



# EERI Earthquake Reconnaissance Team Report: M7.8 Muisne, Ecuador Earthquake on April 16, 2016



Forrest Lanning, Ana Gabriela Haro, Mei Kuen Liu, Alberto Monzón,  
Héctor Monzón-Despang, Arturo Schultz, Adrian Tola

With contributions from the Geotechnical Extreme Events Reconnaissance/ Applied  
Technology Council (GEER-ATC) team (Guillermo Diaz-Fanas, Nonika Antonaki, Sissy  
Nikolaou, Xavier Vera-Grunauer, Ramon Gilsanz, Virginia Diaz)

and Earthquake Engineering Field Investigation (EEFIT) team (Guillermo Franco,  
Harriette Stone, Bayes Ahmed, Siau Chen Chian, Fiona Hughes, Nina Jirouskova,  
Sebastian Kaminski, Jorge Lopez)

October 2016

*A product of the EERI Learning From Earthquakes Program*



© 2016 Earthquake Engineering Research Institute, Oakland, California, 94612-1934

All rights reserved. No part of this publication may be reproduced in any form or by any means without the prior written permission of the publisher, Earthquake Engineering Research Institute, 499 14th Street, Suite 220, Oakland, CA 94612-1934, telephone: +1 (510) 451-0905, email: [eeri@eeri.org](mailto:eeri@eeri.org), website: [www.eeri.org](http://www.eeri.org).

The Earthquake Engineering Research Institute (EERI) is a nonprofit corporation. The objective of EERI is to reduce earthquake risk by (1) advancing the science and practice of earthquake engineering, (2) improving understanding of the impact of earthquakes on the physical, social, economic, political, and cultural environment, and (3) advocating comprehensive and realistic measures for reducing the harmful effects of earthquakes.

Any opinions, findings, conclusions, or recommendations expressed herein are the authors' and do not necessarily reflect the views of EERI, the authors' organizations, or any funding agencies.

This publication is available in PDF format from <http://www.eeri.org>.

ISBN: 978-1-932884-69-2



# PREFACE

In mid-April of 2016, the coastal Ecuadoran province of Manabí suffered a devastating earthquake. Damage was spread up and down the coast, with some towns almost being completely erased. In about a month's time, EERI sent out a reconnaissance team to study the damage. The team was made up of highly energetic structural engineers from both practice and academia. Deploying the team was a race against time, as the central government of Ecuador was in full swing of demolishing all severely damaged buildings. Even by the time the EERI team reached the field, many of the low rise buildings have already been completely cleared out in some of the towns.

This earthquake further strengthens the case that non-ductile, masonry infilled buildings continue to pose a high hazard to lives and buildings in the seismically active areas of the world. For example, most of the hospitals the team visited were inoperative mainly due to the masonry infill and other non-structural damage where in most cases the building structure itself withstood the earthquake. This in turn put more pressure and resources on the response teams to set up temporary emergency hospitals and potentially delayed their ability to take in the injured immediately following the earthquake.

The world, and more specifically the developing world, is dictated by economics. It's always going to be cheaper to fill a wall with locally produced brick masonry over manufactured flexible light-weight building materials. We, the earthquake engineering community, need to find a way of safely using brick masonry where it can be compatible with the building's structure.

This report is filled with images, data and observations. It is part of a growing collection of information the EERI staff, reconnaissance team, and community have developed on the Ecuador earthquake, including an extensive video briefing and a detailed virtual clearinghouse.

The people of Ecuador were very helpful and most of all, welcoming during our visit, especially the Ecuadoran Army Corps of Engineers, who generously provided transportation for the team. Our hearts and our encouragement go out to the people of Manabí Province as they try to rebuild after the devastating earthquake.

Forrest Lanning  
EERI Learning From Earthquakes  
Ecuador Earthquake Reconnaissance Team Leader and Associate  
Miyamoto International, Inc.

September 16, 2016

# TABLE OF CONTENTS

<b>CHAPTER 1: Introduction</b>	<b>6</b>
1.1 Overview of April 16, 2016 Earthquake and aftershocks	6
1.2 Historic Seismicity in Ecuador	9
1.3 Team Members	10
1.3.1 Coordinating with Other Teams and Organizations	11
1.4 Acknowledgments	13
1.5 About EERI and It's Learning From Earthquakes program	13
1.6 EERI and GEER Reconnaissance Team webinar and recorded videos	14
1.7 Virtual Clearing House	14
1.8 Organization of this report	15
1.9 References	15
<b>CHAPTER 2: Selected Geotechnical Observations</b>	<b>17</b>
2.1 Event and GEER-ATC team	17
2.2 Seismological observations	18
2.3 Ground Motions	18
2.4 Geotechnical, infrastructure, and soil-structure interaction	21
2.4.1 Embankments	21
2.4.2 Landslides and Rock Falls	22
2.4.3 Liquefaction and Liquefaction Induced Effects:	25
2.4.4 Dams	28
2.4.5 Earth Retaining Walls	29
2.4.6 Performance of selected foundations	31
2.5 References	31
<b>CHAPTER 3: Building Damage</b>	<b>33</b>
3.1 Introduction	33
3.2 Construction characteristics	33
3.2.1 Formwork Alignment and Overuse	33
3.2.2 Formwork Workmanship and Alignment	34
3.2.3 Corrosion of Reinforcement	35
3.2.4 Construction Joints	37
3.2.5 Steel Structures	39
3.3 Building Interior Partitions and Cladding	40
3.3.1 Partition and Cladding Materials	40
3.3.2 Structure-Partition Interaction	40
3.3.3 Consequences of Poorly Detailed Partitions and Façades	42
3.3.4 Masonry Workmanship	42
3.2.5 Means of Egress	43
3.4 Manta	44
3.4.1 Tarqui District	44
3.4.2 Damage observed in other locations in Manta	46
3.4.3 Hospital IESS of Manta	49
3.4.4 Port of Manta	49

3.5	Portoviejo	51
	3.5.1 Damage to Reinforced Concrete (RC) Buildings	53
	3.5.2 Conclusion	61
3.6	Building damage in pedernales	61
3.7	References	62
<b>CHAPTER 4: Hospitals</b>		<b>63</b>
4.1	Introduction	63
4.2	Hospitals IESS in manta	64
4.3	Hospitals IESS in portoviejo	64
	4.3.1 Hospital SOLCA in Portoviejo	65
4.4	Hospital Miguel H. alcívar in bahía de cÁraquez	66
4.5	Hospital napoleÒn dÁvila in chone	67
4.6	References	
<b>CHAPTER 5: Non-Engineered Construction</b>		<b>68</b>
5.1	Introduction	69
5.2	Masonry construction	69
5.3	Bahareque Construction	72
5.4	Clay brick and timber construction	73
5.5	Wood Construction	
<b>CHAPTER 6: Post-Earthquake Building Shoring</b>		<b>74</b>
6.1	Introduction	75
6.2	The Basic concept of shoring	75
6.3	Shoring in ecuador	77
	6.3.1 Post Eartquake Observations	77
6.4	references	
<b>CHAPTER 7: Post-Earthquake Safety Evaluation of Buildings</b>		<b>79</b>
7.1	Introduction	80
7.2	Usage of evaluation placards	81
7.3	references	
<b>CONCLUDING REMARKS</b>		<b>85</b>
<b>APPENDIX</b>		<b>87</b>
8.1	Recovery from the M7.8 Muisine Earthquake of April 16, 2016: A case study of the earthquake refugee shelters in Manabí Province, Ecuador	85
	8.1.1 Demographic Characteristics	86
	8.1.2 Economic Status	87
	8.1.3 Problems in the Shelters	88
	8.1.4 Future Direction	88
	8.1.5 Information on Survey Respondent Homes	88
	8.1.6 Summary Findings	89
	8.1.7 Acknowledgments	90



# CHAPTER 1

# INTRODUCTION

## 1.1 OVERVIEW OF APRIL 16, 2016 EARTHQUAKE AND AFTERSHOCKS

On Saturday, April 16, 2016 at 23:58:36 (UTC), an earthquake with a moment ( $M_w$ ) magnitude 7.8 and a maximum European Macroseismic Scale (EMS-98) intensity of IX (destructive) struck along the central coast of Ecuador. Figure 1-1 (left) shows the epicenter of the earthquake (USGS, 2016), while Figure 1-1 (right) shows a map of the EMS-98 intensities (Singaucho et al., 2016).

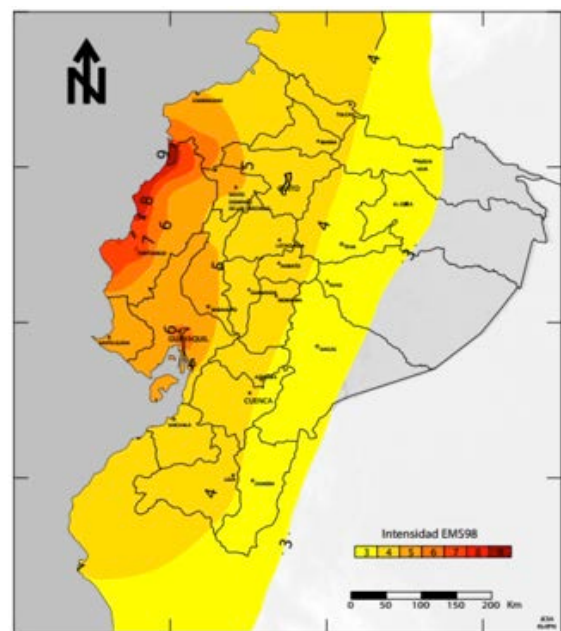


Figure 1-1. (Left) Location of epicenter for earthquake in Ecuador on April 16th, 2016; (Right) Map showing intensity of shaking, based on EMS-98 scale (Singaucho et al., 2016).

Widespread damage was caused throughout the provinces of Esmeraldas and Manabí, including the towns and cities of Muisne, Pedernales, Canoa, Bahía de Caráquez, Portoviejo, and Manta. The maximum PGA recorded in Pedernales was 1.407 g (Singuacho, 2016). Building collapses were observed hundreds of kilometers from the epicenter. In the aftermath of the earthquake, water supply, energy supply, disposal, transportation, and telecommunication systems reported limited service in the most affected areas. The President of Ecuador, Rafael Correa, stated that the earthquake cost the country more than \$1.3 billion, with a final death toll of 668 (La República, 2016). According to the Ecuadorian Secretariat for Risk Management (Secretaría de Gestión de Riesgos, 2016), the aftermath of this earthquake saw 6,274 people injured, twelve people missing, 113 people rescued, and 28,775 people taken to shelters.

This megathrust earthquake was generated at the boundary of the Nazca Plate (Figure 1-2), which is subducting beneath the South American Plate at a convergence rate of approximately 61 millimeters per year; the focal depth of the earthquake was 19.2 km, and the epicenter was 29 km SSE of Muisne (USGS 2016). As of July 8, 2016, there had been 2,106 aftershocks (Instituto Geofísico EPN, 2016), with three having a moment magnitude greater than 6 (Orellana, 2016). There was severe damage to houses and buildings in the coastal region of Ecuador. Typical construction materials in this area, as well as in the majority of the country, are unreinforced masonry for infill/partition walls, and reinforced concrete for columns, beams, and slabs. In most cases, the masonry consists of clay brick, or hollow concrete blocks made of pumice aggregate. Although in Ecuador, masonry walls are usually surrounded by concrete columns and beams, the masonry commonly does not satisfy the requirements to be considered confined masonry, and therefore, houses and other low-rise buildings usually lack a well-defined lateral load-resisting system. In the case of multistory buildings, reinforced concrete moment frames with masonry infills and masonry partition walls are typical (Figure 1-3).

Ductile reinforced concrete (RC) frame structures usually behave satisfactorily during an earthquake when nonstructural elements are also considered during the design process. The use of RC frame systems is a common practice in Ecuador. However, the lack of specific guidelines in local seismic codes for the design of nonstructural components and their attachments to main structures, and to a lesser extent, for the detailing of ductile members and connections, contributed to an overall poor seismic performance.

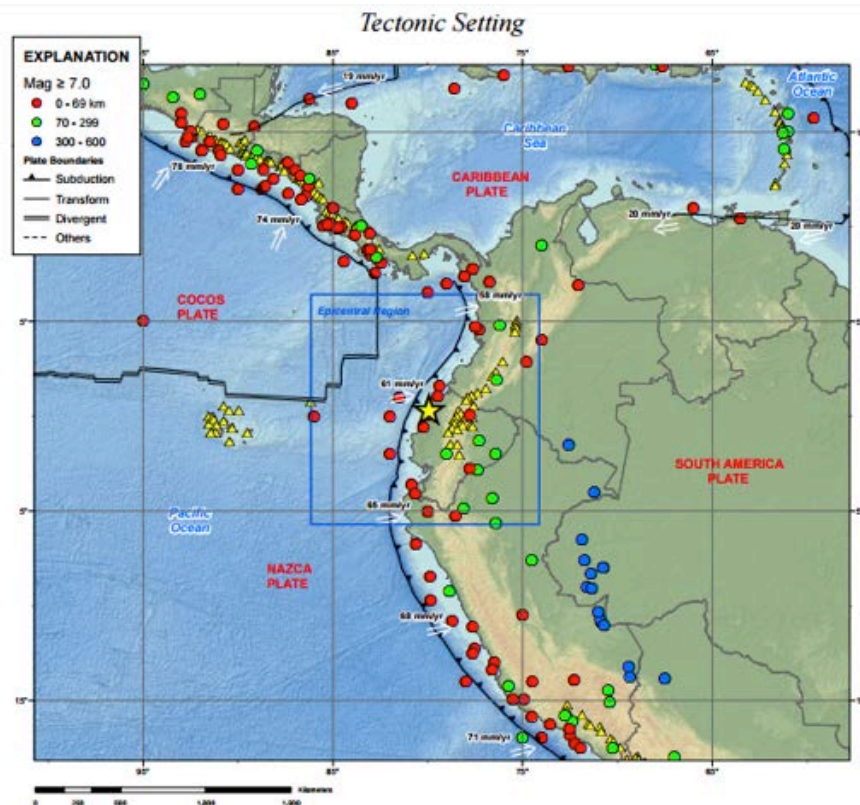


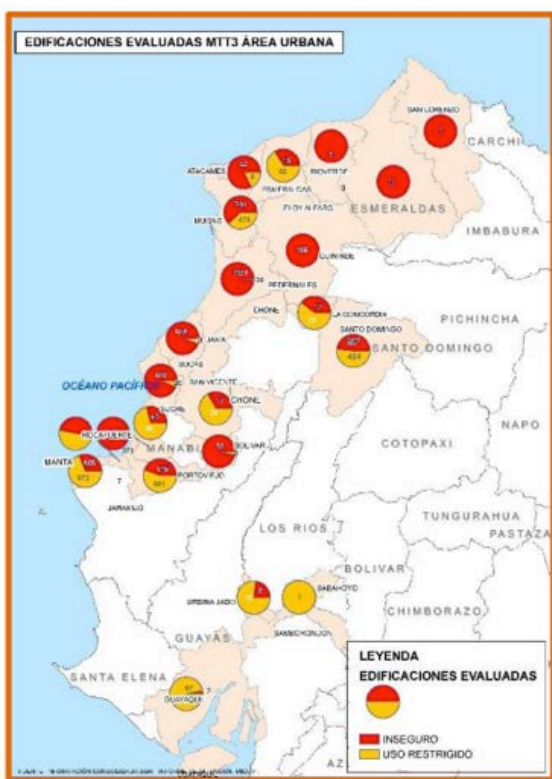
Figure 1-2. Seismic history of the inter-plate region. Courtesy of USGS.

In addition, structural design firms in Ecuador are usually not involved in the construction process, and therefore, there is no guarantee that a building will be built as it was originally designed. Furthermore, structural engineering firms in Ecuador usually do not provide specific details in structural drawings (or at least a set of guidelines to the building contractor) regarding nonstructural components and their attachments, particularly for the case of infill walls.

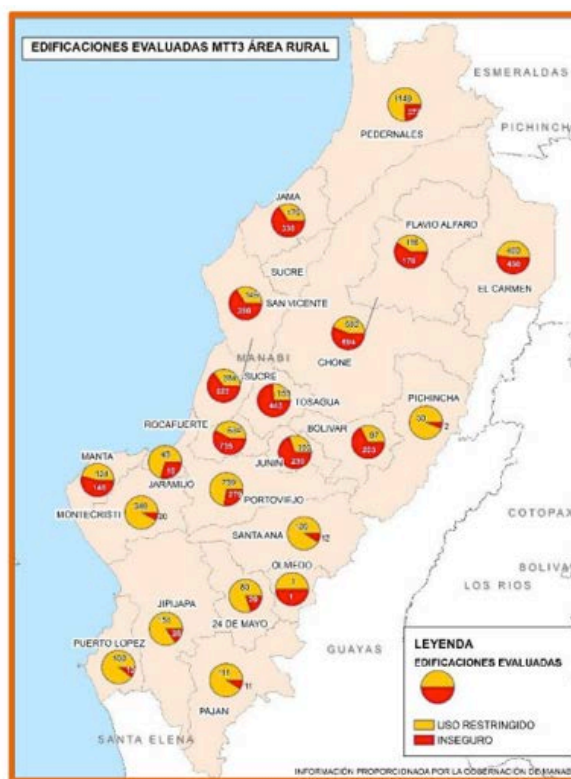
Figure 1-4 illustrates the building evaluation in urban and rural areas conducted by the Ministry of Urban Development and Housing, and the Manabí Province Government, respectively. Red tags represent unsafe structures and yellow tags represent structures with restricted use.



Figure 1-3. Typical masonry used for wall infill on reinforced concrete framed buildings.



10,508 affected buildings



8,157 affected buildings

Figure 1-4. Infrastructure evaluation in urban and rural areas conducted by the Ministry of Urban Development and Housing, and the Manabí Province Government, respectively. Red tags represent unsafe structures and yellow tags represent structures with restricted use.

Nonstructural damage was widespread in mid-rise engineered and non-engineered buildings. Heavy masonry units contributed to the building mass (and hence seismic inertial force) causing extensive losses in critical facilities and businesses.

All of the cities affected by the earthquake are important for the economy of the country in different aspects. For instance, Portoviejo, the capital of the Province of Manabí, has important agricultural and shrimp farming industries, both of which were heavily affected by road damage that halted or limited the ability to transport goods. Damage in the pools used to cultivate shrimp was also reported. Portoviejo also has a large number of small businesses in the downtown areas, where structure collapse was significant.

Manta's seaport has a significant impact in the local and national economy, and such infrastructure suffered damage. Fortunately, Manta's heavy tuna processing industry was not greatly affected. The motor that moves the economy in other cities like Bahía de Caráquez or towns like Canoa is tourism, and because of the damage at these locations, the regular activities and income of their residents might be affected.

## 1.2 HISTORIC SEISMICITY IN ECUADOR

Ecuador's seismic history includes a number of large subduction zone related earthquakes (Figure 1-5). Seven magnitude 7 or greater earthquakes have occurred within 250 km of the April 16, 2016 event since 1900. A M7.8 earthquake occurred on May 14, 1942, 43 km south of the April 16, 2016 event. Several decades earlier, a M8.8 earth-

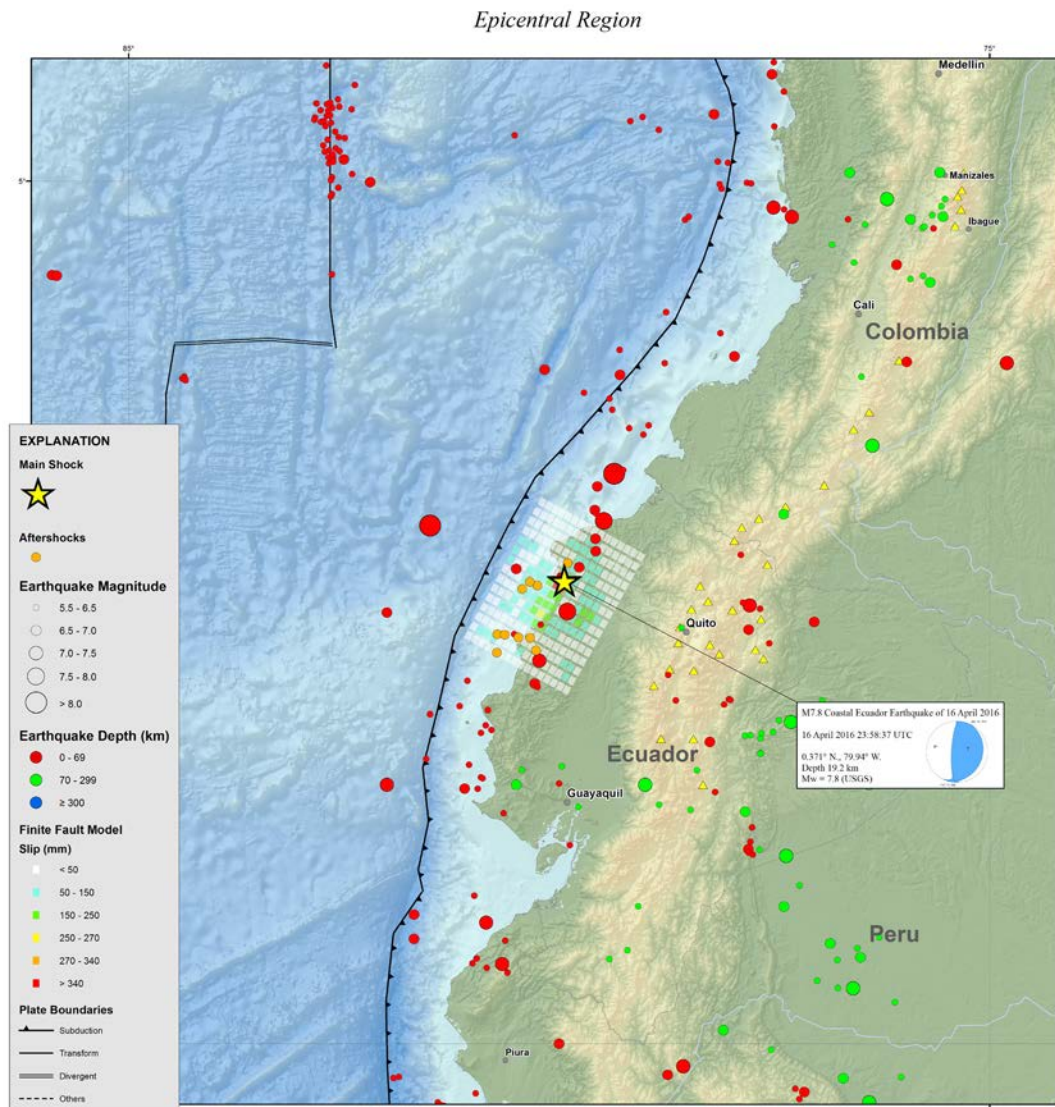


Figure 1-5. Seismic history of the epicentral region. Courtesy of USGS

quake occurred on January 31, 1906. This earthquake was centered on the subduction zone 90 km to the northeast of the April 2016 event, and ruptured a length of 400-500 km of the fault. This earthquake also resulted in a damaging tsunami that caused between 500-1,500 fatalities to the region. The April 2016 earthquake is at the southern end of the approximate rupture area of the 1906 event. More recently, a shallow, upper crustal M 7.2 earthquake occurred 240 km east of the April 2016 event on March 6, 1987 resulted in approximately 1,000 fatalities (USGS).

Ecuador covers a total of 283,560 square kilometers. Four very distinct geographic regions divide the country: the jungle region, the mountain region, the coastal region, and the Galapagos Islands. The central coastal region, which was the most affected area during the April 16, 2016 earthquake, is relatively flat and extends into the rain forests. From time to time, the geography of this region has been altered not only by earthquakes, but also by floods and landslides (Ecuador.com, 2016).

Ecuador is impressively geologically diverse. Regarding only the coastal region, during the Cretaceous and early Tertiary periods, marine deposits of limestone and shale were accumulated in the western area of the country. Submarine pillow lavas alternating with marine sediments were also formed in the region during these periods. The igneous rocks were later uplifted to form the present-day coastal range (Neill, 2016). The landforms were caused by the push of the present oceanic crust of the Carnegie Ridge against the Ecuadorian continent. The Paleo beaches, which are ridges of sand beaches abandoned inside the continent, like those existing in east Manta and the valleys found elsewhere at the coastal cliffs, are all consequences of continental uplifts and the receding ocean (Vera, 2013).

### 1.3 TEAM MEMBERS

EERI issued a call for volunteers to participate on a reconnaissance team on April 20th. A small team was selected from the pool of interested volunteers to travel to Ecuador. Forrest Lanning from Miyamoto International and a current EERI Housner Fellow was selected as the team leader. In addition two members of the Guatemalan Earthquake Engineering Association (AGIES) team were asked to join with EERI, based on a strong working relationship that was developed as part of a World Bank-funded investigation into the November 7, 2012 Guatemala earthquake and its implications for disaster reduction and mitigation. Team members included (see Figure 1-6):

1. Forrest Lanning, Miyamoto International—Costa Rica & Colombia (Team Leader)
2. Ana Gabriela Haro, North Carolina State University
3. Mei Kuen Liu, Forell—Elsesser Engineers, Inc.
4. Alberto Monzón, Guatemalan Association of Structural and Seismic Engineers—AGIES
5. Héctor Monzón Despang, Guatemalan Association of Structural and Seismic Engineers—AGIES
6. Arturo E. Schultz, University of Minnesota
7. Adrian Tola, Virginia Tech



Figure 1-6. Back row: Cnrl. José Ramos, Héctor Monzón Despang, Alberto Monzón, Mei Kuen Liu, Arturo Schultz, Forrest Lanning, Tcrn. Xavier Riofrío. Front row: Xavier Velásquez, Ana Gabriela Haro, Adrian Tola

### 1.3.1 Coordinating with Other Teams and Organizations

EERI worked closely with several other teams in developing their reconnaissance approach. These teams included the Geotechnical Extreme Event Reconnaissance (GEER) and Applied Technology Council (ATC) team, co-led by Sissy Nikolaou, Xavier Vera-Grunauer and Ramon Gilsanz, and the European Earthquake Field Investigation Team (EEFIT), led by Guillermo Franco. Team members from each of these teams are listed in Table 1-1 below.

Financial support was provided by EERI; the Department of Civil, Construction, and Environmental Engineering at North Carolina State University; the Department of Civil and Environmental Engineering of Virginia Tech; Forell/EI-sesser; Miyamoto International Inc.; and The Masonry Society.

*Table 1-1 Members of collaborating EEFIT and GEER-ATCTeams*

NAME	AFFILIATION
<b>EEFIT</b>	
Guillermo Franco, team leader	Global Head of CAT Risk Research, Guy Carpenter
Harriette Stone	Research Engineer, University College London
Bayes Ahmed	PhD candidate, University College London
Siau Chen Chian	Assistant Professor, National University of Singapore
Fiona Hughes	PhD candidate, Cambridge University
Nina Jirouskova	PhD candidate, Imperial College London
Sebastian Kaminski	Structural Engineer, Arup
Jorge Lopez	Structural Engineer, Arup
<b>GEER EDITORS</b>	
Sissy Nikolaou, co-team leader	WSP PB (USA)
Xavier Vera-Granauer, co-team leader	Universidad Católica de Guayaquil and Geostudios (Ecuador)
Ramon Gilsanz	GMS (USA)
<b>GEER-ATC TEAM MEMBERS</b>	
Alexandra Alvarado	IG-EPN (Ecuador)
Daniel Alzamora	FHWA (USA)
Nonika Antonaki	RPI (USA), WSP PB (USA)
Carlos Arteta	UNCO (Colombia)
Adda Athanasopoulos-Zekkos	Univ of Michigan (USA)
Patrick Bassal	WSP PB (USA)
Adolfo Caicedo	UCSG (Ecuador)
Bernardo Casares	Cornell Univ (USA)
Danilo Davila	Geostudios (Ecuador)
Virginia Diaz	GMS (USA)
Guillermo Diaz-Fanas	WSP PB (USA)
Oscar González	Univ of Michigan (USA)
Laura Hernandez	GMS (USA)
Tadahiro Kishida	UC Berkeley (USA)
Panagiota Kokkali	RPI (USA) and WSP PB (USA)
Pablo López	
Roberto Luque	UC Berkeley (USA)

(Chart continued on next page...)

<b>GEER TEAM MEMBERS continued</b>	
Gabriela M. Lyvers	USACE (USA)
Said Maalouf	
Jay Mezher	WSP PB (USA)
Eduardo Miranda	STANFORD (USA)
Enrique Morales	UBUFFALO (USA)
Enrique Morales Moncayo	ECACE (Ecuador)
Jerome S. O'Connor	UBUFFALO (USA)
Tom O'Rourke	Cornell Univ (USA)
Ignacio Ochoa	Geostudios (Ecuador)
Francisco Ripalda	UCSG (Ecuador)
Luis Fernando Rodríguez	Droneando (Ecuador)
Kyle Rollins	BYU (USA)
Andreas Stavridis	UBUFFALO (USA)
Theofilos Toulkeridis	ESPE (Ecuador)
Efthymios Vaxevanis	WSP PB (USA)
Noemí Villagrán León	Geostudios (Ecuador)
Clinton Wood	Univ of Arkansas (USA)
Hugo Yepes	IG-EPN (Ecuador)
Fabricio Yopez	SFQUITOU (Ecuador)
<b>GEER RECORDERS</b>	
Guillermo Dias-Fanas	WSP PB (for GEER-Ecuador)
Virginia Dias	GMS (for ATC-Ecuador)
Fernando "Estefan" Garcia	Univ of California Berkeley (2016 GEER Recorder)

Full documentation on these teams' missions is available in Nikolaou et al 2016; Franco et al 2016 and Franco et al 2017.

## 1.4 ACKNOWLEDGMENTS

A reconnaissance trip is impossible to conduct successfully without the assistance and collaboration of many individuals, both in the affected country and from afar. These individuals provide insights into the context for the earthquake, construction practices, and government policies and programs as well as help with access and transportation to affected areas. The EERI team is deeply indebted to the following individuals, listed in Table 1-2 (next page), who provided them with such assistance.

Table 1-2 Individuals who assisted the EERI reconnaissance team

NAME	AFFILIATION
Grab. Pedro Mosquera Burbano	Chief of the Ecuadorian Army Corps of Engineers
CrnI. José Ramos	Ecuadorian Army Corps of Engineers
Tcrn. Xavier Riofrío	Ecuadorian Army Corps of Engineers
Fabricio Yépez, PhD.	Universidad San Francisco de Quito
Telmo Sánchez, PhD.	Universidad San Francisco de Quito
Xavier Vera-Grunauer, PhD.	Universidad Católica de Guayaquil
Guillermo Ponce	Universidad Católica de Guayaquil
Dra. Gladys Báez	Unidad Educativa Marqués de Selva Alegre
Carolina Salcedo	Ecuadorian Secretariat for Risk Management
Xavier Velásquez	Civil Engineering Consultant
Capt. Xavier Oviedo	Ecuadorian Army Corps of Engineers
Capt. Darwin Carrera	Ecuadorian Army Corps of Engineers
Mervyn Kowalsky, PhD.	North Carolina State University
Pablo Caiza Sánchez, PhD.	Universidad de las Fuerzas Armadas ESPE
Enrique Morales	University at Buffalo
Eduardo Miranda	Stanford University
Dr. Roberto Aguiar Falconi	Universidad de las Fuerzas Armadas ESPE, Ecuador
Santiago Camino	PLANPROCONS Consulting Firm
Patricio Paredes	PLANPROCONS Consulting Firm
Krishna Vatsa	UNDP
Jeanette Fernandez Castro	UNDP

## 1.5 ABOUT EERI AND ITS LEARNING FROM EARTHQUAKES PROGRAM

The Earthquake Engineering Research Institute (EERI) is a nonprofit multi-disciplinary technical society of engineers, practicing professionals, and researchers dedicated to reducing earthquake risk. Since its inception in 1949, EERI has conducted post-earthquake investigations for the purpose of improving the science and practice of earthquake engineering and earthquake hazard reduction. Formalized as the Learning from Earthquakes (LFE) program in 1973, the mission is to accelerate and increase learning from earthquake-induced disasters that affect the natural, built, social and political environments worldwide. The mission is accomplished through field reconnaissance, data collection and archiving, and dissemination of lessons and opportunities for reducing earthquake losses and increasing community resilience. Volunteer EERI field teams are deployed on trips that aim to document impacts, identify knowledge gaps where further research is most needed, and identify practices that will improve mitigation measures, disaster preparedness, and emergency response for future disasters. The LFE program is led by the LFE Executive Committee and its Chair with additional support from EERI Staff and the EERI Board of Directors.

Special help was provided for this reconnaissance trip to Ecuador from various members of LFE and EERI Staff. Charles Huyck, Chair of the LFE Executive Committee, provided critical insight and guidance particularly in the

early phases of the reconnaissance trip planning. The members of the LFE Executive Committee also participated in discussions to make critical early decisions about EERI's response to this earthquake. Marjorie Greene served as the interim coordinator for this event. Members of the EERI staff also provided support including Executive Director Jay Berger, Stephen LaBounty, Sonya Hollenbeck, Juliane Lane, Maggie Ortiz, and Intern Shizza Fatima.

## 1.6 EERI AND GEER RECONNAISSANCE TEAM WEBINAR AND RECORDED VIDEOS

On July 15, EERI conducted a webinar with members of the EERI reconnaissance team that traveled to Ecuador to study the April 16, 2016 earthquake. Team members presented their observations. In addition, the co-leader of the GEER-ATC team offered an overview of geotechnical impacts. Briefing content provided key insights into the various aspects of shaking characteristics, earthquake damage to housing and hospitals and initial response, in particular tagging issues. An overview of damage in Portoviejo and Manta was also included.

A list of the video presentations is shown in Table 1-3. Total viewing time for the video is 1 hour and 40 minutes. The presentations are also available for download as pdf files. The video and pdf files can be accessed here: <http://www.eqclearinghouse.org/2016-04-16-muisne/2016/07/21/ecuador-briefing-webinar-video-now-available/>

*Table 1-3 List of webinar presentations from the Ecuador reconnaissance trip*

TITLE	PRESENTER
Introduction and Overview of the Earthquake	Forrest Lanning
Geotechnical Observations from the GEER-ATC Team	Sissy Nikolaou
Damage Observed in the Ground Zero Zone of Portoviejo	Ana Gabriela Haro
Damage Observed in Manta	Mei Kuen Liu
Performance of Hospitals	Adrian Tola
Performance of Partitions and Cladding of Multistory Buildings	Héctor Monzón Despang
Building Tagging	Arturo E. Schultz

## 1.7 VIRTUAL CLEARINGHOUSE

Additional information on the April 16, 2016 earthquake is available at the clearinghouse EERI set up after the event: <http://www.eqclearinghouse.org/2016-04-16-muisne/>. This clearinghouse includes the presentations listed in Table 1-3, as well as reports from other organizations and government agencies. The interactive map contains links to much information that has been made available by various agencies. In addition over four thousand photos from EERI team members have been catalogued and uploaded, where they are accessible to all.

EERI created the concept of online virtual earthquake reconnaissance clearinghouses in 2009, with the website for the Muisne, Ecuador earthquake being the twentieth launched by the Learning from Earthquakes program. The 2015 Nepal Earthquake clearinghouse brought the innovation of assigned curators to research, summarize, and post information on a range of topics, deepening and expanding the value of virtual clearinghouses.

EERI's Younger Members Committee formalized a Virtual Earthquake Response Team (VERT) to have curators ready to respond immediately after the launch of a virtual clearinghouse. Enthusiastic members of VERT scour the Internet and use their contacts to find reports, video, photos, and maps to link to and post. In addition, VERT members are prepared to provide logistical and informational support to in-field members of EERI reconnaissance teams, and it is expected that their role will continue to grow in future earthquakes. Table 1-4 is a list of the VERT volunteers for the Ecuador clearinghouse.

Table 1-4 Virtual Earthquake Reconnaissance Team Members for Ecuador

NAME	AFFILIATION
Diego Aguirre	North Carolina State University
Candice Avanes	Arup
Patrick Bassal	WSP PB
Veronica Cedillos	ATC
Sahar Derakhshan	PEER
Erica Fischer	Degenkolb Engineers
Manny Hakhamaneshi	EERI Younger Members Committee
Ana Gabriela Haro	North Carolina State University
Ezra Jampole	Stanford University
Jeena Jayamon	Virginia Tech
Cuiyan Kong	North Carolina State University
Ammar Motorwala	SKA Engineers
Yasutaka Narazaki	University of Illinois
Nicole Paul	Arup
Bishal Subedi	Aurecon
Emrah Tasdemir	North Carolina State University
Anna Weiser-Wooward	Walter P Moore

## 1.8 ORGANIZATION OF THIS REPORT

This report has been organized into the following chapters.

Chapter 2 presents a summary of geotechnical damage, prepared by the GEER/ATC team.

Chapter 3 presents an overview of structural damage, including a discussion of construction characteristics that may have contributed to damage, and a review of specific damage observed in Manta, Portoviejo and Pedernales.

Chapter 4 presents a discussion of damage to the 5 hospitals observed by the EERI team.

Chapter 5 summarizes types of non-engineered construction in Ecuador and observed performance in this earthquake.

Chapter 6 presents a discussion of building shoring that was used after the April 16 event.

Chapter 7 summarizes issues the team observed surrounding the tagging of buildings.

## 1.9 REFERENCES

- Ecuador.com. "Jungles, Coastal Plains and Highlands—The Diverse Geography of Ecuador." Accessed June 12, 2016. <http://www.ecuador.com/geography/>.
- Franco et al. (2016) "The April 16 2016 MW7.8 Muisne Earthquake in Ecuador—Observations & Conclusions from the EEFIT Reconnaissance Mission of May 24–June 7." Earthquake Engineering Field Investigation Team, Institution of Structural Engineers, London, UK.
- Franco et al. (2017) "The April 16 2016 MW7.8 Muisne Earthquake in Ecuador—Preliminary Observations from the EEFIT Reconnaissance Mission of May 24–June 7." In Proceedings of the 16th World Conference on Earthquake Engineering, 16WCEE 2017, Santiago Chile, January 9th to 13th 2017, Paper N° 4982.

- Instituto Geofísico Escuela Politécnica Nacional (EPN), 2016. Informe Sísmico Especial N.- 25 *Actualización de las Réplicas*, Instituto Geofísico Escuela Politécnica Nacional. Quito.
- La Republica. "Correa dice que subió a 668 la cifra de muertos por terremoto en Ecuador." Accessed June 10, 2016. *La Republica.ec*.
- Neill, David A. "Geology," *Catalogue of the Vascular Plants of Ecuador* (1999): 5-7. Accessed 12 June 12, 2016. <http://www.mobot.org/mobot/research/Ecuador/geology.shtml>.
- Nikolaou, S., Vera-Grunauer, X., and Gilsanz, R., eds. (2016). "GEER-ATC Earthquake Reconnaissance: April 16 2016, Muisne, Ecuador," Geotechnical Extreme Events Reconnaissance Association Report GEER-049, Version 1, October 2016. [http://www.geerassociation.org/component/geer\\_reports/?view=geerreports&id=77&layout=default](http://www.geerassociation.org/component/geer_reports/?view=geerreports&id=77&layout=default)
- Orellana J. R., 2016. *Informe Sísmico Especial*, No.14. Continúan las réplicas del sismo de Pedernales. (Instituto Geofísico Escuela Politécnica Nacional, Quito. 2016).
- Singaicho J. C., Laurendeau A., Viracucha C., Ruiz M., 2016. *Informe Sísmico Especial*, No. 18. *Observaciones del sismo del 16 de abril de 2016 de magnitud Mw7.8. Intensidades y Aceleraciones*. (Instituto Geofísico Escuela Politécnica Nacional, Quito. 2016).
- Secretaría de Gestión de Riesgos, 2016. Informe de Situación, No. 71. 19/05/2016 (20h30) Terremoto 7.8–Pedernales, Secretaría de Gestión de Riesgo, 2016. Accessed July 2016. <http://www.gestionderiesgos.gob.ec/>
- USGS: United States Geological Survey USGS. "M7.8 - 29km SSE of Muisne, Ecuador." USGS. Accessed June 12, 2016. <http://earthquake.usgs.gov/earthquakes/eventpage/us20005j32#executive>
- Vera, Ramón. *Geology of Ecuador* (Iberia) 2013.



## **CHAPTER 2**

# **SELECTED GEOTECHNICAL OBSERVATIONS**

### **2.1 EVENT AND GEER-ATC TEAM**

A team from the Geotechnical Extreme Events Reconnaissance (GEER) Association, sponsored by the National Science Foundation (NSF), and with partial support from the Applied Technology Council (ATC) was deployed shortly after the main event, on April 26th, to document and investigate the widespread earthquake-induced geotechnical, infrastructure, and soil-structure impacts for a week in the field. The GEER-Ecuador team was co-led by Dr. S. Nikolaou of WSP | Parsons Brinckerhoff from the US and Dr. X. Vera-Grunauer of the Universidad Católica de Santiago de Guayaquil and the Geostudios firm from Ecuador. The US GEER-Ecuador team included Professors K. Rollins (Bingham Young Univ.), A. Zekkos (University of Michigan), C. Wood (Univ. of Arkansas), Mr. D. Alzamora (Federal Highway Administration), and Ms. G. Lyvers (US Army Corp of Engineers). The team included ATC-funded structural engineers Mr. R. Gilsanz and Ms. V. Diaz of Gilsanz Murray Steficek LLP. The team was joined by additional members who were already in Ecuador, including Prof. E. Miranda (Stanford Univ.), Mr. E. Morales (Univ. at Buffalo), and Mr R. Luque (UC Berkeley). The GEER recorder for this event was Mr. G. Diaz-Fanas (WSP | Parsons Brinckerhoff). The GEER-ATC team collaborated closely with their local counterparts from academia and practice, and had unique opportunities to meet with principal Ecuadorian government officials to discuss the needs for immediate rebuild and long term goals for the recovery of their country.

This chapter will present selected geotechnical reconnaissance observations from the main Mw7.8 Muisne, Ecuador earthquake, including seismological, ground motion, liquefaction, and effects on infrastructure. Details are in the GEER-ATC report: [http://www.geerassociation.org/component/geer\\_reports/?view=geerreports&id=77&layout=default](http://www.geerassociation.org/component/geer_reports/?view=geerreports&id=77&layout=default).

## 2.2 SEISMOLOGICAL OBSERVATIONS

The tectonic setting in Ecuador consists of a mix of a subduction zone with crustal earthquakes and volcanism. This area has felt megathrust subduction earthquakes, including the 1906 Mw8.8 Esmeraldas, 1942 Mw7.8 Jama, 1958 Mw7.8 Esmeraldas, 1979 Mw8.2 Colombia, and 1998 Mw7.2 Bahia events. The area that ruptured during the 1906 earthquake covers the west coast of Ecuador. According to Chlieh et al. (2014), a potential for an earthquake of magnitude greater than Mw7.5 existed due to a seismic gap. The gap, depicted in Figure 2-1, was not covered by the historic megathrust events following the 1906 event as mentioned above. The rupture area of the 2016 Mw7.8 Muisne earthquake coincides with the Chlieh et al. (2014) seismic gap.

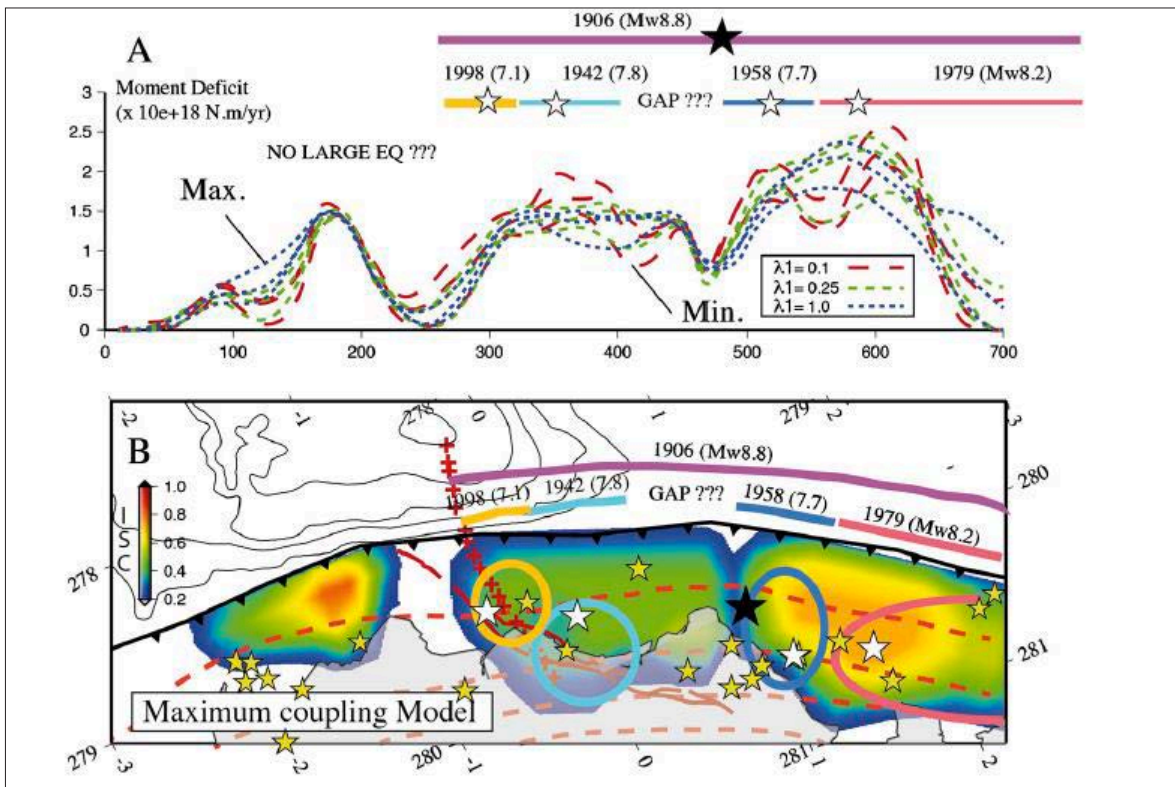


Figure 2-1. Historic seismicity of Ecuador and the seismic gap (modified from Chlieh et al., 2014).

## 2.3 GROUND MOTIONS

Strong ground motion records were provided by the Ecuadorian Geophysical Institute from the National Polytechnic School (IG-EPN) and presented in Singaicho et al. (2016). A total of 30 three-component uncorrected digital acceleration time series were provided to the GEER-ATC Ecuador team. Most of the instruments that recorded the motions are part of the RENAC (Accelerometers National Network) that is managed and maintained by IG-EPN, but other instruments belong to the OCP (oil pipeline) or the LMI project (a collaboration between IG-EPN and the Institute of Research for Development (IRD) of France). These records were processed following the PEER standard procedure (Ancheta et al. 2014), which includes inspection of record quality, selection of time windows, such as P-, S-, and coda waves, and component-specific filter corner frequencies to optimize the usable frequency range. All but the PRAM station record were useable and of acceptable quality.

Table 2-1 shows information from ten of the RENAC stations that recorded the main event, including the location (nearest city, geographic coordinates), closest distance to the rupture plane (RRUP) using the finite USGS fault solution (USGS, 2016), the shear wave velocity in the top 30 m of overburden ( $V_{S,30}$ ) and the recorded Peak Ground Acceleration (PGA) of the three components (East, North, and Vertical). Figure 2-2 shows the USGS Intensity ShakeMap with the projected rupture plane to the surface with the station locations that are color-coded according to the geometric-mean of the PGA horizontal components. In general, both the intensity map and the Strong Motion

Stations (SMS) shows stronger shaking intensity towards the south of the rupture plane. Also, both intensity tools type (ShakeMap and SMS) show clear evidence of site effects in the soft alluvial deposits of Guayaquil city, located at source-to-site distances (RRUP) between 160 and 180 km.

Table 2-1. Important parameters of 10 stations from which ground motion records were processed by the GEER team

Station	City	Geographic Coordinates		R <sub>RUP</sub> (km)	V <sub>S30</sub> (m/s)	PGA (g)		
		Latitude	Longitude			EW	NS	VER
PDNS	Pedernales	0° 6' 39.6" N	79° 59' 27.6" W	21	-	1.034	0.942	0.573
APED	Pedernales	0° 4' 4.8" N	80° 3' 25.2" W	20	342 <sup>a</sup>	1.408	0.83	0.742
AES2	Esmeraldas	0° 59' 27.6" N	79° 38' 45.6" W	51	-	0.154	0.111	0.044
ACHN	Chone	0° 41' 52.8" S	80° 5' 2.4" W	34	200 <sup>a</sup>	0.328	0.371	0.173
APO1	Portoviejo	1° 2' 16.8" S	80° 27' 36" W	73	224 <sup>a</sup>	0.317	0.381	0.105
AMNT	Manta	0° 56' 27.6" S	80° 44' 6" W	76	496 <sup>a</sup>	0.404	0.525	0.162
EPNL	Quito	0° 12' 43.2" S	78° 29' 31.2" W	104	-	0.027	0.02	0.013
AGYE	Guayaquil	2° 3' 14.4" S	79° 57' 7.2" W	155	1800 <sup>b</sup>	0.019	0.024	0.015
AGY1	Guayaquil	2° 15' 3.6" S	79° 54' 36" W	175	178 <sup>b</sup>	0.059	0.065	0.02
AGY2	Guayaquil	-2° 11' 56. 4" S	79° 53' 56.4" W	170	101 <sup>b</sup>	0.094	0.098	0.038

*a* Measured by Geoestudios (2016). *b* Measured by Vera-Grunauer (2014).

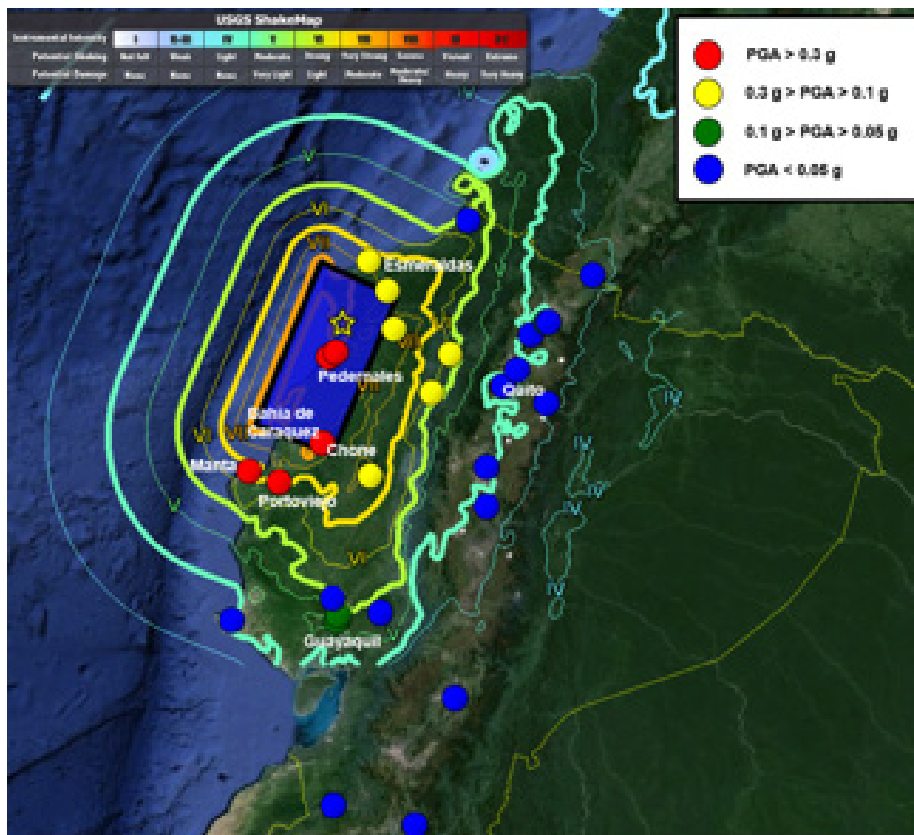


Figure 2-2. Contours of Intensity (ShakeMap) from USGS and strong motion stations (SMS) color-coded by the intensity of the motion in terms of the geo-mean Peak Ground Acceleration (PGA).

The strongest recorded motion with PGA = 1.41 g corresponds to the EW component of the APED station, located in Pedernales, with an approximate RRUP of 20 km and VS,30 of 342 m/s (Geoestudios, 2016). At the same station, the NS component recorded a PGA = 0.83 g. Another station in Pedernales, PDNS, with RRUP = 21 km recorded 1.03 and 0.94 g in the EW and NS components, respectively.

Figure 2-3 shows the acceleration time histories for the EW component for selected stations. Station AV21, located near Esmeraldas, is shown on the map because it has a smaller distance than ACHN (25 vs. 34 km), but recorded half of the PGA amplitude at ACHN. APED, PDNS, AMNT and APO1 recorded ground motions with PGA greater than 0.3 g. AGYE and AGY1 are founded on rock with VS,30 of 1,800 m/s and soft soil deposits with VS,30 of 101 m/s, respectively, with different recorded PGA amplitudes of 0.02 and 0.094 g, respectively.

A comparison of the acceleration, velocity and displacement time histories for four stations (APED, AMNT, ACHN, APO1) is shown in Figure 2-4. Visual inspection of the velocity time series indicates high frequency contents for APED station. AMNT and APO1 show lower frequency content, with periods in the order of 2 to 3 seconds. The interesting case is ACHN, where the acceleration time series show lower frequency content (higher periods) than AMNT and APO1, but the velocity time series show higher frequency than the same two stations, roughly between 1 and 2 seconds.

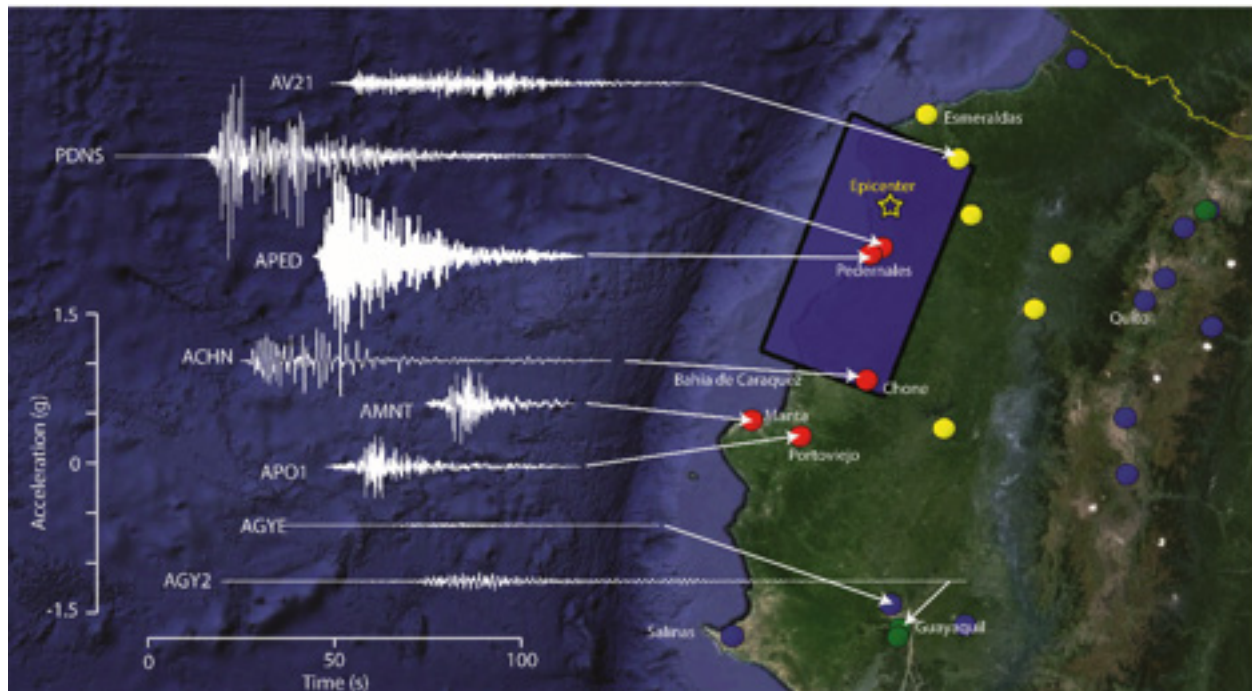


Figure 2-3. Acceleration time series in the EW component overlying map of Ecuador with cities and stations.

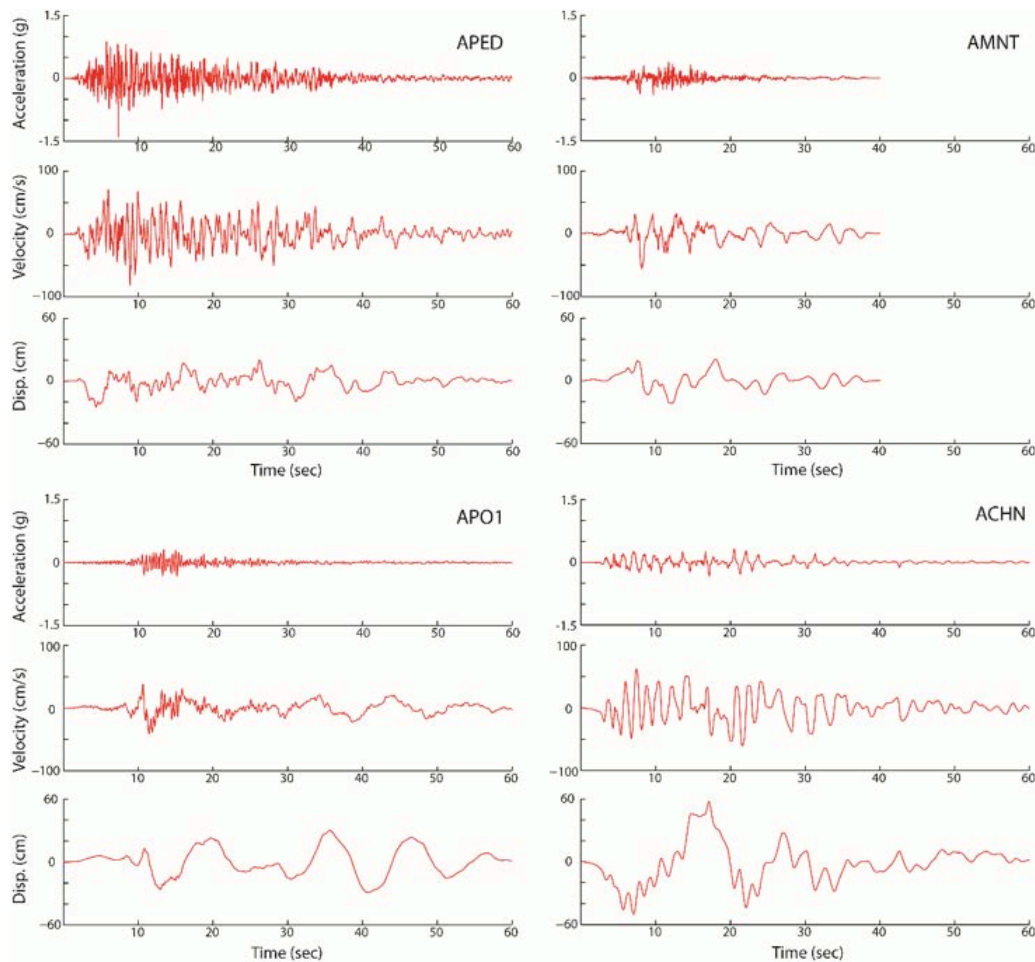


Figure 2-4. Acceleration, velocity and displacement time histories for the EW component of stations APED, AMNT, ACHN and APO1

## 2.4 GEOTECHNICAL, INFRASTRUCTURE, AND SOIL-STRUCTURE INTERACTION

### 2.4.1 Embankments

Failures of embankments as well as any other aspect of transportation road network affect connectivity, ability to quickly receive supplies, and access of emergency vehicles. Even though the majority of highway embankments throughout the affected areas of Ecuador performed well, maintaining a serviceable road and in some cases possibly requiring minor repair, a few embankments performed from poorly to collapse. Two examples of major failure are the Rio Chico Bridge ( $0^{\circ}58'35.65''\text{S}$ ,  $80^{\circ}25'21.29''\text{W}$ ) and the Mejia Bridge ( $0^{\circ}59'22.73''\text{S}$ ,  $80^{\circ}28'11.14''\text{W}$ ), both built using a well-graded material and at a 2H:1V slope.

The Rio Chico Bridge had several modes of failure acting on the embankment. We observed large coherent cohesive blocks settle, slide, rotate and in several cases present a combination of these modes, which became evident with measurements of large cracks and displacements. At the Mejia Bridge the embankments appeared to have failed in a general global stability mode and damage was mostly found on the south embankment. Most of the damage to the bridge, walls, and embankments was focused on the south approach. There was some instability on the north side but it was relatively minor. Figures 2-5 shows some important observations.



Figure 2-5. Failure Modes of Embankments (a) Rio Chico Bridge ( $0^{\circ} 58' 38.09''S$ ,  $80^{\circ} 25' 25.67''W$ ); (b) Mejia Bridge ( $0^{\circ}59'24''S$ ,  $80^{\circ}28'11''W$ ) (photos: COE-3).

### 2.4.2 Landslides and Rock Falls

The Ecuadorian Emergency Operations Committee (COE3) recorded hundreds of landslides and rock falls along the west coast of Ecuador. The GEER-ATC team was able to identify many of them in the west roads between Manta and Pedernales. It was observed that, in general, roads along the Ecuadorian coast do not have any type of slope reinforcement, and that, if needed, a protection wall is built to safeguard the roads. The only slope treatment is typically flattening, which explains why landslides was such a common type of failure. Typical observed landslides and rock falls are shown in Figure 2.6.

Several landslides occurred in the province of Manabi, but it is of interest to present the case of the macro-landslide events in the land owned by Mr. Gonzalo Loor and Dr. Cesar Navas. The macro-landslides were triggered by the main April 16th Mw7.8 earthquake due to increment in water pressures, reduced soil resistance and/or liquefaction.

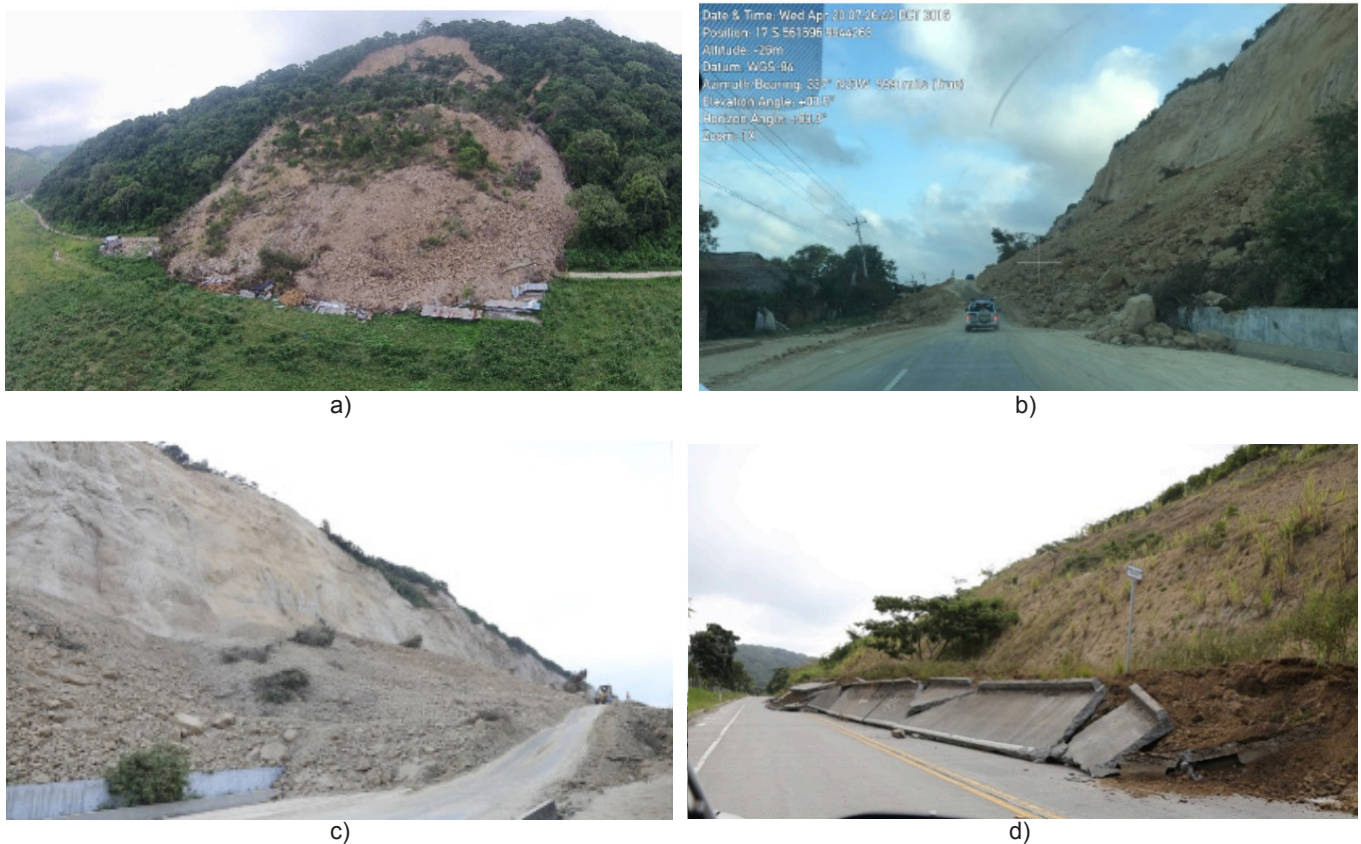


Figure 2-6. Typical landslides and rock falls in Ecuadorian west coast roads: (a)  $0^{\circ} 33' 5''S$ ,  $80^{\circ} 25' 42''W$ ; (b)  $0^{\circ}30'15''S$ ,  $80^{\circ}26'44''W$ ; (c)  $0^{\circ}30'15''S$ ,  $80^{\circ}26'44''W$ ; (d)  $0^{\circ}25'44''S$ ,  $80^{\circ}26'59''W$  (photos: COE-3).

The landslides did not coincide with known geologic faults in the area, and showed no evidence of the typical Angostura formation sands at the Navas' property; instead mudstone predominated at the surface after the landslides succession. The Loor site suffered from significant landslides, an approximate 29 Has (hectares) of the site suffered vertical and lateral displacement. The residents of the area observed that minutes before the main event, the water stored in tanks at the site was actively moving. Consistently, the records of IGPEN show that a Mw5.7 foreshock took place 11 minutes before the main event roughly at the same location.

The ground water was unusually high throughout this site, and could even be seen at the base of the slope due to intense precipitation the previous days. The landslide happened in a succession of three main events as illustrated in Figure 2-7.

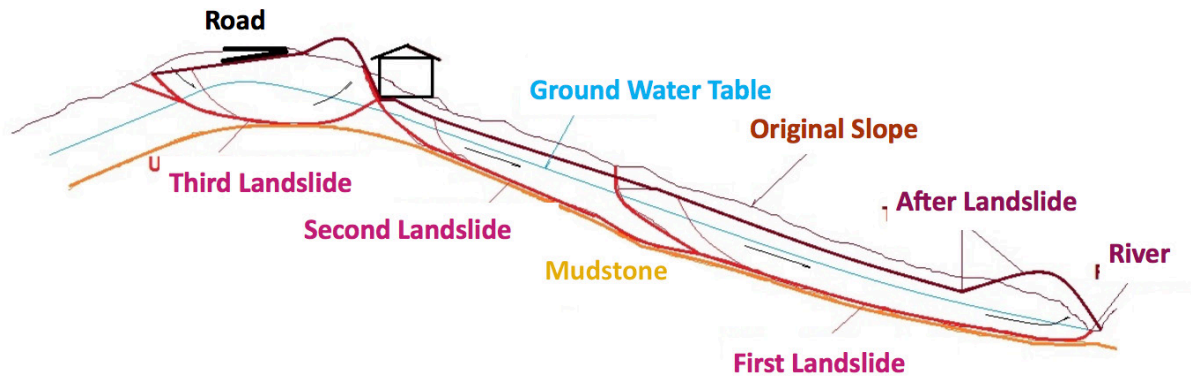


Figure 2-7. Scheme of succession of landslides at Loor Site (image: Ripalda 2016b).

The main event triggered a first landslide that affected the inferior zone of the slope, and possibly the middle zone as well. This first landslide seemed to be translational at the top and rotational at the base of the slope. The translational portion is evident due to lateral movement of soils, with standing trees that didn't lose their verticality. The rotational portion showed rotated and fallen trees, and earth lifting at the base stopping at the river. This first landslide left the upper portion, where the house and barn were located, without support, leading possibly to a second landslide almost instantly.

The second landslide was triggered seconds after the first one. Earth lifting at the west of the house, rotation of the house, and cracks through the house and barn were observed after the second landslide.

A third landslide took place in a rotational mechanism at the head of the slope.

Combination of photographs obtained by drones and the Google Earth survey prior to the landslides was performed to create a 3D model and sections of the area (Figures 7-8 – 7-11).

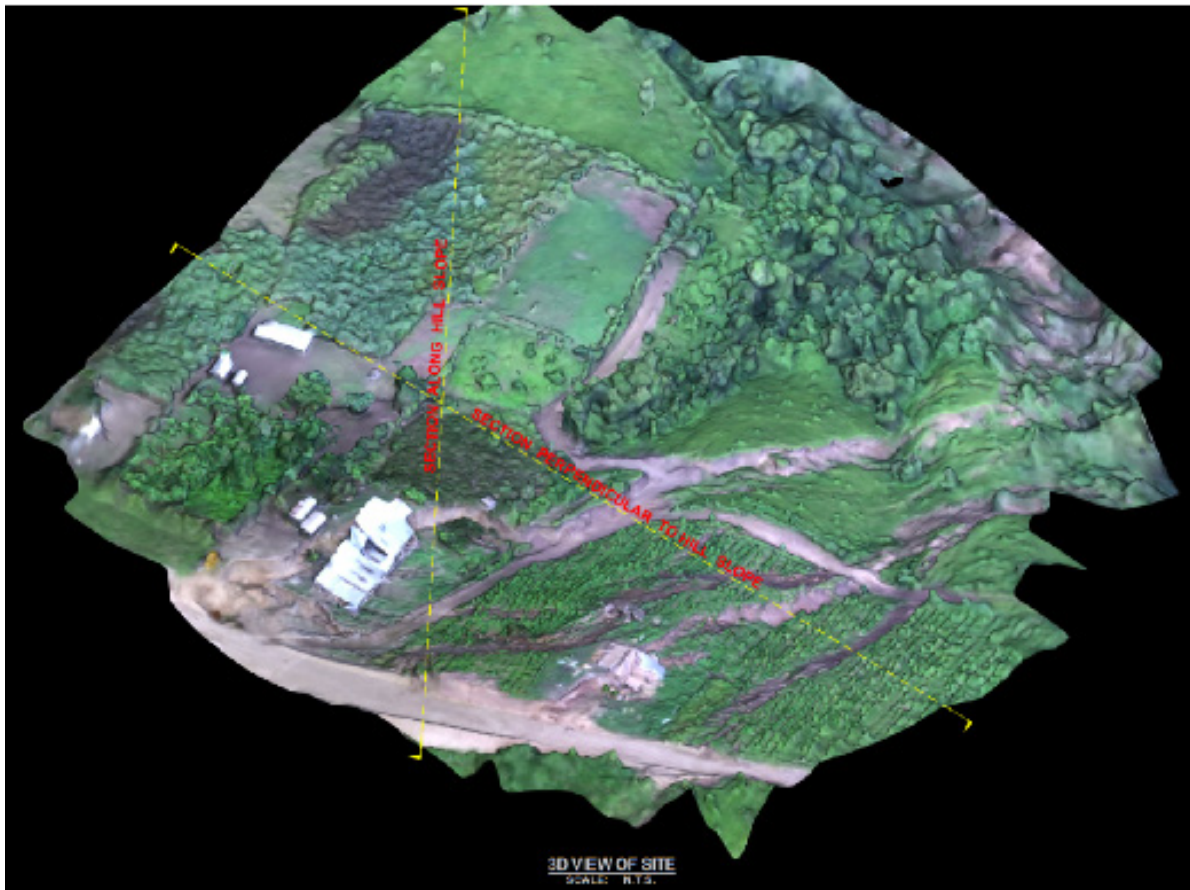


Figure 2-8. 3D view of Loor Site with sections from Figs. 15 and 16 defined.

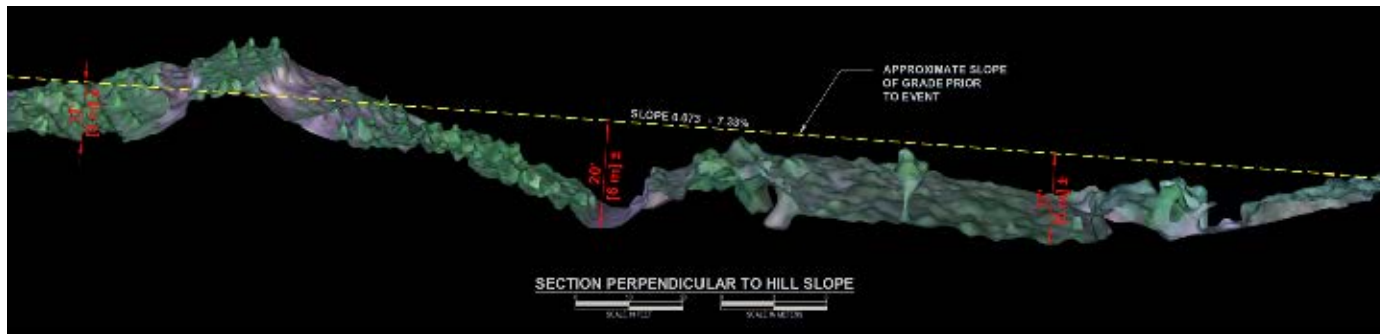


Figure 2-9. Section perpendicular to hill slope at Loor site.

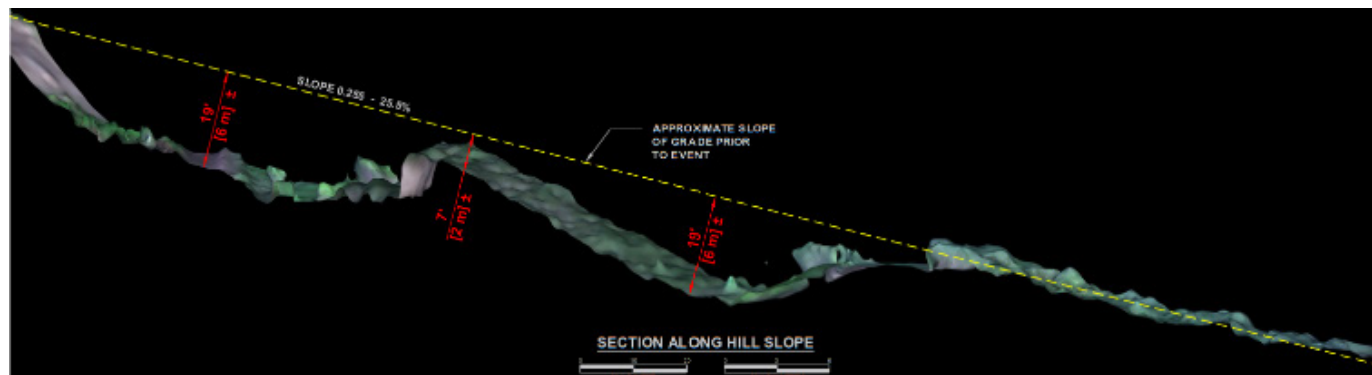


Figure 2-10. Section along hill slope at Loor site.

### 2.4.3 Liquefaction and Liquefaction Induced Effects:

For the liquefaction section, two sections will be covered: 1) a case study for the Manta Port covered by the GEER team during the reconnaissance mission, and 2) observations from EERI team in city of Calceta.

Manta is one of the five major ports of Ecuador. A Google Earth image of the port is provided in Figure 2-11. The port consists of a pile supported wharf, two pile supported piers, a rock-fill breakwater and an imported car storage area constructed by placing backfill material behind a rock berm. Liquefaction and liquefaction-induced distress was prominent at a number of locations at the port. In addition, damage and displacement of pile-supported structures occurred.

A Google Earth image of the import car storage area behind the rock berm is provided in Figure 2-11b. Liquefaction-induced lateral spreading towards the rock berm produced a number of cracks parallel to the rock berm along with ejecta. In addition, large sand boils erupting from a single point developed at several locations. The soil type of the ejecta ranged from sand to silt and samples were obtained for subsequent laboratory testing. Figure 2-12a shows one of the large soil boils that erupted primarily from a single vent in the pavement. Eyewitness accounts indicated that water sprayed out of the ground as high as a meter immediately following the event. In contrast, Figures 2-12b and 2-12c show sand ejecta that emanated from transverse cracks in the pavement as a result of lateral spreading.

Liquefaction and lateral spreading caused foundations for light poles to rotate and sink into the ground. Rotation was approximately  $2^\circ$  towards the rock berm and  $1.5^\circ$  towards the west. A boat ramp on the southeast side of the area (see Figures 2-12d and 2-12e) with 4 m high reinforced concrete retaining walls moved about 40 cm outward at the top of the wall as shown in Figure 2-12d. This led to significant vertical cracks in the walls on either side of the boat ramp. In addition, the floor slab at the base of the boat ramp heaved upwards and developed significant longitudinal cracks (see Figure 2-13e).

To document the lateral spreading displacements that occurred in this area, crack widths along five lines normal to the rock berm were measured. In addition, the distance to each crack was measured relative to the face of a concrete panel wall running roughly parallel to the top of the rock berm as shown in Figure 2-11b. Figure 2-13 provides plots of cumulative lateral displacement up to the wall, which is considered the zero reference point for each line. The average lateral spreading displacement was about 37 cm, with a range between 8 and 70 mm. Lateral displacement increased substantially within about 10 m of the wall as the edge of the rock berm slope was approached. Displacements were less than about 2 cm beyond 90 m behind the wall. The measured variation in the lateral spreading displacements could potentially be useful in evaluating the effect of subsurface stratigraphy and soil properties in lateral spreading displacement prediction models.

A significant vertical offset in the pavement was observed running roughly parallel to the wall at a distance of about 3.5 m landward from the wall (Line A-A in Figure 2-11b). Typically, the ground settled downward on the landward side relative to the seaward side. To quantify the variation in offset, offset measurements were made at 5 m intervals along the line. Figure 2-14 shows the offset plotted versus distance along the line. The maximum offsets was 50 cm and -14 cm with an average of 15 cm.

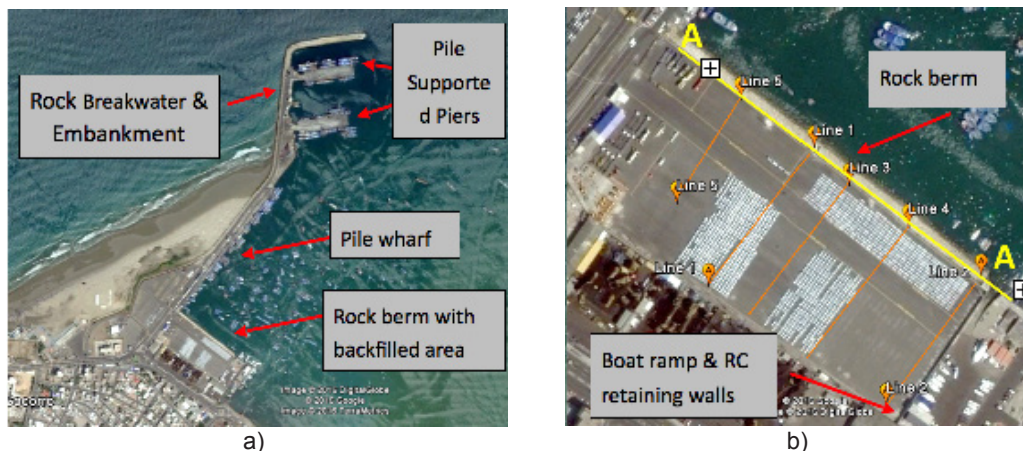
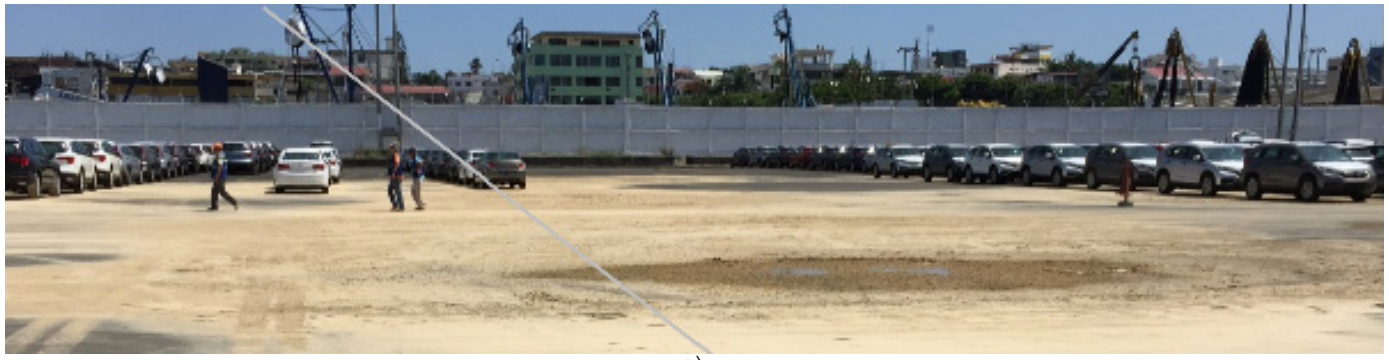


Figure 2-11. Aerial View of (a) Port at Manta (b) backfilled area behind rock berm used to store imported cars. Lines along which settlement and lateral displacement were measured are also shown (D. Globe ©2016).



a)



b)



c)



d)



e)

Figure 2-12. Photograph of (a) concentrated sand blow in the center of the pavement, (b & c) sand vents erupting from cracks in the pavement formed by lateral spreading (d) Lateral movement (40 cm) of 4 m tall retaining walls adjacent to boat ramp, and (d & e) heave and longitudinal cracking of base slab (GPS coordinates: (a) 0° 56' 27.61"S 80° 43' 29.36"W (b) 0° 56' 26.91"S 80° 43' 29.53"W (c) 0° 56' 29.45"S 80° 43' 27.77"W (d & e) 0° 56' 28.87"S, 80° 43' 26.78"W

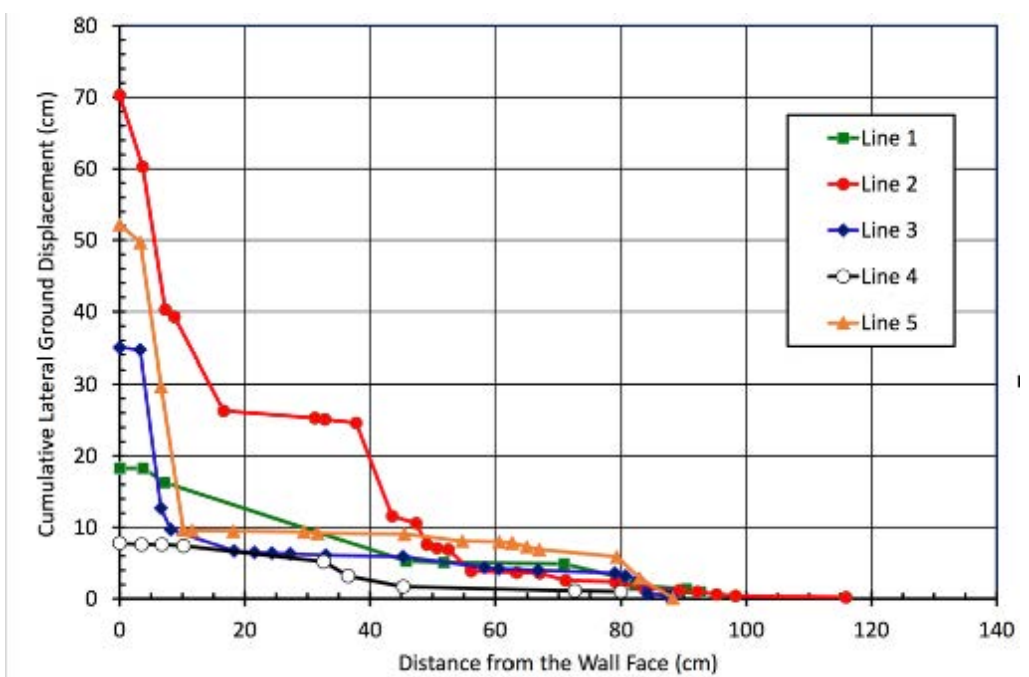


Figure 2-13. Cumulative lateral spread displacements measured along five lines perpendicular to the shoreline.

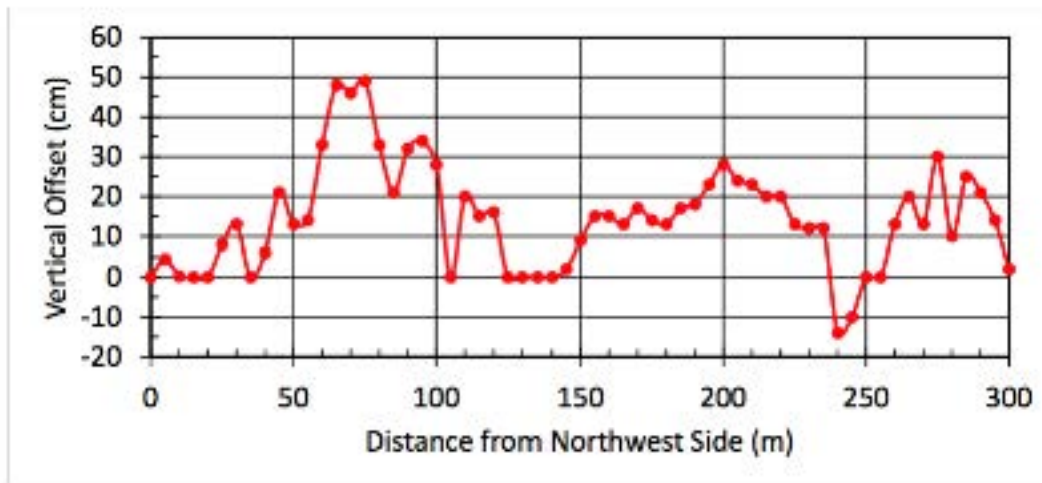


Figure 2-14. Vertical offset in concrete pavement produced by lateral spreading along line A-A at 5 m intervals. Line A-A is roughly parallel to the concrete wall at a distance of about 3.5 m from the wall face

Calceta is a town located between the cities of Portoviejo and Chone. The town is situated on the Rio Carrizal inland on the coastal plain. The observed ground damage described in the form of liquefaction and lateral spreading in this area was observed by the EERI team.

Half of a city block laterally displaced in the direction of the Rio Carrizal by 50 cm due to lateral spreading, as shown on Figure 2-15a. The buildings that are located on the section of block which moved experienced little structural damage. However, the buildings located on the section of block which didn't move, suffered more damage. In general, the area shown in red below experienced lateral spreading and moved toward the river by 50cm.

The column on Figure 2-15b laterally displaced 50 cm to the right, while the column on the left, which is part of the neighboring building remained relatively still.



Figure 2-15. (a) Area of lateral displacement (Image: Google Earth ©2016); (b) Lateral displacement of building.

Outside of the town of Calceta, the team visited the Coliseum Manuel Felix Lopes at the Escuela Superior Politecnica Agropecuaria de Manabi. The coliseum sites within is 40 m of tributary of the the Rio Carrizal. Both Lateral spreading and liquefaction were observed in and around the coliseum, as shown on Figures 2-16 and 2-17. Figure 16 shows damage on access road. Figures 2-17a and 2-17b illustrate laterally displacement of 25cm and vertical displacement of 24cm in coliseum due to lateral spreading and liquefaction in the soils under the foundation.



Figure 2-16. Lateral spreading along the roadway to the coliseum.



Figure 2-17. Lateral and vertical displacement inside of coliseum.

#### 2.4.4 Dams

After the seismic event of April 16, 2016, the Ministry of Urban Development and Housing (MIDUVI) in coordination with the Public Water Utility (EPA-EP), organized inspections of four dams in the area of Manabí and the northern section of Santa Elena. The inspection of these dams was not only necessary due to the seismic event but also due to heavy rains in the area on April 10th and 11th, 2016. The inspections were performed on April 26, 2016 by a group of geotechnical and hydraulic engineering experts. This section will only cover main observation for the Chone Dam. For additional information of dams performance refer to the GEER-ATC report: [http://www.geerassociation.org/component/geer\\_reports/?view=geerreports&id=77&layout=default](http://www.geerassociation.org/component/geer_reports/?view=geerreports&id=77&layout=default).

Chone Dam is a multipurpose dam currently under construction in the province of Manabí to be finished this year. The dam is a zoned embankment dam with a maximum height of 57.5 m and a total crest length of 276 m. At the dam embankment, no settlement or deformations were visible to the inspection teams. Leaks at the downstream face and spillway contact were not visible either. No significant damage was observed at the spillway, chute or stilling basin. Some cracking at the spillway training walls, counterfort and slab was visible as shown in Figure 18a, but it is unknown when these cracks occurred. Some, but not all of the cracks appear to have vegetation growth so the assumption is that they have been present for some time although this cannot be confirmed. There was some damage visible to the gate seal of the low flow outlet. Based on project personnel, the defect in the gate seal had occurred prior to the seismic event and a replacement was planned. Grout injections are also planned in the outlet tunnel to mitigate leakage. This work was also planned prior to the seismic event. The outlet tunnel which is 3 m in diameter was not dewatered or inspected. Slope instability at the cuts at the right and left abutment were visible at the time of the inspections. Based on discussions with project personnel, some instability had occurred due to the heavy rains a few days before the seismic event. Further instability may have occurred due to the earthquake. Slope instability is shown in Figures 2-18a and 2-18b.



a)



b)

Figure 2-18. a) Cracks in spillway slab, wall and counterfort, Chone Dam, Manabí, Ecuador, 2016 (GPS coordinates: 0° 42' 02.01" S, 79° 59' 25.89" W); (b) Slope instability at right abutment, above Chone Dam, Manabí, Ecuador, 2016 (GPS coordinates: 0° 42' 01.62" S, 79° 59' 10.85" W).

### 2.4.5 Earth Retaining Walls

Earth retaining wall behavior ranged from extremely poor to satisfactory throughout the west coast of Ecuador. The GEER-ATC team inspected 7 sites with earth retaining walls. It was observed that the most northern sites (closest to epicenter) showed minor to no damage in earth retaining walls (both cast-in-place), while the southern walls, except for Rio Chico Bridge, required extensive repair or even replacement because of structural or geotechnical failure. The typical damage observed in these soil-structure systems was vertical and lateral displacements, lateral soil movement at the toe of the abutment, cracks, and partial collapse or rotation of wall, as shown in Figure 2-19.



a)



b)



c)



d)

Figure 2-19. Typical damage observed (a) Damage to eastern abutment, wing wall, and gabions in Mejia Bridge (GPS coordinates: 0°59'22.73"S, 80°28'11.14"W); (b) Collapse of unreinforced stone masonry of Bahia wall (0°36'30.61"S, 80° 5'25.03"W); (c) Damage and partial collapse of the wall at the Manta Port (0°56'28.86"S, 80°43'26.69"W); (d) Wall at Velboni supermarket in Portoviejo (1°3'37.78"S, 80°27'29.27"W)

## 2.4.6 Performance of selected foundations

To highlight the performance of foundations, we present the study of the Port of Manta due to the varied performance of piles throughout the site. The port consists of a pile-supported wharf, two pile supported piers, a rock-fill breakwater and an imported car storage area constructed by placing backfill material behind a rock berm. The GEER-ATC team observed that:

1. The northern end pier was supported by multiple rows of 0.5 m x 0.5 m reinforced concrete piles. Most of the piles were not battered, but the ends of each row had battered piles to provide greater lateral restraint (Figure 2-20a). The piles supporting the two piers on the northern end of the port were relatively undamaged, with damage only consisting of cracking in shear beams used to attach an additional pile to the pile cap (Figure 2-20b), and some cracking and compression failure at the heads of battered and square piles at the northwest corner of the southern pier.



Figure 2-20. (a) Relatively undamaged rows of piles supporting the two piers on the northern end of the port and (b) shear cracking in shear beam attaching adjacent pile to pile cap (GPS coordinates: 0° 55' 58.2" S, 80° 43' 18.8" W)

2. The wharf is supported by alternated battered 0.4 m x 0.4 m reinforced concrete piles spaced at 3 m with 1H: 5V slope. The piles supporting the wharf running parallel to the shoreline experienced considerable damage (Figure 2-21). After the earthquake a crack with a vertical and horizontal offset developed at the west side of the pier relatively to the ground on the west side. The piles with a reverse batter exhibited considerable damage and offset at the pile head while piles with a forward batter did not. Port engineers indicated that many of the piles had been retrofitted to improve the strength of the pile-to-pile cap connection. Unfortunately, the retrofit was not generally successful and reinforcing bars pulled out or sheared off at the pile head. For a given lateral deflection towards the sea, the piles with a reverse batter, would be in tension while the piles with a forward batter would be expected to be in compression. It is likely that this difference in loading is associated with the observed damage pattern. There is no visible indication of cracking or lateral spreading in the gravel berm behind the piles, although liquefaction and lateral spreading may have occurred in the immediate vicinity of the piles.



Figure 2-21. Photos showing cracking and shearing of pile head connection for piles with backward batter in comparison with minimal damage to piles with a forward batter at two locations along the wharf. (a) GPS coordinates: 0° 56' 14.42" S 80° 43' 27.41" W (b) 0° 56' 14.22" S 80° 43' 27.32" W

3. A 3-story building that serves as operation offices located within the port's embankment between two of the piers, is supported by 0.4 m x 0.4 m reinforced concrete piles. The piles go through the slope of the embankment possibly to a firm soil layer beneath the foundation soils of the embankment. The embankment spread laterally towards the building, resulting in measured lateral displacement of 0.4 m as can be seen in Figure 2-22 (a) and (b). Figure 2-25 (a) and (c) show vertical settlement of 0.4 m relative to the pile-supported structure. Tilt measurements indicate that the piles were tilting at angles of 4 to 6° near the heads of the piles. The head of the piles experienced some damage at the concrete as can be seen in Figure 2-22.

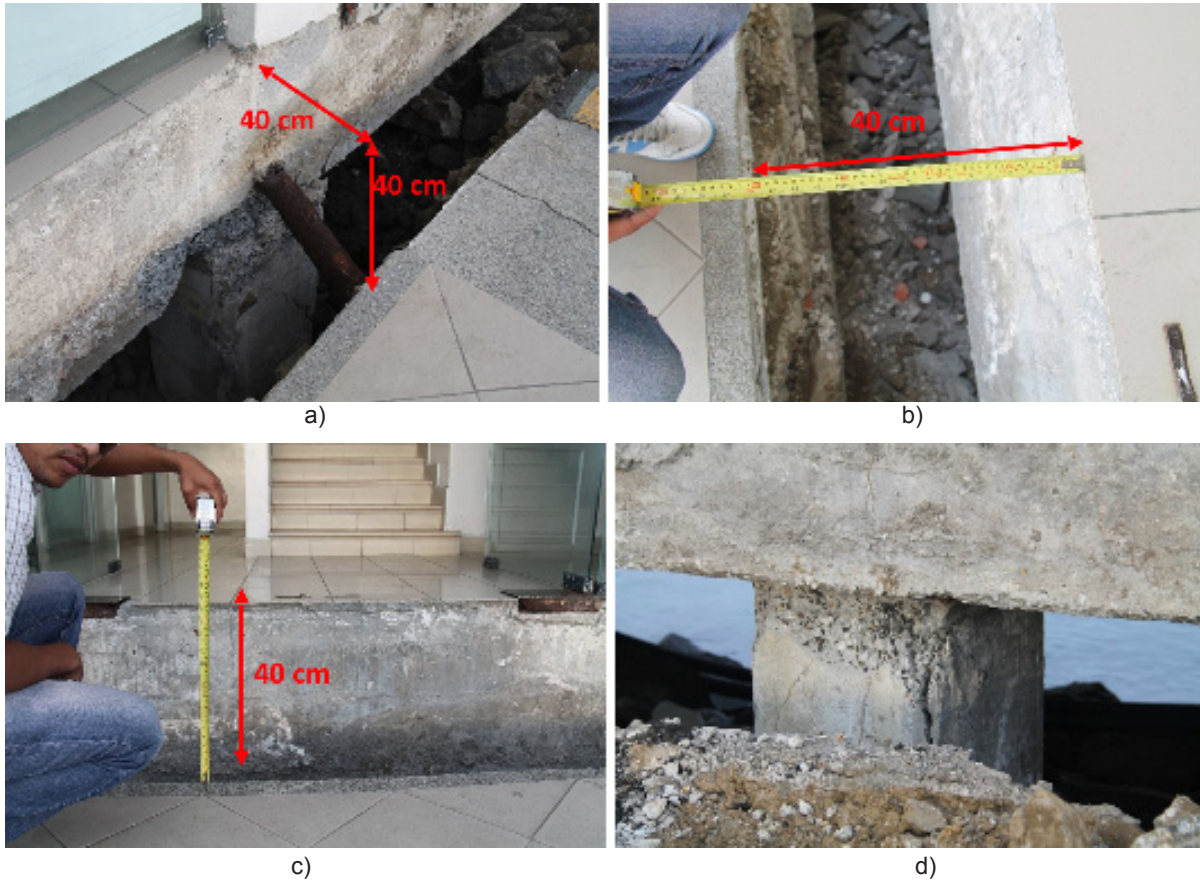


Figure 2-22. (a) Horizontal and vertical displacement of embankment relative to the building; (b) horizontal relative displacement between building and embankment; (c) vertical settlement of the embankment relative to the pile-supported building; (d) damage in the head of the building's pile (GPS coordinates: 0° 55' 55.2" S 80° 43' 19.56" W)

## NOTE

Further details on geotechnical and soil-structural observations, as well as other aspects of the GEER-ATC reconnaissance mission are provided in the GEER-ATC report: GEER-ATC report with link [http://www.geerassociation.org/component/geer\\_reports/?view=geerreports&id=77&layout=default](http://www.geerassociation.org/component/geer_reports/?view=geerreports&id=77&layout=default).

## 2.5 REFERENCES

- Ancheta, T.D., R.B. Darragh, J.P. Stewart, E. Seyhan, W.J. Silva, B.S.J. Chiou, K.E. Wooddell, R.W. Graves, A.R. Kottke, D.M. Boore, T. Kishida, and J.L. Donahue (2014). NGA-West2 database, *Earthquake Spectra* 30, 989-1005.
- Chlieh, M., Mothesb, A., Nocqueta, J.-M., Jarrinb, P., Charvisa, P., Cisnerosc, D., Fonta, Y., Collota, J.-Y., Villegas-Lanzad, J.-C., Rolandonee, F., Valléef, M., Regniera, M., Segoviab, M., Martina, X., and Yepes, H. (2014). "Distribution of discrete seismic asperities and aseismic slip along the Ecuadorian megathrust". *Earth and Planetary Science Letters* 400 (2014): 292-301.

- Geoestudios (2016). "Measurement of shear wave velocity in strong motion stations from Ecuador".
- GEER-ATC Report (GEER-049), Nikolaou, S., Vera-Grunauer, X., Gilsanz, R. eds., "2016 Ecuador GEER Report version 1". Published in [geerassociation.org](http://www.geerassociation.org): [http://www.geerassociation.org/component/geer\\_reports/?view=geerreports&id=77&layout=default](http://www.geerassociation.org/component/geer_reports/?view=geerreports&id=77&layout=default)
- Ripalda, O. (2016a). "Technical Report of the Inspection of Poza Honda, La Esperanza, Rio Grande (Chone) and San Vicente Dams".
- Ripalda, O. (2016b). "Technical Report Macro-Landside – Loor Site. San Isidro Area Report".
- Singaucho J. C., Laurendeau A., Viracucha C., Ruiz M. (2016). "Observations of the 16 April 2016 Mw 7.8 earthquake: Intensity and accelerations". To be published in the Polytechnic Journal.
- USGS (2016). "M7.8 - 29km SSE of Muisne, Ecuador". Access date: June 18th 2016. URL: <http://earthquake.usgs.gov/earthquakes/eventpage/us20005j32#general>
- USGS (2016). "M7.8 - 29km SSE of Muisne, Ecuador". Access date: June 18th 2016. URL.
- The CATDAT Damaging Earthquakes Database via: <http://earthquake-report.com/> Access date: June 18th 2016



## **CHAPTER 3**

# **BUILDING DAMAGE**

### **3.1 INTRODUCTION**

This Chapter reviews basic construction characteristics of midrise buildings in the coastal cities of Ecuador, particularly those that led to problems with earthquake performance, and reviews structural damage in three specific towns. One- to three-story dwellings are discussed separately in Chapter 5. Construction characteristics that are discussed below include poor alignment, frame details, corrosion of reinforcement, masonry workmanship, means of egress and joints within building complexes. There is a brief discussion of the steel structures observed by the team, and a more detailed discussion of general damage patterns in Manta and Portoviejo. There is also a short discussion contributed by the EEFIT team of damage in Pedernales.

### **3.2 CONSTRUCTION CHARACTERISTICS**

#### **3.2.1 Formwork Alignment and Overuse**

Midrise buildings in the coastal area affected by the Muisne earthquake are usually reinforced concrete, 5 to 12 stories high. The two structural systems mostly used are flat slabs on columns (no girders) and reinforced concrete frames. Housing typically uses a column-flat slab structure with infilled masonry walls; columns are very slender (wall thickness: 15cm or 20cm). Construction using steel frames is limited.

The heavy flat slab structures supported by reinforced concrete columns are older buildings (roughly built more than 15 years ago). Structural grid size is about 30 square meters with side dimensions between 4.50 to 6 meters, and seldom larger. There are no reinforced concrete walls to take the lateral forces. All lateral force demands, elastic and inelastic were taken by small-section columns. The columns were typically about 45 to 50 cm square and lacked adequate confinement. This led to severe structural damage and collapses in many cases. In some instances, unreinforced masonry partitions and facades unintendedly took the lateral forces barely preventing total collapse.

More recent buildings are reinforced concrete column-girder frames having about the same grid size. The columns were about 45 to 50 cm square and girders were around 30 cm x 60 cm. Shear walls to stiffen and strengthen the frames are not typically used in the region visited by the team. The RC frames generally lack many of the reinforcement detailing needed to develop a good inelastic performance during strong shaking, hence, slight to moderate structural damage was observed frequently.

The typical building has interior partitions and facades made of unreinforced masonry. Since the frame structures are rather flexible and the partitions were stiff and weak, this led to extensive interior damage. Section 3.3 addresses the issue of poor performance of partitions and facades.

Lack of attention to several important seismic details was an important source of damage, including captive columns (short columns), missing confining reinforcement in columns and column-girder joints, and inadequate stirrups as illustrated in Figure 3-1.

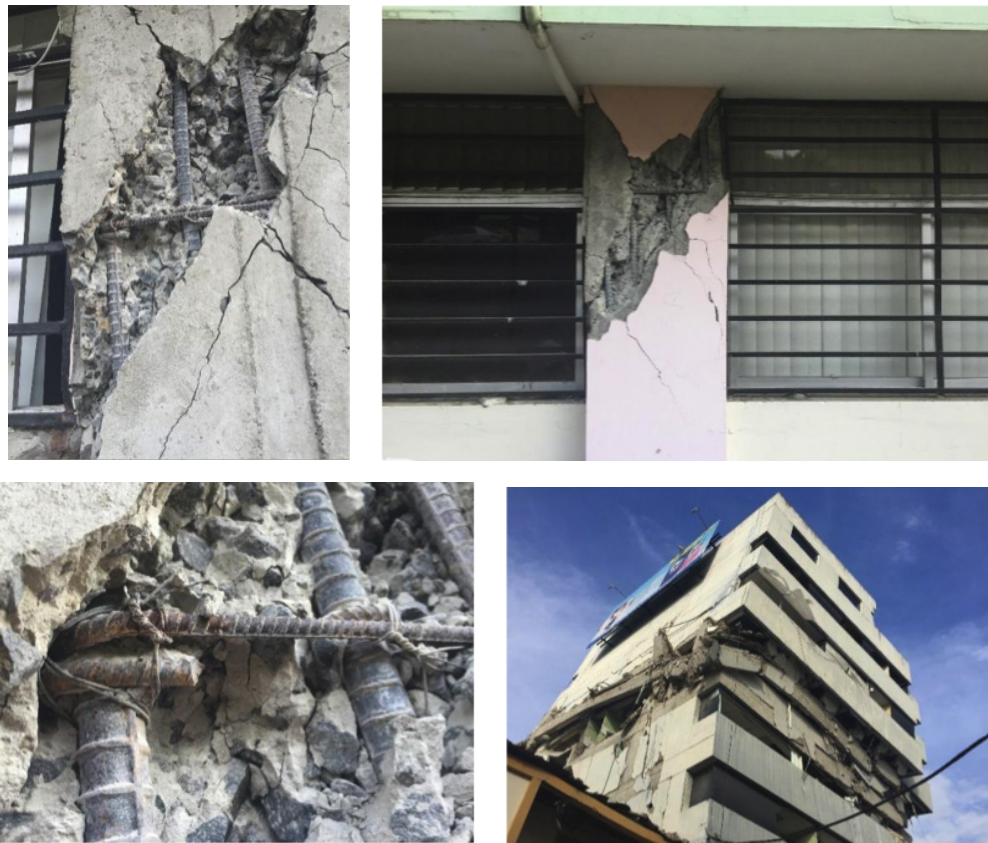


*Figure 3-1. Top left: Short exterior column of the Applied Sciences Faculty Building of Portoviejo's National University; damage caused by partial height masonry walls on adjacent sides of the column. Top right: Enlarged view of the column damage, showing large tie spacing and poor concrete quality. Bottom left: Seismic hooks on confinement hoops are nonexistent in most frame columns. Bottom right: Inadequate transverse confinement reinforcement may have been a contributing factor for the collapse of this mid-rise building in Portoviejo.*

### **3.2.2 Formwork Workmanship and Alignment**

Buildings such as the Hospital Napoleón Dávila Cordova in Chone and Miguel Hilario Alcívar Hospital in Bahía showed problems caused by poor formwork workmanship and low quality of the forms. Multiple examples of out-of-plumb columns and uneven beams caused random concrete cover. In several buildings, the team observed concrete column plan shape transition with no corresponding rebar transition, which led to excessive concrete cover. There were frequent instances of nearly exposed reinforcement at one end of the element and thick spalled covers at the opposite end indicating that the reinforcement cage itself was out-of-plumb. (Figure 3-2). Rough uneven surfaces indicated overuse of untreated formwork wood, thus, contributing to the rapid deterioration of the molds. This, in turn, contributed to irregular sections and misaligned shapes of reinforced concrete elements.

Out-of-plumb surfaces and irregular sections require thick plaster finishes to recover verticality and surface alignment. Spalling of such finishes during the earthquake resulted in a significant amount of debris falling with consequent hazards during the earthquake and significant collateral damage.



Figure 3-2. Left: Thick mortar finish for vertical alignments. Thickness of this mortar reached up to 6 cm. Right: Debris caused by unbraced infill walls to the main structure.

### 3.2.3 Corrosion of Reinforcement

In the coastal area of the country, there is a widespread reinforcement corrosion problem. Spalling of concrete cover during the earthquake exposed corroded reinforcement in both older and newer buildings. See Figure 3-3. Many factors seem to promote corrosion:

- Irregular and random thickness of concrete cover (addressed in the Formwork Alignment and Overuse section); often, reinforcement turns out to be too close to the surface.
- A corrosive environment especially near the ocean.
- Inadequate or nonexistent protective concrete cover of the reinforcement in locations with direct exposure to sea breeze. See Figures 3-4 and 3-5.
- Segregated and porous concrete as noted by local engineers. Builders often choose to use hand-mixed concrete because: a) mixers don't supply concrete in small volumes and b) it is less expensive than ready-mixed concrete. Use of mechanical vibrators to compact concrete is not a general practice. While newer buildings are much better off in this aspect, older structures and smaller structures tend to have lower concrete quality.
- Beach sand is often used without any treatment to reduce chloride contents.
- The team was not able to determine whether corrosion-resistant cement is used in these aggressive environments.



Figure 3-3. Spalling of concrete cover and longitudinal reinforcement buckling was found in frames of small residential structures, typically in beam-column joints and at the base of columns.



Figure 3-4. Left: Corrosion in rebar due to exposed reinforcement in Bahía de Caráquez. The structure is located near the bay's shore. Right: An abandoned mid-rise building in Bahía shows a column with little concrete cover, which is typical and enables and accelerates corrosion.



Figure 3-5. Left: Corrosion of reinforcement in a column at Portoviejo's National University. Right: One story structures are typically constructed with the intention to build a second floor in the future. Second-floor columns are built with the first slab. Rebar dowels are not protected from the environment and are prone to corrosion.

### 3.2.4 Construction Joints

Several mid-sized buildings in the affected area were composed of smaller, independent structures; in some of these cases, the effective clear space between adjoining structures was insufficient. For instance, in the case of the Hospital of Chone, the gap between some adjoining structures was 5 cm, which in turn became a serious liability because of toppling partitions, ripping apart ducts and conduits and obstructing paths. Figure 3-6 (right) illustrates this problem.

Exterior stair towers that are structurally independent from the area that they serve were particularly affected. See Figures 3-6 and 3-7.



Figure 3-6. Left: Hospital in Chone. Consequences of pounding between structural units, Main building at background pounded against two-story unit seen in middle ground. Right: Hospital in Chone. Severely damaged interface along narrow joint due to impact between structural units



Figure 3-7. Main Judiciary Building in Portoviejo. Minor structural unit wedged between two larger units. The 5 cm gaps were too narrow during the seismic event. All three units underwent severe interior damage. The consequences of pounding are apparent in the glazing. A heavy ledge on the small unit collapsed.



Figure 3-8. Steel stadium from the National University at Calceta. Liquefaction and lateral spreading of soil caused adjacent segments of the structure to drift differentially and away from each other. Damage in the structure was found only in the masonry infill walls (photos: Forrest Lanning).

### 3.2.5 Steel Structures

Steel was found primarily in non-building structures such as bridges, industrial structures, ports, and major electrical transmission lines. There are a few buildings made with steel, such as the 911 office in Portoviejo, but these buildings are small in number compared to reinforced concrete buildings.

Because of the small quantity of steel structures, the team was able to observe the performance of only a few of these structures. No cases of collapsed or heavily damaged steel buildings were observed.

Two steel buildings were evaluated: the ECU911 in Portoviejo and the steel coliseum in Calceta, which belongs to the National University. The latter structure showed minor structural damage, primarily due to soil liquefaction. The structure was comprised of several structural segments and, in one instance, two adjacent segments moved approximately 27 cm from each other. However, it should be noted that no critical damage was found in the steel structure. The masonry partitions were the only elements that showed substantial damage, and these elements are not part of the main structure. See Figure 3-8. The coliseum, however, was not completely made of steel. The building had piers made of concrete and the structure supporting the roof was made of steel members.

#### ECU911 Centre

No damage was found in the steel structure. Some partition walls served unintentionally as a lateral load resisting system and showed shear cracks. The metal deck had signs of corrosion.

The connection in the steel moment resisting frames and the beam-column joints consisted of beams field-welded all around with the column. In the exterior elements, the frames are covered with concrete. See Figure 3-9.



Figure 3-9. Damage in Portoviejo's 911 Centre was minor and primarily in nonstructural elements. After the earthquake, repairs began in the partition walls and the steel cladding, which is made of cement plaster (photos: Forrest Lanning).

## 3.3 BUILDING INTERIOR PARTITIONS AND CLADDING

The seismic performance of masonry interior partitions and masonry cladding of frame buildings was not satisfactory in many of the affected buildings in the cities and towns located in the area affected by the April 16 earthquake in Ecuador. This section describes the construction characteristics of these elements as observed in the region and briefly summarizes their seismic performance.

Most of these buildings were apartments, but there were hotels in some areas as well as office buildings and public buildings, including hospitals. The observed performance problems were quite uniform in all buildings independent of use or construction date.

### 3.3.1 Partition and Cladding Materials

It was common for buildings in the region to have masonry façade elements. Some non-bearing panels and infills were full height, while others were low or high window sills. Lighter cladding panels made of a more lightweight material were not seen and only occasional instances of full-height glass façades were observed.

The other common feature found in buildings in the region was the extensive use of non-load bearing masonry interior partitions. Typical partition height was from the floor to the upper slab or girder, but instances of masonry partitions that only extended from the floor to the hanging ceiling without lateral bracing at the top of the wall were also observed. The wall panels are typically placed between main frame columns and are generally lacking adequate anchorage, or sufficient seismic separation, to the main structure. Vertical reinforcement within the masonry units was not observed. Horizontal small gauge reinforcement is sometimes placed in bed joints to connect masonry walls to columns of the main structural system; however this reinforcement is usually in form of dowels and does not provide any additional reinforcement against in-plane shear. All masonry partitions and cladding the team observed were practically unreinforced. Gypsum board partitions with metal or timber studs were seldom seen, not even in hospitals or office spaces.

Two common types of masonry units were used in the masonry interior partitions. One type is cement-sand block; standard 20 cm x 40 cm configuration, either 15 or 20 cm thick. The other very common type is clay brick, either artisanal hand-compacted solid units (about 10 cm x 30 cm, usually some 15 cm thick) or somewhat larger extruded hollow tile units (horizontal cells and very thin walled shells about 1/4"). Sand-cement mortar is used.



Figure 3-10. Typical brick masonry partition (photo: Hector Monzón).

### 3.3.2 Structure-Partition Interaction

The in-plane partition stiffness was inferred by the team to be much higher than the frame stiffness given structural geometry and material properties. Out-of-plane overturning of partitions was a commonly observed failure mode as the anchoring of partitions to the structure was inadequate. During the April 16 earthquake, it was commonly observed that facades plummeted to the ground along the building perimeter, and interior partitions collapsed onto interior floor space blocking ingress and egress for the damaged buildings. See Figure 3-11 and Figure 3-12.

In general, the upper stories had considerably less partition damage than lower ones, and this observation suggests smaller interstory drift demands in the upper stories relative to the lower ones.

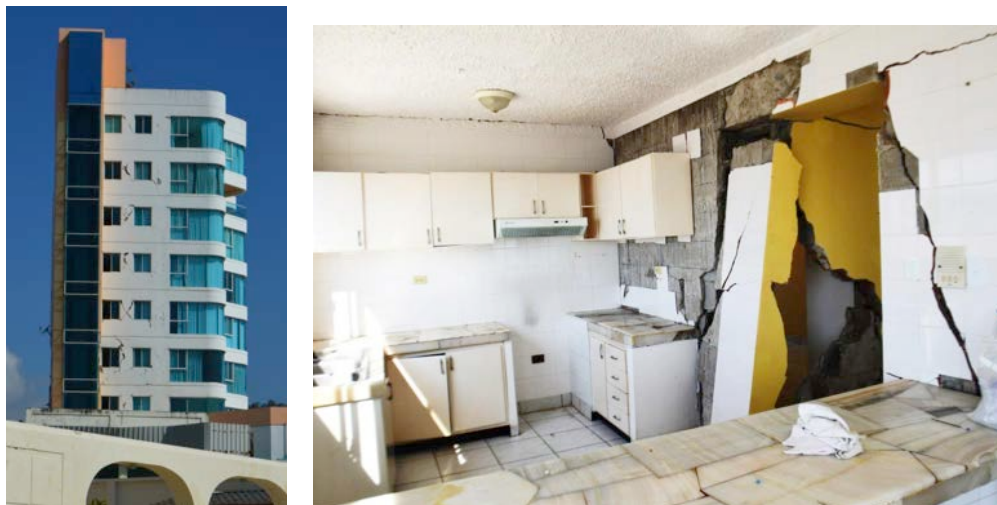


Figure 3-11. While the building exterior appears undamaged, there was heavy interior partition damage and some facade damage (photo: Hector Monzón).



Figure 3-12. (Left) Partition and hanging ceiling collapsed on an unoccupied bed in a Hospital in Chone; (Right) Unreinforced partition collapse and facade panel on hospital records in Bahia de Caraquez Hospital (photo: Hector Monzón).

### 3.3.3 Consequences of Poorly Detailed Partitions and Façades

Several lessons can be drawn from this earthquake for the use of masonry partitions and façades in multistory buildings. There should be greater compatibility in the in-plane stiffness of the frame structure that contains the masonry elements and the infills and partitions, unless the masonry elements are effectively isolated from the frame to prevent loading under seismic excitation. Details are needed that provide maximum out-of-plane restraint. Additionally, if the masonry panels are to be isolated from in-plane seismic demands, then the details should minimize in-plane resistance.

The use of panels comprising gypsum board with backup metal or timber studs can be incorporated into systems that tolerate seismic drifts while minimizing damage. However, caution must be exercised with the elimination of masonry infill panels in existing buildings, either as cladding or partitions. The resulting frames will be considerably more flexible than those with the masonry elements, and they may prove to be drift-critical. The elimination of masonry infills should only be done following detailed dynamic analysis of the building to ascertain adequate drift performance. Additionally, masonry infills that survive an earthquake are able to provide an alternate load path for building weight if the vertical load capacity of the frame is undermined. Thus, removal of infills is recommended only for ductile frame buildings. It is apparent that a first effective step is to design stiffer structures.

### 3.3.4 Masonry Workmanship

Wall workmanship was observed to be of poor quality. The faces of brick walls are very uneven and sometimes different types of units are used in the same panel. As a result, the final verticality and evenness of the wall panel is achieved with a plaster finish. Plaster thicknesses can vary widely, sometimes up to 5 cm on longer walls. Such thick finishes tend to spall during earthquake shaking, resulting in a large amount of debris. The extruded clay units tend to spall off because of their thin shells. Cement block panels tend to split in halves during the shaking, with one entire face of the panels spalling out

In summary, the anchorage technique for masonry walls could be improved. Consideration should be given to the main structure drift and its interaction with the infill panels. See Figures 3-13, 3-14, and 3-15.



Figure 3-13. Left: Typical interior masonry wall in the Justice Building in Portoviejo. Use of unreinforced masonry is a normal practice. Right: School building in Bahía de Caraquez. Two-story buildings made of small concrete frames with masonry infill with extensive damage.



Figure 3-14. Left: Public school building in Bahía de Caraquez, showing visible damage in infill walls. Right: Masonry infill in a private, mid-rise residential building in Bahía. There are two types of masonry materials: the older masonry is fired-clay masonry, the 1998 earthquake partially destroyed the panel. Concrete masonry was added to repair the partition, no reinforcement was added in the repair.



Figure 3-15. Left: Apartment building in Bahía. Unreinforced and poorly anchored masonry facade panels collapsed or cracked. Right: Inadequately anchored masonry panels collapsed on an ambulance parking canopy roof (photo: Hector Monzón).

### 3.2.5 Means of Egress

In several buildings, minimally reinforced stair shafts were completely destroyed during the earthquake, obstructing the exit path; in some cases, the staircase itself collapsed because it was supported on the brittle shaft. In less serious, but still dangerous situations, stair-shaft interior finishes, such as tiles or thick mortar layers, spalled off and obstructed means of egress. A more extended use of reinforced concrete wall shafts, integral with the column-girder frame, seems desirable to increase overall seismic performance and reliability. See Figure 3-16.



Figure 3-16. Left: Public building in Portoviejo. Staircase enclosure walls collapsed due to inadequate reinforcement in a frame building without structural damage. These were the only exit stairs. Fortunately, no injury was caused because the earthquake took place on a Saturday evening. Right: Oncology Unit Portoviejo: The corridor leading to the only exit stairs and elevators. Brick debris was ground from the top of unreinforced, unbraced masonry partition. The debris is mixed with large non-tempered glass shards from a large window (not seen) at right.

## 3.4 MANTA

The coastal city of Manta is the fifth most populous city in Ecuador (population 221,000) and was severely affected by the earthquake on April 16, 2016. The most affected area within the city was the Tarqui district, which was visited by the EERI team on May 9, 2016. The following sections detail the damages observed of a bridge along November 4th Avenue, the neighborhood of the Manta Clinic, the Hospital “IESS” in Manta, and the Port of Manta.

Even though Manta is located more than 100 km away from the epicenter of the earthquake, it recorded one of the highest peak ground accelerations (PGA) of about 0.52g. According to the Minister of Housing, also called MIDUVI, out of a total building stock of 82,922, 716 buildings were destroyed, whereas 5,675 buildings were damaged. This translates to 26,163 residents being affected in Manta alone.

As compared to structural damages observed in Portoviejo, the team observed more structures with story collapses in Manta. However, it is unclear whether the soft-story mechanism was more prevalent in Manta, because at the time of visit, cleanup in Portoviejo was further along than in Manta.

### 3.4.1 Tarqui District

The Tarqui district, located along the coast, was denoted the “Ground Zero” of Manta due to its severe damage. During the reconnaissance, some parts were still restricted for safety reasons, and the EERI team observed a deserted area of this typically lively district.

The damage observed in Tarqui buildings varied from non-structural damage to complete collapse. Some of the buildings still standing were shored with sections of bamboo (See Figure 3-17), a material readily available in this part of Ecuador. Although this type of temporary shoring could work as an immediate measure to protect the buildings, it is not clear how long the bamboo will hold—its performance in aftershocks and over time remains unknown. There were also several buildings with long cantilevers on the front elevations, making them more susceptible to vertical accelerations in ground shaking.



Figure 3-17. Temporary shoring of buildings using sections of bamboo (photos: Adrian Tola and Mei Kuen Liu).

While some buildings in Tarqui were standing at the time of the team visit, they were structurally unstable. Figure 3-18a shows the La Barca Restaurant building complex, where one of its two buildings was leaning toward the right; the building had not collapsed, possibly because of the unintended support provided by the adjacent two-story building. The concrete exposed at the bottom of one of the building columns (Figure 3-18a) revealed poor construction quality; cohesion of the existing concrete was very weak, as it was possible to pick away pieces of it using fingers. Confinement ties in the column were spaced much farther than recommended and only had 90-degree hooks, as opposed to the 135-degree hooks recommended for construction in seismic regions.

Figure 3-18b shows the Las Gaviotas Hotel building. Many of the concrete columns failed, possibly due to “short column” behavior, in which partial height masonry walls were constructed immediately adjacent to concrete columns, in

essence reducing the buckling length and inducing an unintended large amount of shear force in the column, causing shear failure. Lap splices of longitudinal rebar in these columns were placed at the same elevation, whereas the current recommendation is to have the splice location staggered to avoid a weakened plane in the column section. It was peculiar that the upper longitudinal rebars terminated in 180-degree hooks (see right part of Figure 3-18b), which may suggest that the splices may not have had enough development length. It is worth noting that smooth (un-deformed) rebar was used for both longitudinal and confinement reinforcement at the failed columns in this building; this fact might have corresponded to the materials and applicable regulatory codes available at the time of construction.



a) La Barca Restaurant



b) Las Gaviotas Hotel

Figure 3-18. Damage observed in the District of Tarqui (photos: Adrian Tola and Mei Kuen Liu).

The hotel Vista Alegre, which is located in the same block as La Barca Restaurant and Las Gaviotas Hotel, is shown in Figure 3-19. There was severe damage to the unreinforced masonry façade. See the masonry infill section of this report for further discussion on this topic. Also, from Figure 3-19, it is apparent that masonry debris from upper floors poses a falling hazard and could easily cause injuries to pedestrians. It should be noted again that this section of Tarqui had been evacuated and limited access was granted to few.

The EERI team observed other buildings with severe damage in Tarqui, and two of them are presented in Figure 3-20. The figure shows before and after photos of these buildings (the before photos coming from Google Street View [“Manta, Ecuador” 2015a, b]) contrasting the damage of these buildings and their surrounding areas 23 days after the earthquake.

The left side of Figure 3-20a shows the Centro Comercial Navarrete four-story building, while the right side shows the debris from the collapsed building—all that remained 23 days after the earthquake. Ninety-one people lost their lives in this building, according to the local newspaper. The collapse of this building alone accounted for approximately one-third of deaths in Manta from the April 16 earthquake.

Figure 3-20b shows the Pacifico Hotel building (white-blue) leaning toward the Las Rocas Hotel (yellow) due to a probable soft-story mechanism in one of the upper floors of the Pacifico Hotel.



Figure 3-19. Hotel Vista Alegre (photos: Adrian Tola and Mei Kuen Liu).



a) Centro Comercial Navarrete



b) Hotel Pacifico

Figure 3-20. Some of the buildings with severe damage observed in the District of Tarqui in Manta before (left) and 23 days after (right) the earthquake (photos: Adrian Tola and Mei Kuen Liu).

### 3.4.2 Damage observed in other locations in Manta

The following two buildings and one bridge were observed near the intersection of 2nd Street and 11th Avenue.

Figure 3-21b shows a building that collapsed due to a soft-story mechanism, while Figure 3-21a shows the same building before the earthquake, obtained from Google Street View. Soft-story mechanism failures were relatively common in areas affected by the earthquake throughout the country, due to a typically taller ground floor story height and fenestration.

Figure 3-22 shows the Hotel Lun Fun, which is adjacent to the building shown in Figure 3-21. It suffered severe damage in the base of the columns, as shown in the figure below.



a) Before the earthquake



b) After the earthquake

Figure 3-21. Soft-story mechanism in a building at 11th Avenue and 2nd Street (photos: Adrian Tola and Mei Kuen Liu).



Figure 3-22. Hotel Lun Fun (photos: Adrian Tola and Mei Kuen Liu).

A bridge along the November 4th Avenue is shown in Figure 3-23. The earthquake displaced the concrete box girder relative to its pier and toward the two shear keys located at the end of each bridge support. The shear keys were cracked or pushed to the ground due to the strong lateral force induced from the box girder. The shear keys that were damaged during the earthquake were already undergoing reconstruction at the time of the EERI team visit.

Another building observed was the seven-story Clinica Manta building, located near the intersection of November 4th Avenue and J-12th Street. This building was used for medical care, and as shown in Figure 3-24, it had several contributing factors to the building's apparent instability. The building experienced damage in the façade (Figure 3-24a and c), as well as structural damage due to short-column mechanisms as explained earlier in this section (Figure 3-24b). Concrete spalled off several joints, revealing no joint confinement reinforcement (Figure 3-24c). There was also severe cracking in interior columns at the ground level (Figure 3-24d).

Damage was also observed in a building adjacent to the Clinica Manta. As shown in Figure 3-25, this four-story building was reduced to a small pile of debris (before photo from Google Street View). Suspended floor slabs were visible, as seen in Figure 3-25b. The pile of debris appeared small for a four-story building. It was not clear whether any debris had been taken away but the team did observe local youth playing in and with the debris.



Figure 3-23. Bridge along November 4th Avenue (photos: Adrian Tola and Mei Kuen Liu).



a) Manta Clinic and adjacent building



b) Short column mechanism



c) Compromised joint without joint confinement reinforcement



d) Cracks in 1st floor column with short column mechanism

Figure 3-24. Clinica Manta (photos: Adrian Tola and Mei Kuen Liu).



a) Before the earthquake



b) Twenty-three days after the earthquake

Figure 3-25. Building adjacent to the Clinica Manta (photos: Adrian Tola and Mei Kuen Liu).

### 3.4.3 Hospital IESS of Manta

This hospital suffered major non-structural damage during the April 16 earthquake. The hospital building's medical and mechanical systems were relocated on the campus. Most of the damage observed was in the form of partial or complete collapse of unreinforced masonry walls. This occurred in the perimeter as well as in interior walls. Damage was also evident by the collapse of large portions of the mechanical distribution system (ducts) that used to hang from the slab of the floor above. The hospital damage is discussed in more detail in a separate section of this report.

### 3.4.4 Port of Manta

The port of Manta is one of the most important commercial facilities in the city as so much of its economic activity depends on it. Figure 3-26a shows the location of the port with respect to the city of Manta. The port consists of a long circulation line for vehicles and for loading/unloading of small ships, as well as two perpendicular modules (Module 1 and 2 in Figure 3-26b) that are dedicated to the loading/unloading of cargo from big ships.



Figure 3-26. Location of the port with respect to Manta (photos: Adrian Tola and Mei Kuen Liu).

Long cracks were visible, parallel to the circulation line. There was also a change of vertical elevation on both sides of the cracks (See Figure 3-27a), which measured approximately 45 cm at certain points. Moving toward Modules 1 and 2, there were more cracks parallel to the circulation line (See Figure 3-27b), suggesting that this cracking might have occurred due to lateral spreading of the soil under the port. Toward the end of the pier, a metal fence was partially suspended in the air, evidence that substantial differential ground settlement occurred (see Figure 3-27f).

Access from the circulation line to Module 1 was under reconstruction at the time of the team visit (see Figure 3-27c). One of the engineers in charge of the reconstruction informed the EERI team that the access to Module 1 collapsed during the earthquake, most likely due to an undesired rigid connection between Module 1 and the circulation line. Module 2 was operating, but the maximum allowed loads on the module have been lowered because of damage observed in the piles under it.



a) Long cracks parallel to circulation line



b) Long cracks parallel to circulation line



c) Re-construction of access to Module 1



d) View of Module 2



e) Damaged piles under modules



f) Metal fence detached from slab, suggesting ground settlement

Figure 3-27. Damage observed in the Port of Manta (photos: Adrian Tola and Mei Kuen Liu).

## 3.5 PORTOVIEJO

On May 10, 2016, the reconnaissance activities continued in Portoviejo (population 250,000), capital of the Manabí province. The city is one of the oldest cities in Ecuador, founded in 1535. This large city is located 19 miles from the Pacific coast and 105 miles from the epicenter of the 7.8M earthquake that occurred on April 16, 2016. Overall, the damage was concentrated in the historical and commercial center of the city, identified as Ground Zero-Portoviejo, where RC frame buildings with unreinforced masonry infills were predominantly affected. This type of construction is the most common in Ecuador. Figure 3-28 shows that out of 2,365 buildings inspected in this area by the Secretariat for Risk Management of Ecuador where more than 60% are RC frame buildings. Figure 3-28 also displays information about the total number of buildings tagged with unsafe (634), restricted use (757), and safe (974) placards, based on an adapted version of the ATC-20-1 Field Manual: postearthquake safety evaluation of buildings.

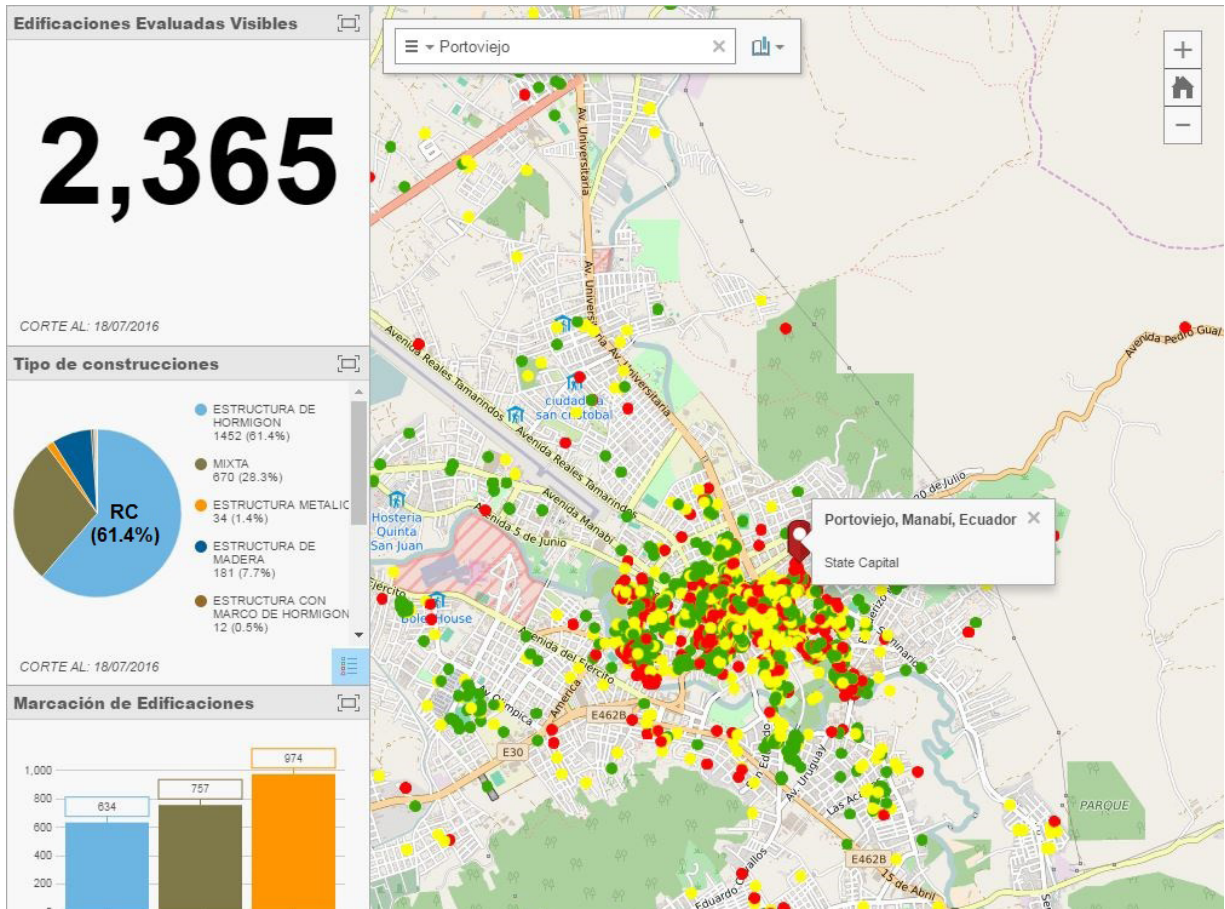


Figure 3-28. Buildings inspected by the Secretariat for Risk Management of Ecuador.  
Source: <http://gestionriesgosec.maps.arcgis.com/>

The peak ground accelerations recorded at the APO1 Station in Portoviejo were 3.12, 3.73, and 1.02 m/s<sup>2</sup> for the EW, NS, and UP directions, respectively (Singaucho J. C., 2016). The maximum peak ground acceleration was recorded for the NS component and was close to 0.4g. See Figure 3-29.

The EERI reconnaissance team was able to access the Ground-Zero zone controlled by the Ecuadorian Army Forces, and rapid visual observations of the exterior and interior of select buildings were conducted. In general, the team noticed that the RC frame buildings were extremely flexible to withstand the lateral displacements induced by the earthquake since small cross sections are used in columns and beams. In addition, the team observed that the debris of many low-rise collapsed buildings had already been cleared, and further demolition and debris clearance was in progress during the team visit. See Figure 3-30.

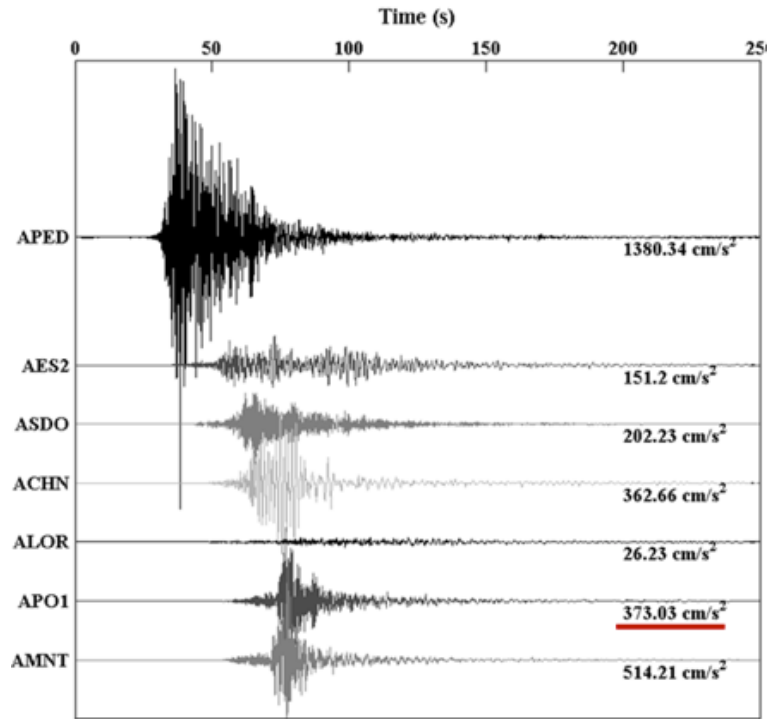


Figure 3-29. Ground accelerations recorded at different stations in Ecuador (Singaicho J. C., 2016).



Figure 3-30. Cleared areas of collapsed buildings (photos: Ana Gabriela Haro).

### 3.5.1 Damage to Reinforced Concrete (RC) Buildings

Figure 3-31 shows the Palace of Justice of Portoviejo, which is a nine-story frame building with two main sections placed in an “L” shape. According to a source within the Army, the foundation consists of piles. The main building and its annexes were separated by approximately 2-inch (50 mm) wide seismic joints, which appeared ineffective in the places where they were filled with inappropriate material. Unreinforced hollow concrete block masonry was used in facade and interior partitions. Failure of structural elements was not evident, but as observed in other buildings throughout the affected area, masonry elements were substantially damaged. Regarding the contents of the building, significant disruptions were observed as the building had been vacated. This indicated a greater need for adequate workplace security, resiliency measures, and planning for post-disaster operations.



a)



b)



c)



d)

Figure 3-31. Palace of Justice of Portoviejo: a) general view of the structure; b) damage to joints; c) shear failure in partitions; d) fallen contents (photos: Ana Gabriela Haro).

Numerous low- and medium-rise buildings exhibited non-structural failure associated with shear cracks in masonry infill walls, as stated previously. Figure 3-32 shows some cases with minor to severe damage where brittle, heavy, unreinforced facades were not designed and detailed for deformation compatibility with the lateral deformations of the frame buildings. The observed damage suggests that a change in the procedures to connect the infill walls to the main structure could improve building performance in future earthquakes.



a)



b)

Figure 3-32. Examples of facade damage in Portoviejo. (photos: Ana Gabriela Haro).

Several medium-rise buildings collapsed partially, jeopardizing the adjacent structures. Figure 3-33 shows the Mutualista Pichincha building, which originally had ten levels. Stories five to seven completely collapsed causing the upper levels to lean toward the west. Short columns with reduced cross sections were observed in the upper level.



a)



b)



c)



d)

Figure 3-33. Mutualista Pichincha Building: a) general view of the damage; b) close view of the collapsed floors; c) short column and shear failure on beam; d) location (Google Maps) (photos: Ana Gabriela Haro and Arturo Schultz).

The upper two stories of the two annexes of the Centro Comercial Municipal collapsed as shown in Figure 3-34, where the original configuration of the structure before the earthquake has been included for reference. Poor detailing and a lack of structural robustness and redundancy contributed to the partial collapse, see Figure 3-34b. The main structure is a nine-story building, which experienced damage to the infill walls, especially in the stairs.

Figure 3-34a also shows the location of the IESS and the Hotel Alejandro buildings before the April 16 earthquake, both seven-story RC structures. Figure 3-35b also shows the space left by the first building after its complete collapse due to a first floor soft-story collapse, and the partial collapse of the second building where the upper four levels collapsed, endangering the small structure on its right.



a)



b)

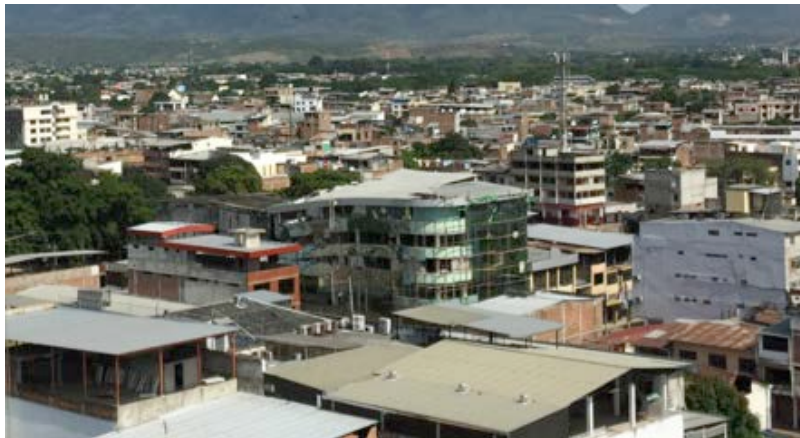


c)



d)

Figure 3-34. Centro Comercial Municipal: a) structure before earthquake (Google Street View); b) general view of damaged building; c) close view of the collapsed floors; d) damage on infill walls. (photos: Ana Gabriela Haro and Arturo Schultz)



a)



b)

Figure 3-35. Banco Comercial de Manabí: a) structure after the April 16 earthquake (photo: Arturo Schultz) ; b) structure after the May 18 tremors (photo: courtesy of Diego Aguirre Burneo–Ecuadorian Inspector)

The Banco Comercial de Manabí building was severely damaged during the April 16 earthquake when a large portion of this six-story RC building collapsed, Figure 3-35a. The cause of the damage is attributed to weak structural elements, particularly on the upper levels. During the 6.7M and 6.8M tremors on May 18, 2016, only the first three floors survived, as observed in Figure 3-35b. These new seismic events are apparently aftershocks of the main earthquake and occurred after the EERI team left Ecuador.

All around the Ground-Zero area, relevant damage in seismic joints due to pounding between adjacent buildings was observed, see Figure 3-36. Often, adjacent slabs are not at the same height, and have different rigidities. Overall, the seismic separations are insufficient in width to avoid the effects of pounding, which could lead to structural failure.



Figure 3-36. Pounding between buildings: a) Contraloría General del Estado building affected by two adjacent structures; b) adjacent slabs at different heights; c) restricted differential movement. (photos: Ana Gabriela Haro and Arturo Schultz)



Figure 3-37. RC three-story building partially collapsed: a) general view of the structure; b) column failure; c) joint failure and beam detail; d) attempt to prevent total collapse. (photos: Ana Gabriela Haro and Arturo Schultz)

Figure 3-36c shows a particular case where a joint was not respected (parapet wall seen crossing joint without allowance for differential movement) and, consequently, the parapet was damaged during the earthquake.

The top of the columns at the first floor of some buildings experienced shear failure, which led to instability as can be seen in Figure 3-37 (an example of a three-story building). Poor reinforcement detailing in columns and joints was detected. Stirrups were built with smooth bars and closed with 90-degree hooks instead of the standard 135-degree seismic hook. With the purpose of preventing the total collapse of the building, steel and bamboo elements were employed as temporary shoring at the time of the team visit.

Many residential and commercial buildings in Portoviejo's Ground Zero use a colonnade frame, which usually lacks seismic design. Tall and slender columns placed on the sidewalk are used to support the upper levels. In order to avoid problems caused by slenderness, false beams are provided, but mostly only in one direction. If these false beams are connected inadequately to the columns, they suffer significant damage when a building is subjected to horizontal displacements during an earthquake, as observed in Figure 3-38.



Figure 3-38. Beam-column connections damage. (photos: Arturo Schultz and Ana Gabriela Haro)

Inelastic response was observed at the base of the first floor columns in some buildings. There was evidence of poor quality concrete and inappropriate confinement reinforcement detailing where corroded stirrups were spaced about twice the distance required to prevent buckling of longitudinal rebars. Figure 3-39 shows a five-story RC building where the described problems are exposed, including rebar buckling and concrete crushing.



Figure 3-39. Plastic hinges evidenced in a five-story RC building. (photos: Ana Gabriela Haro)



a)



b)



c)

Figure 3-40. Cases of structural alterations. (photos: Ana Gabriela Haro)



a)



b)

Figure 3-41. Church at Vicente Amador Flor Park: a) general view; b) damage localized at one of the dome supports. (photos: Ana Gabriela Haro)



a)



b)



c)



d)

Figure 3-42. Church at Vicente Amador Flor Park: a) general view; b) damage localized at one of the dome supports; c) damaged connections; d) damage in masonry (photos: Ana Gabriela Haro and Arturo Schultz)

Structural alterations of RC buildings were also observed during the reconnaissance, which can lead to building vulnerability. An increment in the gravity loading increases the lateral loading when an earthquake strikes, and consequently buildings are subjected to forces that were not considered during their design. The situation becomes more critical when the conception of these structural alterations lacks basic design and construction procedures to resist earthquake forces. In Portoviejo's Ground Zero, some added systems were different from the original construction system of the building and the lack of seismic design of these alterations was clearly noted as illustrated in Figure 3-40.

The two inspected churches were partially damaged and performed better than most of the other RC buildings in Portoviejo. Figure 3-41a shows the general view of the church located at Vicente Amador Flor Park; and Figure 3-41b shows detailing of the main dome support, which was damaged during the earthquake. Concrete cover spalling was observed at this support.

The Cathedral Jesús del Buen Pastor, experienced minor damage in infill walls. In addition, the connections between the towers and the adjacent parapets failed, as can be seen in Figure 3-42c and 3-42d. The main structure, consisting of big domes, apparently performed well, as can be seen in Figure 3-42b. Flexural cracks were observed in the structure surrounding the top of the stained glass circular window, probably caused by the stresses transmitted from the interaction between the towers and the connecting curved beam.

### 3.5.2 Conclusion

In summary, the failure modes observed in Portoviejo's Ground Zero suggest the necessity of enforcing design and construction codes to improve the seismic structural performance of new and existing buildings to prevent future catastrophes.

The main causes of damage were attributed to the following aspects:

- Extremely flexible RC frame buildings associated with lack of robustness and redundancy.
- Heavy and brittle infill walls became safety hazards during the April 16, 2016 earthquake.
- Poor quality of materials and reinforcing detailing.
- Evidence of lack of quality control during construction processes.

## 3.6 BUILDING DAMAGE IN PEDERNALES

Pedernales was reported to be one of the most affected towns. While the EERI team did not visit the town, the EEFIT team did and shared their preliminary observations, which are included here:

The army reported that 402 buildings had been demolished prior to the EEFIT team's arrival. The EEFIT team surveyed structures using a rapid visual protocol in the town centre and in the area around the seismometer station (APED). Additionally, detailed surveys were conducted in the cathedral, and the main municipality building, both located on Plaza Central.

The rapid visual survey included approximately 200 buildings in Pedernales town center and 100 around the seismometer station (APED). The building typologies were primarily low-rise RC or timber masonry infilled buildings. Structural damage was generally light to moderate, however many of the most damaged buildings had been demolished. The observed non-structural damage was primarily in- and out-of-plane masonry infill wall damage.

A detailed survey of the cathedral was also conducted (See Figure 3-43). The cathedral is primarily RC construction with an architectural steel truss roof. Masonry was used throughout for infill, gable, and external walls. Non-structural damage was heavy, with some significant masonry wall damage, and dislodged heavy ceiling tiles. Roof cladding panels had also fallen during the earthquake and caused fatalities. The observed structural damage was light and appeared to be caused by connections to the masonry infill walls.



Figure 3-43. Pedernales cathedral on Plaza Central (photo: EEFIT).



Figure 3-44. The main municipality building in Pedernales (photo: EEFIT).

A detailed survey of the main municipality building (Figure 3-44) was also conducted. This building is a five-story building of RC frame construction with masonry infill in the internal and external walls. The team surveyed the building internally on level 1 and externally, and observed moderate structural damage, including cracks and spalling of concrete in the top of the columns, and heavy damage to the RC staircase. Non-structural damage was heavy with the failure of full wall panels internally and externally.

### 3.7 REFERENCES

- Franco et al. (2016) “The April 16 2016 MW7.8 Muisne Earthquake in Ecuador—Observations & Conclusions from the EEFIT Reconnaissance Mission of May 24–June 7.” Earthquake Engineering Field Investigation Team, Institution of Structural Engineers, London, UK.
- Franco et al. (2017) “The April 16 2016 MW7.8 Muisne Earthquake in Ecuador—Preliminary Observations from the EEFIT Reconnaissance Mission of May 24–June 7.” In Proceedings of the 16th World Conference on Earthquake Engineering, 16WCEE 2017, Santiago Chile, January 9th–13th, 2017, Paper N° 4982.
- “Manta, Ecuador.” Map. Google Maps. Google, 23 Feb. 2015a. Web. 6 June 2016. Available at <https://www.google.com/maps/@-0.9539051,-80.7160702,3a,75y,319.52h,107.94t/data=!3m6!1e1!3m4!1sWuFj1ryAwPYx-wE6Wy7xgxl2e0!7i13312!8i6656>
- “Manta, Ecuador.” Map. Google Maps. Google, 23 Feb. 2015b. Web. 6 June 2016. Available at <https://www.google.com/maps/@-0.952374,-80.7166508,3a,75y,330.32h,113.87t/data=!3m6!1e1!3m4!1srX3tDNTQlxQX5eO-alH5ACA!2e0!7i13312!8i6656>
- “Manta, Ecuador.” Map. Google Maps. Google, 23 Feb. 2015c. Web. 6 June 2016. Available at [https://www.google.com/maps/@-0.9527527,-80.718883,3a,75y,336.55h,106.73t/data=!3m6!1e1!3m4!1sf\\_-iE02jSKu6PW-zUalo2Lg!2e0!7i13312!8i6656](https://www.google.com/maps/@-0.9527527,-80.718883,3a,75y,336.55h,106.73t/data=!3m6!1e1!3m4!1sf_-iE02jSKu6PW-zUalo2Lg!2e0!7i13312!8i6656)
- “Manta, Ecuador.” Map. Google Maps. Google, 23 Feb. 2015d. Web. 6 June 2016. Available at [https://www.google.com/maps/@-0.9605109,-80.7128499,3a,75y,190h,101.34t/data=!3m6!1e1!3m4!1sPn5zOqb3nnLSgq-pf\\_fa\\_dQ!2e0!7i13312!8i6656](https://www.google.com/maps/@-0.9605109,-80.7128499,3a,75y,190h,101.34t/data=!3m6!1e1!3m4!1sPn5zOqb3nnLSgq-pf_fa_dQ!2e0!7i13312!8i6656)
- Singaicho J. C., L. A. (2016). Observaciones del Sismo del 16 de Abril de 2016 de Magnitud Mw 7.8. Intensidades y Aceleraciones. Revista Politécnica.
- Wikipedia. (18 de April de 2016). Portoviejo. Retrieved 30 de May de 2016 from <https://en.wikipedia.org/wiki/Portoviejo>. <http://gestionriesgosec.maps.arcgis.com/apps/MapJournal/index.html?appid=da3427b0e35f473b-b3029467a9b4f1fc>



# CHAPTER 4

# HOSPITALS

## 4.1 INTRODUCTION

This section reviews the performance of the five hospitals that the EERI team visited in the Province of Manabí, as listed in Table 4-1 below. Of the five hospitals, one remained fully operational, one remained partially operational, and the rest suffered significant damages and had to be evacuated. Despite the severe damage in non-structural components, verbal inquiry indicates that only a small number of casualties occurred at these hospitals immediately after the April 16 earthquake.

*Table 4-1. Hospitals visited in Manabí*

Name of the Hospital	City	Status
Hospital IESS	Manta	Not Operational
Hospital IESS	Portoviejo	Fully Operational
Hospital SOLCA	Portoviejo	One story block: Operational. Multi-story block: Not Operational
Hospital Miguel Hilario Alcívar	Bahía de Caráquez	Not Operational
Hospital Napoleón Dávila	Chone	Not Operational

All five hospitals have structures comprised of reinforced concrete frames (beams and columns), concrete “waffle” slabs, and unreinforced masonry extensively used for exterior walls and interior partition walls. Some of the exterior and interior walls are infill panels within a reinforced concrete frame, while others are non-load-bearing panels that do not coincide with the plane of the frame, but may still have some connection to it. An exception is the Hospital Miguel H. Alcívar in Bahía, which was comprised of concrete shear walls added to the original concrete moment frame system. Typical geometry for these hospitals is comprised of several structural independent buildings (blocks) with different height and layout.

Soft-story mechanisms or other global structural damage were not observed in the Hospital IESS in Manta, however, the team observed structural damage at the SOLCA and Napoleon Dávila hospitals. Details about the performance of each hospital are provided in the following sections.

## 4.2 HOSPITALS IESS IN MANTA

Visual inspections of the columns and beams of the Hospital IESS in Manta did not reveal visible damage (although detailed inspection of every beam, column, and joint would be needed for definitive conclusions), but both exterior and interior unreinforced masonry walls were severely damaged throughout the building (see Figure 4-1). Debris from infill walls was a falling hazard (see Figure 4-2), and it most likely caused obstructions for building occupants trying to exit the building. The attachments for non-structural elements such as ceilings, pipes, ducts, and ceiling-supported equipment performed poorly. Major mechanical and medical equipment had been taken out of the building and relocated elsewhere on the hospital complex. Excessive cover (over four inches) was noted in some of the columns.



Figure 4-1. Widespread damage to exterior infill walls (photo: Adrian Tola).



Figure 4-2. Obstructions caused by infill wall material debris (photo: Adrian Tola).

## 4.3 HOSPITALS IESS IN PORTOVIEJO

Of the five hospitals visited, the Hospital IESS in Portoviejo (see Figure 4-3, left) had the least amount of damage. The building includes a large segment, one story in height, and a smaller segment three stories in height, and both of them were fully operational at the time of our visit (see Figure 4-3, right). No cracking of walls was observed. Minor damage was seen in the building at a seismic joint on the ground floor (see Figure 4-4). Hospital employees reported that people evacuated the hospital on April 16 for security reasons; however, because of the minor damage, it was re-opened a few days after the earthquake.



Figure 4-3. (Left) No observed damage at the interior of the hospital. (Right) Exterior of the fully operational hospital (photo: Adrian Tola).



Figure 4-4. Minor damage at ground floor seismic joint (photo: Adrian Tola).

#### 4.3.1 Hospital SOLCA in Portoviejo

Hospital SOLCA contained cracked walls that were concentrated in the first two levels of the building (See Figure 4-5a). Most walls at these levels were cracked but still standing, but a few walls collapsed. In the upper floors, there was minor cracking of walls and mechanical equipment was unaffected.



Figure 4-5. Damage in the walls in the first two floors in Hospital SOLCA (photo: Adrian Tola).

Structural damage was observed in one of the columns on the second floor (see Figure 4-6b). The concrete at the top of this column spalled and the longitudinal bars buckled in this region; also, no cross ties were observed in the top of this column, immediately below the column-beam joint, which caused too far spacing of ties in a critical region of this column.



Figure 4-6. Structural damage in a column on 2nd floor in hospital in SOLCA.

## 4.4 HOSPITAL MIGUEL H. ALCÍVAR IN BAHÍA DE CÁRAQUEZ

Hospital Miguel H. Alcívar in Bahía de Caráquez was retrofitted after the magnitude 7.2 earthquake on August 4, 1998. However, following the April 16, 2016 earthquake, the building was deemed not operational. The team observed employees actively removing medical equipment from this building for the nearby temporary hospital.

The original building lateral system consisted of reinforced concrete moment frames. The 2000 retrofit added six new reinforced concrete shear walls (Aguiar, 2016): one each at front and back, and two in each transverse direction (see Figure 4-7a and 4-7b). Also, as part of the retrofit, some of the columns, including the ones forming the boundary zone of the new shear walls, were strengthened by enlarging their plan dimensions, adding new confining reinforcement, and adding steel angles as longitudinal reinforcement (see Figure 4-6c). The April 2016 earthquake caused the concrete cover of some columns to spall and the EERI team was able to see the retrofit measures taken in 2000.

The performance of this hospital is described in more detail in a report by Dr. Roberto Aguiar, who was the structural engineer in charge of the seismic retrofit in 2000 (Aguiar, 2016). Aguiar concludes that the shear walls contributed notably to the good performance of the building, and that beams, columns, and joints remained in the elastic range during the earthquake.



Figure 4-7. Damage in Hospital Miguel H. Alcívar in Bahía de Caráquez (photo: Adrian Tola).

No diagonal cracks were observed in the reinforced concrete shear walls. Concrete spalling in the concrete columns forming the boundary zone of the concrete shear walls was observed (see Figure 4-7c). Unreinforced masonry walls were used for both exterior and interior walls. Notably, an unanchored, unreinforced masonry wall adjacent to the elevator lobby failed out-of-plane and debris fell into the elevator lobby (see Figure 4-7d). Diagonal shear cracks on the interior walls on the ground floor were observed, but most walls did not fail out-of-plane (see Figure 4-7a), possibly due to smaller drifts expected with the presence of the shear walls.

There was less damage in upper levels and some rooms appeared to be almost undamaged. Nonstructural observations include toppled tall, unbraced bookshelves (see Figure 4-8b), while lighter ceiling-mounted equipment was still in place.



Figure 4-8. Damage in non-structural components in Hospital Miguel H. Alcívar (photo: Adrian Tola).

## 4.5 HOSPITAL NAPOLEÓN DÁVILA IN CHONE

Figure 4-9a emphasizes three structurally independent blocks of particular interest in this hospital, where the observed seismic joint between Blocks 1 and 2, and between Blocks 2 and 3, were approximately two inches in width. There was extensive structural damage at the seismic joints due to pounding of adjacent structures, which illustrates the lack of adequate joint separation between these blocks. The pounding also led to the collapse of unreinforced masonry walls and damage to mechanical equipment in one of the blocks. Significant rebar corrosion at walls, slabs, and beams adjacent to seismic joints was observed.

Figure 4-9a and 4-9b show the front and back view of the hospital with the pounding damage to Blocks 1, 2, and 3. Figure 4-9c shows the debris from collapsed walls in Block 2 at the second floor. Figure 4-7d shows that the upper floor of Block 2 seemed to be out of plumb with the floors below. Block 1 and 3 had significantly less damage to non-structural components, as compared to Block 2.



a) Front view



b) Back view. Damage in Block 2 and Block 3.



c) Damage at interior of Block 2, floor 2.



d) Possible out of plumb of upper floor in Block 2.

Figure 4-9. Damage in Hospital Napoleón Dávila in Chone due to pounding of adjacent buildings (photo: Adrian Tola).

In Block 2, many interior unreinforced masonry partitions collapsed. Cementitious parge coats on the wall surface was quite thick and in some instances it was nearly one-and-a-half inches thick. The excessively thick cement parge was crushed during the April 16 earthquake and spalled in large chunks (see Figure 4-10).



Figure 4-10. Damaged walls inside Block 2 (photo: Adrian Tola).

## 4.6 REFERENCES

Aguiar R. (2016), "Hospital de Bahía de Caraquez Miguel H. Alcivar, Luego del Terremoto del 16 de Abril de 2016." Revista Internacional de Ingeniería de Estructuras, To be published.



## CHAPTER 5

# Non-Engineered Construction

### 5.1 INTRODUCTION

This section briefly reviews the performance of several types of non-engineered construction that the team observed in Ecuador. Such construction is called “non-engineered” because no structural analysis or design is done; usages are dictated by empirical practice. These structures are usually built by master craftsmen (‘maestros de obra’) without formal training.

### 5.2 MASONRY CONSTRUCTION

Housing and small commercial buildings in the coastal region visited by the EERI team were generally of non-engineered masonry construction, up to three or four stories high. Masonry is either artisanal clay brick or cement block. Small RC columns are cast at corners and at wall intersections, brick or block panels (typically unreinforced) are then built between columns, a RC slab is cast, and the process is repeated for subsequently stories. Finally, a reinforced concrete bond beam is cast and a truss roof, of metal or wood, completes the structure. Alternatively, a complete building frame may be constructed first and the masonry infill walls are placed last. This makes for a flexible frame system with heavy, non-structural and poorly connected infill walls. Since the walls are infilled at a later stage, there is no effective bonding between masonry, concrete, and reinforcement; the small RC elements (about 20 cm x 20 cm in section as seen in the photographs) are seldom able to adequately resist the seismic forces; and the infills tend to topple out of the wall plane.

It is important to note that in many earthquake-prone countries of Latin America (but not Ecuador), construction of non-engineered buildings utilizes the “confined masonry” technique. This is a straight-forward, prescriptive method, used by master craftsmen, and sometimes by architects and engineers. Confined masonry has proven to provide satisfactory behavior during earthquakes provided that certain rules are followed. The EERI team suggests that the system used in the coastal area of Ecuador could be easily modified to become a confined masonry system with little difference in cost. This can be accomplished by slightly changing the construction sequence, namely to cast the concrete columns and bond beams after erecting the masonry panels.



Figure 5-1. Non-engineered block masonry house (photo: Héctor Monzón)



Figure 5-2. Non-engineered construction (photo: Héctor Monzón)

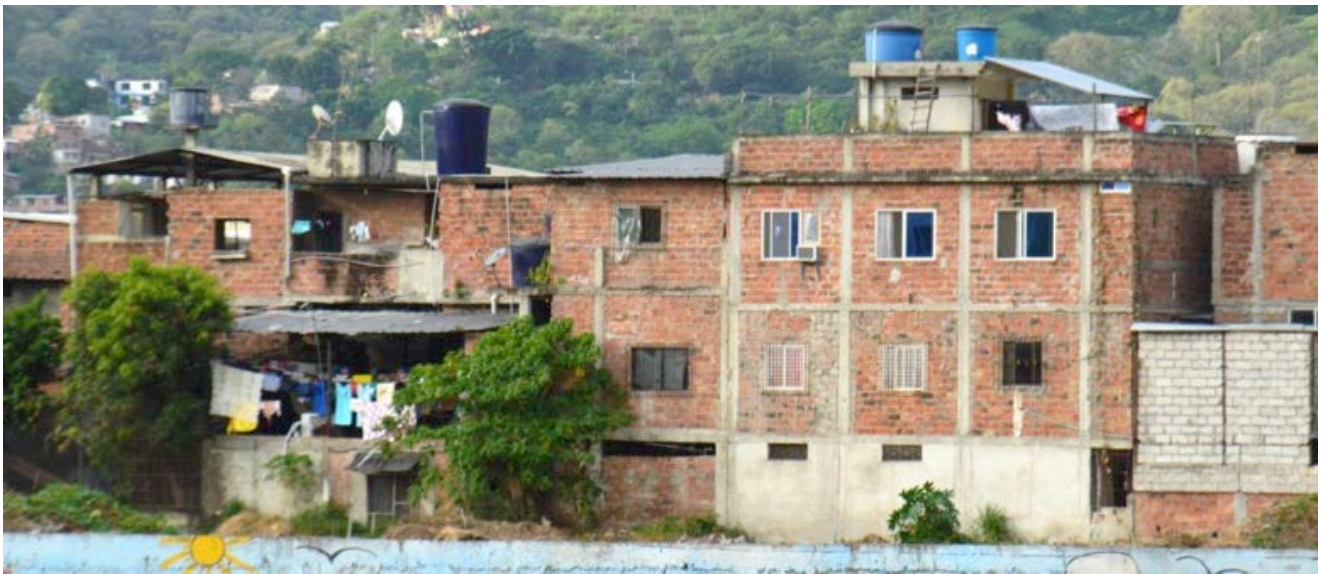


Figure 5-3. Non-engineered construction (photo: Héctor Monzón).



Figure 5-4. Masonry construction near downtown Portoviejo (photo: Héctor Monzón).



Figure 5.5. Severe damage to non-engineered construction in Canoa (photo: Héctor Monzón).

Figure 5-1 is of a house on the Coastal highway, 70 km south of Manta in a low seismic intensity fringe of the April 2016 earthquake. The top stories illustrate the building system as described on the previous page. (The partial height walls appear to be intentional.) Figure 5-2 is another non-engineered construction, probably brick masonry, on the Coastal highway, about 50 km south of Manta. It is unclear whether the top stories incurred severe damage and the debris had already been removed (photograph was taken 25 days after the April 2016 earthquake) or if the construction was yet to be completed, but it clearly illustrates the weaknesses of the building system.

Figure 5-3 is an example of hand compacted brick masonry in downtown Portoviejo—a high seismic intensity area during the April 2016 earthquake. Only minor damage was observed in some units such as the one at the right of the photo. However, wall panels collapsed in the unit at the left. Such random performances were often observed.

While there weren't many collapsed units, Figure 5-4 shows many collapsed walls in the upper stories of buildings near downtown Portoviejo. Figure 5-14 shows severe damage to non-engineered construction in a small town north of Bahía called Canoa. In the high intensity shaking area, there were about 30 % collapses—judging from empty plots. In Figure 5-5, all debris from the upper story in the dwellings shown above has been removed.



Figure 5-6. An older construction system of combined wood and masonry (photos Héctor Monzón).

### 5.3 BAHAREQUE CONSTRUCTION

Another type of non-engineered construction, bahareque, is found throughout Latin America, including coastal Ecuador. It is made using a combination of some or all of the following: guadua bamboo, timber, mud, straw, cow manure, and plaster. Many variants exist, but the most common (basic) form in Ecuador comprises a bamboo or timber (mangrove, oak, or lignum vitae selected for strength and durability) frame with posts embedded in a compacted soil or concrete foundation, bamboo or wood laths attached to the bamboo or timber frame, mud (often mixed with straw) to fill the gaps and provide a continuous wall surface, and a plaster covering to protect the other components. Typically, a light roof is used (bamboo, timber, thatch, or corrugated metal) making bahareque houses very light structures and with a modest supply of ductility in the bamboo or timber elements. Low-rise (one- or two-story) bahareque structures that are well connected and have been protected from deterioration of the plant-sourced materials have been shown to perform well under seismic excitation (Gutierrez, 2004).

Figure 5-7 shows a two-story unplastered bamboo wall in the back of a building housing a restaurant and bar in the beachside town of Canoa. The front of the building was damaged from inadequate out-of-plane support of the streetside wall (Figure 5-8), but the back wall performed well. Traditional bahareque is more common in rural areas of coastal Ecuador. In urban areas, the mud and straw are often replaced with clay brick, and bamboo is often replaced by timber. Figure 5-9 shows a building in the historic sector of downtown Bahía de Caráquez that is made of mixed construction including timber-framed walls with wood laths, and plaster along the street façade. The building



Figure 5-7. Unplastered bamboo wall in Canoa (photo: Arturo E. Schultz).



Figure 5-8. Failed façade of bamboo building in Canoa (photo: Arturo E. Schultz).



Figure 5-9. Timber framed building in Bahía de Caráquez with damaged party wall (photo: Arturo E. Schultz).



Figure 5-10. Timber and bahareque building in Tarqui district of Manta (photo: Arturo E. Schultz).

has been shored, but most of the damage is concentrated around the masonry infill panels in the party wall with the collapsed building in the foreground. Figure 5-10 shows the bottom of the overhang above the streetside colonnade in a building in the Tarqui district of Manta. The building is of mixed construction, including timber beams and posts encased in brick (Figure 5-11) and plastered bamboo laths, but these components have been covered by plaster and textured in the second floor to simulate block masonry construction. Unfortunately, the timber members (Figure 5-4) and bamboo laths (Figure 5-12) are heavily deteriorated in many locations.

## 5.4 CLAY BRICK AND TIMBER CONSTRUCTION

Another variant of traditional, non-engineered construction in Ecuador uses clay brick infill instead of plastered laths in timber frames given the greater durability of clay masonry (Figure 5-13). In this construction system, it is common to include inclined timber members in addition to the vertical and horizontal posts for greater strength and stability. The bricks are placed as “rowlock stretchers or shiners” to minimize wall thickness. Exposed façades, especially along streets, are typically plastered (Figure 5-14). Performance of this system is often better than that of the non-engineered concrete frames with brick infill because the timber provides more ductile member behavior, and the smaller brick panels are better restrained. In fact, Saraf et al. (2012) studied an Indian version of this building system and have quantified the influence of brick panels and timber member lengths on the in-plane shear strength of the walls. However, the improvement, if any, provided by the inclined timber posts on out-of-plane strength and stability is not known.



Figure 5-11. Timber post encased in brick masonry and plaster (photo: Arturo E. Schultz).



Figure 5-12. Deteriorated bamboo laths and timber posts and beams (photo: Arturo E. Schultz).



Figure 5-13. Brick-infilled timber frame construction (photo: Arturo E. Schultz).



Figure 5-14. Plaster over brick-infilled timber frame construction (photo: Arturo E. Schultz).

## 5.5 WOOD CONSTRUCTION

Wood elements were found in small structures only, such as houses. Some houses are made entirely of wood (including columns, beams, floors, and partitions). These houses were found in small coastal towns. Some houses totally collapsed, including both one and two-story houses. This may be because of the inadequate structuring of the elements in terms of quality of material, location, and quantity of supporting and load-resisting elements.

Other houses were constructed of concrete frames with masonry infill with wood elements. These elements are embedded in the masonry walls and are not part of the lateral force resisting system. This typology had a regular performance in this earthquake. Collapsed or heavily damaged houses of this type were not found, but rather showed spalling of concrete finishing (see pictures on the following pages).

Another type of building consists of wood frames with masonry infill. In some cases, wood was found embedded in the masonry. There was a significant amount of mass in the second floor from the partitions and some examples of poor performance in the earthquake. There were also houses constructed of concrete frames in the first floor and frames of wood infilled with masonry in the second floor. A few collapsed houses with this typology were observed.

The performance of wood structures was not generalized. Typically, as expected, only small houses with poor construction quality did not perform well in the earthquake.



Figure 5-15. Houses with spalling concrete finishing.



## CHAPTER 6

# Post-Earthquake Building Shoring

### 6.1 INTRODUCTION

This section discusses the post-earthquake shoring of buildings in Ecuador, after briefly reviewing the basic concept of shoring. The overall goal of post-earthquake shoring is to provide temporary support to stabilize buildings and other structures that are damaged during an earthquake. Stabilization is needed to afford safety to those who may be trapped in the building, to urban search and rescue personnel, and to anyone in the vicinity of the damaged structure. Shoring is temporary by nature and has a useful life determined by the search and rescue efforts, and the repair, reconstruction, or demolition processes.

### 6.2 THE BASIC CONCEPT OF SHORING

The basic concept of shoring is often described schematically as a symmetric double-funnel (Figure 6-1) in which the top funnel represents the components that collect load from the distressed structure, and the vertical line represents the elements that transfer the load to components that distribute load to the ground or foundation (bottom funnel). Other desirable characteristics of shoring systems are adjustability, positive connections, lateral bracing, ductility, and warning of overload. In the United States, recommendations for temporary shoring are made by the Federal Emergency Management Agency (FEMA) and the Department of Homeland Security (DHS) (FEMA 2013, DHS 2011). States have the authority to enforce, adapt, modify, or replace the FEMA/DHS recommendations, even though they are usually adopted with addenda to address issues not deemed to be addressed adequately in the FEMA/DHS documents (CALBO 2013, Turner 2015).

Vertical shores are typically assembled from the basic configuration shown in Figure 6-2, which comprises a vertical wood post and two horizontal wood members serving as header and sole, all with the grain of the wood oriented along the longitudinal axis of the individual members. The vertical post will be loaded parallel to the grain of the wood, so that it will be stronger than the header and sole, which are loaded perpendicular to the grain. Moreover, when the

header and/or sole fail, the process will be slow and noisy, affording both time and warning to evacuate the damaged building. However, successful performance of this ductile system requires that buckling of the posts be prevented, thus restrictions are placed on the post length-to-thickness ratio ( $L/t$ ). For the typical grades of lumber used in the United States for shoring, a limit of 50 is recommended for  $L/t$ , and it is suggested that this value be reduced to 25 (FEMA, 2014). Additionally, positive connections are needed between the posts, header, and sole, as well as to the damaged structure (through the header) and the ground (through the sole). Thus, a typical shore will incorporate gusset plates, braces, and other components, as shown in Figure 6-3.

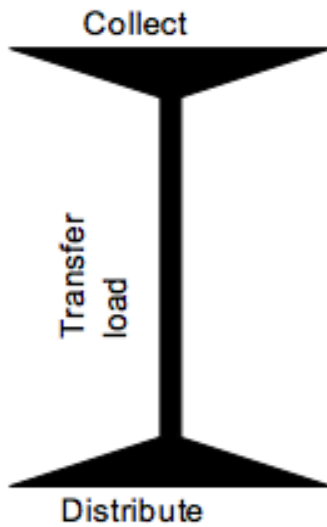


Figure 6-1. Schematic diagram of basic shoring concept (adapted DHS 2011).



Figure 6-2. Basic configuration for vertical shores (FEMA 2014)

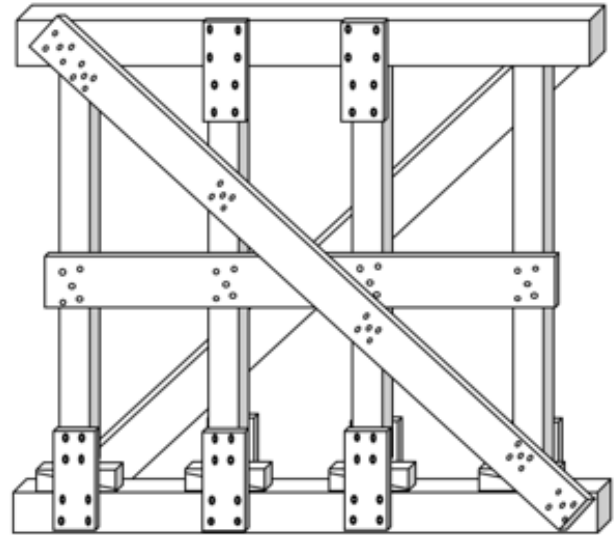


Figure 6-3. Typical vertical shore (DHS 2011)

Shores for lateral loads typically rely on an inclined raker (Figure 6-4) to resist the out-of-plane forces and motions on the building façade, as well as vertical and horizontal plates to stabilize the raker, and positive connections between all members. Large damaged façades require assemblages of multiple rakers with additional braces and other components to provide structural integrity (Figure 6-5).

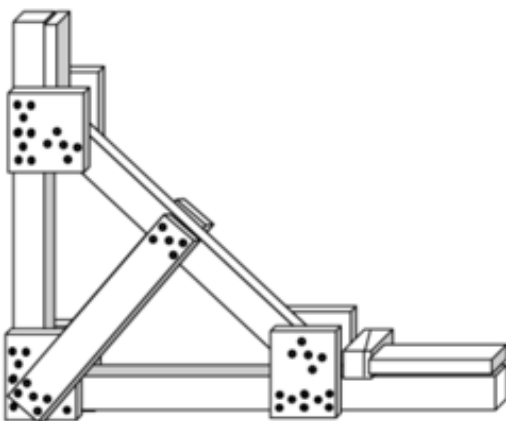
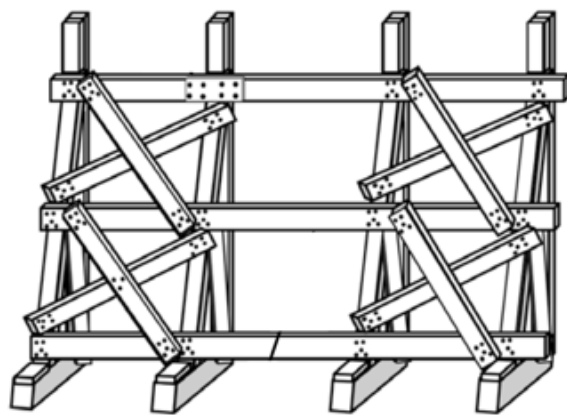


Figure 6-4. Typical raker for lateral shoring (DHS 2011).



## 6.3 SHORING IN ECUADOR

Guadua bamboo is most commonly used in Ecuador for the construction of temporary shoring and is widely available in South America. Guadua bamboo produces strong, stiff, and durable culms (hollow stems) that can be easily cut to desired lengths for use in shoring. The properties of guadua bamboo are variable, like most plant materials, but even the lowest values for modulus of elasticity, compressive strength, and shear strength are at least as large as, if not larger than, those for typical construction lumber (RWTH Aachen). Assuming conservatively that guadua bamboo serves as an equivalent replacement material to SPF lumber—that is, the elastic moduli are approximately equal—then the requirements for slenderness of shoring posts and rakers must be modified for the hollow circular geometry of bamboo culms.

Bamboo culms grow such that the exterior diameter is approximately constant over the height of the culm, a feature of which makes bamboo an excellent construction material for shoring since longitudinal cutting or shaping is not needed. However, wall thickness is naturally tapered along culm height as the older material at the base grows to greater thickness than the newer material at the top. Kappel et al. (2004) note that the ratio of the cross-sectional radius to wall thickness ( $r/t$ ) for bamboo culms varies typically from 0.5 to 0.1. Assuming here that the critical axial load at buckling is defined with an approximate median value for the radius-to-thickness ratio ( $r/t = 0.3$ ), then the corresponding moment of inertia for a hollow bamboo section is approximately 50% of that for a square post of comparable dimensions. Comparable dimensions are assumed for a square post with cross-sectional area equal to the gross area of the circular post. Therefore, for equal buckling load capacity, bamboo shores must be limited to  $L/t$  ratios that are about 70% of those for square posts of comparable dimension. The resulting upper limit for  $L/t$  is 17.5, instead of the corresponding value of 25 for the square post of comparable dimensions, if bamboo shores are to have similar buckling loads to those for square wood posts

### 6.3.1 Post Earthquake Observations

The EERI reconnaissance team observed shoring construction practices in Ecuador that did not follow the slenderness limitation suggested above ( $L/t \leq 17.5$ ), nor the FEMA and DHS recommendations discussed earlier. In addition, a number of features were observed that do not conform with accepted practice for temporary seismic shoring. The features included shores comprising individual bamboo posts, without headers or soles. The problems associated with the omission of headers and soles include loss of stability and structural integrity, as well as the loss of ductility afforded by the crushing of these members. By using individual posts, lateral bracing between posts was also omitted, with the concomitant loss of stability for motion parallel to the building façade. Moreover, there was no positive connection between the individual posts and the ground and support building façade, and the bamboo shoring in Ecuador relies principally on friction for the transfer and distribution of shoring forces.



Figure 6-6. Hotel Capri in the Tarqui district of Manta (photo: Arturo Schultz)

In spite of these shortcomings, the EERI team did not observe either failed or collapsed bamboo shores. It is possible that the  $L/t$  ratios adopted from U.S. shoring practice are too strict, and that more relaxed values can be adopted for bamboo shores. Alternatively, the EERI team was unable to ascertain if bamboo shores actually failed or collapsed during the numerous aftershocks following the April 16, 2016 event, but that the aggressive demolition and cleanup program led by the government of Ecuador removed evidence of these failures before the EERI team was able to conduct their reconnaissance of the affected region. Four cases of building shoring are discussed in the sequel.

Figure 6-6 shows the façade of Hotel Capri along 105th Steet near the waterfront in the Tarqui district of Manta (Malecón de Tarqui). This district is a destination for local tourism and offers hotels, restaurants, and other tourism-related business, especially along the streets closest to the Malecón. The Hotel Capri, like many buildings of its period, includes a street-side walkway with a cantilever overhang to maximize interior space in the stories above the first. Due to concerns about the stability of the cantilever overhang, the street-side façade was shored using bamboo posts following the April 16, 2016 earthquake. The aspect ratio ( $L/t$ ) for these shores clearly exceeds the recommended limit of 17.5, as well as the upper limit of 35. Additionally, the bamboo posts do not have headers, soles, or lateral braces to create a complete and stable shoring system.



Figure 6-7. Chavez Hotel Inn in the Tarqui district of Manta (photo: Arturo Schultz)



Figure 6-8. Close-up of bamboo shores used for the Chavez Hotel Inn (photo: Arturo Schultz)



Figure 6-9. Fish & Dive store in the Tarqui district of Manta (photo: Arturo Schultz)



Figure 6-10. Hotel New York in Portoviejo (photo: Arturo Schultz)

The configuration of bamboo shores shown in Figure 6-6 was observed throughout the region affected by the April 16 earthquake. Figure 6-7 shows the Chavez Hotel Inn near the intersection of 106th Street and 106th Avenue, also in the Tarqui district of Manta. Individual bamboo posts are used to shore the cantilever overhang, but in this case, the posts span a two-story height, making their aspect ratio considerably larger than the suggested limits. Headers, soles, and lateral braces are not present either. Figure 6-8 shows a close-up of the detail between the top of the bamboo posts and the cantilever overhang in the Chavez Hotel Inn. The tops of the posts have been cut into a notch to enhance restraint by locking onto the edge of the building.

The Fish and Dive sport store (See Figure 6-9) catered to the water sporting needs of Tarqui tourists and was located on 105th Street near the intersection with and 106th Avenue in Manta. The cantilever overhang was shored using the common method relying on bamboo posts. Some of the shorter posts, which support the bottom of the overhang, appear to have developed curvature under load. The longer posts, which support the top of the window openings, do not exhibit such curvature.

The 3-story RC building (See figure 6-10) was located in the Francisco de P. Moreira Street near the intersection with Olmedo Avenue and near the Eloy Alfaro Park. The building was damaged heavily during the April 16 event, and was subsequently shored to prevent collapse of the cantilever overhang. Steel pipes were used to shore the building, but the shores buckled and became ineffective. The pipes appear to be excessively slender given the lack of lateral braces between pipes, and the connections between pipe segments do not appear to be sufficiently robust to ensure flexural continuity between connected pipes. This was the only shoring failure observed by the EERI team.

## 6.4 REFERENCES

- California Building Officials (CALBO). (2013). CALBO's Interim Guidance for Barricading, Cordoning, Emergency Evaluation and Stabilization of Buildings with Substantial Damage in Disasters. Sacramento, CA, November, 17 pp.
- Department of Homeland Security (DHS). (2011). Field Guide for Building Stabilization and Shoring Techniques. Report No. BIPS 08, Washington, DC, October, 190 pp.
- Federal Emergency Management Agency (FEMA). (2013). National Urban Search and Rescue (US&R) Response System—Training Program Administration Manual. Washington, DC, February, 151 pp.
- Federal Emergency Management Agency (FEMA). (2014). Structural Collapse Technician Course—Student Manual. Washington, DC, February, 296 pp.
- Guadua Bamboo: Bamboo facts—Mechanical properties of bamboo. [www.guaduabamboo.com/facts/mechanical-properties-of-bamboo](http://www.guaduabamboo.com/facts/mechanical-properties-of-bamboo). Accessed 29 July 2016.
- Kappel, R., Mattheck, C., Bethge, K. and Tesari, I. (2004). "Bamboo as a composite structure and its mechanical failure behavior." Design and Nature II, WIT Transactions on Ecology and the Environment, Collins, M.W. and Brebbia, C.A. Ed. WIT Press, Southampton, UK., pp. 285-293.
- RWTH Aachen: Construction with bamboo—Mechanical properties of bamboo. [http://bambus.rwth-aachen.de/eng/reports/mechanical\\_properties/referat2.html](http://bambus.rwth-aachen.de/eng/reports/mechanical_properties/referat2.html). Accessed 29 July 2016.
- Turner, F., Khorram, D. and Koutsouros, T. (2015). "California Building Officials' Interim Guidance on the Barricading and Stabilization of Buildings with Substantial Damage in Disasters." Proceedings of the Second ATC & SEI Conference on Improving the Seismic Performance of Existing Buildings and Other Structures, ASCE, Reston, VA, December, pp. 670-680.



## CHAPTER 7

# Post-Earthquake Safety Evaluation of Buildings

### 7.1 INTRODUCTION

This section discusses the post-earthquake safety evaluation of buildings. After an earthquake, one of the first steps a community must take is the evaluation of the building stock to establish if the structures are safe to occupy. In the United States, and increasingly in countries around the world (with modifications), the ATC-20-1 Field Manual: Post-earthquake Safety Evaluation of Buildings (ATC 2005) provides guidelines for rapid assessment for trained personnel to use in the ATC-20 methodology. The ATC-20-1 comprises three levels of rapid assessment:

**INSPECTED (green).** No apparent hazard is found, although non-structural repairs may be required. The original seismic resistance is not significantly reduced. No restriction on use or occupancy.

**RESTRICTED USE (yellow).** A hazardous condition exists (or is believed to exist) that requires restrictions on the occupancy or use of the structure. Entry and use are restricted as indicated on the placard.

**UNSAFE (red).** Extreme structural or other hazard is present. There may be imminent risk of further damage or collapse from instability or aftershocks. Unsafe for occupancy or entry, except as authorized by the local building department.

Following the April 16 earthquake, safety evaluations were conducted mainly by volunteers and government entities adapting the forms and placards from the ATC-20 and ATC-45 field manuals, which marks the first use of such standards in Ecuador. A Spanish version of ATC-20 was in development at the University of San Francisco in Quito (USFQ) by the Department of Civil Engineering, but had not been completed when the Muisne earthquake struck. Therefore, days after the main event and in an effort to standardize the procedure, the Ministry of Urban Development and Housing in Ecuador created modified versions of the placards from the ATC-20 posting cards with its symbol, and

deployed trained personnel to affected cities including Manta, Portoviejo, and Bahía de Caráquez in Manabí province. A smart phone app, GeoODK, for the collection and storing of geo-referenced data, was found to enhance the speed of the data collection.

The team organized by the Ministry of Urban Development and Housing had to deploy to the affected region within 48 hours of the April 16 event. During the reconnaissance trip, the EERI team found some inconsistencies in the tagging evaluations, which are presented next. Usually, these anomalies happen in the aftermath of an earthquake, especially when a country is not prepared to face a natural disaster, and does not already have emergency response teams ready to mobilize in short notice for rapid structural inspection.

## 7.2 USAGE OF EVALUATION PLACARDS

Various versions of the placards used in this event were based on the ATC-20-1 procedures; however, the assessment forms were not always used in conjunction, especially during the days immediately after the April 16 earthquake, where different jurisdictions focused on rescuing survivors from collapsed structures and not classification of building safety. The placards and forms were improved and standardized a few days after the event. However, throughout the field observations conducted by the EERI team three weeks after the event, some issues were still noted in the management and implementation of post-earthquake safety evaluation procedures.

In some cases, placards were issued not necessarily to limit or restrict access to buildings, but to apparently inform the owner about the damages and future actions. In other cases, the placard associated with a GREEN tag was used as a general form. Figure 7-1 shows an INSPECTED (green) tag adapted as a RESTRICTED USE (yellow) tag in the main hospital of Bahía de Caráquez. This placard had no color and no information on the restrictions, further reducing the effectiveness of the placard. The ATC-20 procedures establish that restrictions should be displayed on the placard to inform occupants of the hazardous conditions in the building.

Some cases showed that the placards were placed at locations other than entrances, which could lead to confusion. Figure 7-2 depicts a case where the placard was posted on a wall that was not visible from the main entrance. At the time of the team's visit, other residential buildings in Bahía de Caráquez had not been evaluated since placards were not found, even though they suffered damage from the earthquake. Figure 7-3 shows a case where a placard is missing.

In Manta, two buildings shared a RESTRICTED USE (yellow) placard as shown in Figure 7-4. It can be observed that the structure on the right hand was also posted with an INSPECTED (green) placard, which could lead to ambiguity.

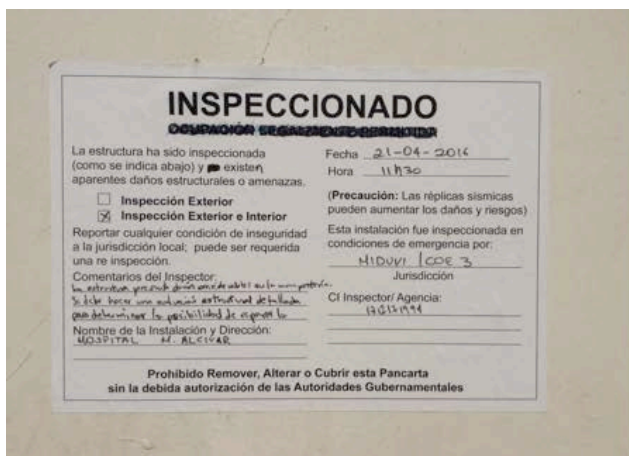


Figure 7-1. An INSPECTED placard used as a RESTRICTED USE placard. No information on the restrictions is indicated (photo: Alberto Monzo).



Figure 7-2. Placard posted on an inconvenient place Bahía de Caráquez (photo: Ana Gabriela Haro).

In Portoviejo, a “Demolition” recommendation was found in a reinforced concrete building tagged with an UNSAFE (red) placard. What was suggested in the placard presented in Figure 7-5, exceeds the purpose of the rapid assessment procedures established in the ATC-20. Since ATC-20 was based on very limited visual information, and except in very obvious cases, we do not agree that it should be used to inform building owners on further actions. Certain repairable buildings appear to have been demolished when they could have been repaired. Figure 7-6 depicts a case in the same city where a building had an INSPECTED (green) placard. It was noticed that it is not indicated if an external or internal inspection was carried on.

The main hospital in Chone was tagged with a blank UNSAFE (red) placard (Figure 7-7). In some cases tenants did not follow the placards. Figure 7-8 shows a shop in Calceta that was still open despite the building was posted with a RESTRICTED USE (yellow) tag. In Chone, we noted multiple cases where the UNSAFE (red) placard, which implied “unsafe for occupancy or entry, except as authorized by the local building department,” was not respected in residential buildings.

Overall, the EERI team noted many instances where the criteria of tagging appear to be inconsistent among different buildings, and in some cases they appear to be over-conservative. The consequence of inappropriate interpretation of the UNSAFE (red) placard is that buildings that can be repaired are often automatically slated for demolition by virtue of the placard. The decisions regarding repair vs. demolition are complex and incorporate many factors, of which structural damage is but one.



Figure 7-3. Missing placard in a residential building in Bahía de Caráquez (photo: Ana Gabriela Haro).



Figure 7-4. Structures sharing a RESTRICTED USE (yellow) placard in Manta (photo: Arturo Achultz).

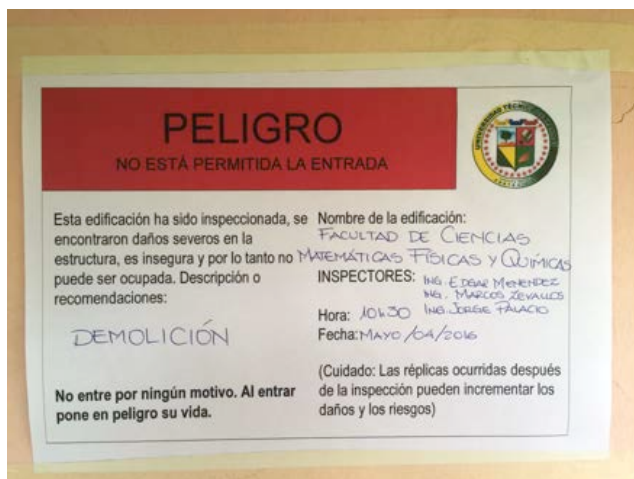


Figure 7-5. “Demolition” suggested on a RED placard used in an RC building in Portoviejo (photo: Alberto Mozon).



Figure 7-6. INSPECTED (green) tag on a building in Portoviejo where the type of evaluation was not established (photo: Mei Liu).



Figure 7-7. Unfilled UNSAFE (red) placard in Chone (photo: Alberto Monzon).



Figure 7-8. RESTRICTED USE (yellow) placard in a shop still open in Calceta (photo: Forrest Lanning).



Figure 7-9. Portoviejo branch of Banco de Pichincha (photo: Arturo Schultz)

The Portoviejo branch of Banco Pichincha was located downtown on Olmedo Avenue near the intersection with Simón Bolívar Street (Figure 7-9). The four-story reinforced concrete building with unreinforced concrete block infill appears to be 30–40 years old, has a large atrium with staircases supported on cantilever overhangs, and a cantilever balcony along Olmedo Avenue. Heavy damage in non-structural components was observed, but the only structural damage was cracking along the supports for the stairs (Figure 7-10) and the street-side balcony. An UNSAFE (red) placard, visible in the lower right of Figure 7-10, is likely due to concern with potential collapse of these cantilever structures. The concern is commensurate with the hazard, but the structural damage is easily repairable. It is unclear if the building will be demolished, but the bank branch has been moved to a building at another location.

The Comercial Bigote Building is located on 109th Avenue and 103rd Street in the Tarqui district of Manta (Figure 7-11). The five-story reinforced concrete frame building with unreinforced concrete block infill appears to be well over fifty years old and harkens back to an Art Deco period. The building has a street-side colonnade supporting the overhanging floor in stories above the first. The building also features balconies on the corner of the two street-side façades. Earthquake damage was observed to infills, but not to the frame members.



Figure 7-10. Cracking damage to staircase (photo: Arturo Schultz)



Figure 7-11. 'Comercial Bigote' Building in Tarqui district of Manta (photo: Arturo Schultz)

Damage to the first floor balcony poses a falling debris hazard, and the main entry of the building is compromised. This hazard earned it an UNSAFE (red) placard, and the concern is commensurate with hazard. However, the building is repairable, misinterpretation/misuse of the placard could result in the demolition of an architecturally important building in a historic sector of Manta.

A final note is made that since some significant aftershocks are to be expected following a major earthquake, the original tagging would need to be revised following strong aftershocks. Building occupants and owners should understand this potential downgrading of tagging and its implication on building safety.

### 7.3 REFERENCES

ATC. 2005. ATC-20-1. Field Manual: Postearthquake Safety Evaluation of Buildings. Second. Redwood City, California.

# Concluding Remarks

- » The main causes of the structural damage observed by the EERI team included the following:
  - RC frames were not properly proportioned to resist the magnitude of the seismic forces, of which the columns were far too small in all of the heavily damaged buildings observed.
  - The reinforcement details for the columns, beam-column joints and the beams (whenever beams were present) were woefully inadequate, and features such as missing ties (or excessively spaced ties) led to inadequate confinement of the columns (and frequent bar buckling) and beam-column joints, and insufficient shear strength for columns, beams and beam-column joints.
  - Many of the buildings observed had soft first stories and were torsionally irregular due to the open building front on the first story. These configuration problems, coupled with highly non-ductile characteristics of the frames, generally result in catastrophic failures (i.e. collapses, partial or total).
  - The common practice of partial height infills and partitions created short columns which exacerbated the column weaknesses mentioned above.
- » Observations concerning hospital performance specifically:
  - Hospitals suffered significant damage in nonstructural components, which made/rendered them not operational after the earthquake.
  - Poor performance of interior/exterior URM walls. Major damage was concentrated at the first two stories for multi-story building segments, with the exception of the Hospital IESS in Manta, where all the stores had poor behavior of URM. Such walls, when used, would require confined masonry reinforcement techniques. A more extensive use of interior dry-wall partitions is advisable.
  - Minor damage observed in structural system (beams & columns) but significant damage observed in non-structural system due to large interstory drift. Designer should account for expected sway in design of non-structural components, or where appropriate, limit drift of structure.
  - Non-structural damage was extensive in spite of the retrofit measures done in the Alcivar Hospital after the 1998 M7.2 Bahía de Caráquez earthquake. In general, flexibility triggered the damage, but the main reason for the virtual disintegration or collapse of brick partitions and facades was the lack of internal reinforcement and very inadequate attachments to the main structure.
  - Despite the damage in hospitals, there were only minor casualties associated with their performance.
  - Damage caused by inadequate separation at seismic joints could have been avoided by proper design or retrofit mechanisms.
  - Hospitals at other locations in the country need immediate assessment for seismic evaluation and potential actions for retrofitting.
  - Ecuadorian seismic code requires guidelines to designers for proper design of attachments of non-structural components at health facilities and other buildings of equivalent importance.
- » Poor quality of concrete and corrosion was observed at some buildings; therefore, the quality control of new concrete and proper measures to reduce or assess corrosion should be considered in new buildings.
- » The observed performance of masonry interior partitions and masonry cladding of frame buildings was typically not satisfactory. Extensive damage was observed in the masonry façade and infill panels in the form of inclined and diagonal cracking from in-plane shear, crushing at the jambs from compressive loading, horizontal cracking from either in-plane shear or out-of-plane bending, and partial or total collapse, typically out of plane.
- » The majority of the shoring observed was made using guadua bamboo, which in several cases exceeded typical slenderness limitations, were lack of lateral bracing, or did not show appropriate connections between pieces and to the ground. In spite of these shortcomings, no total failures were observed due to shoring issues.

- » Significant drifts on the concrete moment frames most likely triggered the cracking of the façades and interior partition walls.
- » Many buildings of different construction systems and configurations were extremely close to each other, causing structural damage due to repeated impact from pounding.
- » Later alterations or additions to buildings led to vulnerabilities caused by increased gravity loads that were not contemplated during the design of the original structure.
- » The clearing of debris after the earthquake, including demolition of unstable structures, was done very rapidly.
- » Observations concerning geotechnical performance (details available in the GEER-ATC report [http://www.geer-association.org/component/geer\\_reports/?view=geerreports&id=77&layout=default](http://www.geer-association.org/component/geer_reports/?view=geerreports&id=77&layout=default)):
  - Ground motions were intense and in some cases exceeded design levels. The strongest motion with PGA = 1.41 g was recorded in Pedernales, in the EW component of the APED station.
  - Most of the coastal area's subsurface conditions consist of site class "F" sites: either thick soft and plastic clays or potentially liquefiable loose sands. Site effects were evident in recordings and observations of the natural and built environment.
  - Liquefaction was evident across the coastal affected areas, in the form of ejecta, lateral spreading, and settlements. The phenomenon was extensive in the major Port of Manta. Reconnaissance and design information was collected and post-liquefaction in-situ testing was performed by the GEER-ATC team.
  - Hundreds of landslides and rock falls were recorded. Drone images and digital photos from helicopter flyovers were used to compose 3D models of some of the major landslides and overlay them with the condition before the earthquake.
  - Dams were observed and design information was collected, with only minor damage recorded by the GEER-ATC team. However, there is no risk assessment procedure and condition assessment procedure is formally available for dams.
  - Earth retaining wall systems and embankments observed at the west coast exhibited, in some cases, extremely poor behavior and even complete failure, but also satisfactory in other cases. The majority of highway embankments throughout the affected areas of Ecuador performed well, maintaining a serviceable road.
  - Damage to infrastructure systems was severe in some cases due to structural and non-structural damage induced by the strong shaking and liquefaction-induced loss of soil strength and ground deformations. Serious fires were not observed post-earthquake, mostly because there is no gas pipeline network in the country which uses individual gas bottles in homes for energy supply.
  - The generated tsunami was minor and did not induce any significant additional damage to the coastal areas. Predictions for future events include tsunami hazard exposure due to the topographic and tectonic setting.



## Appendix

### RECOVERY FROM THE MW7.8 MUISINE EARTHQUAKE OF APRIL 16, 2016: A CASE STUDY OF THE EARTHQUAKE REFUGEE SHELTERS IN MANABÍ PROVINCE, ECUADOR

A contribution from the Earthquake Engineering Field Investigation Team (EEFIT)<sup>1</sup>: by Bayes Ahmed

Addressing community vulnerability in disaster risk reduction (DRR) is an important aspect that is often neglected. This research, conducted as part of the EEFIT reconnaissance investigation, takes into account the perception of people at risk and affected by the April 2016 earthquake. Three different earthquake refugee shelters in Manabí province, Ecuador, were selected for analysis of community vulnerability. The earthquake camps are located in the Aeropuerto Reales Tamarindos, Portoviejo (1°2'45" South 80°28'5" West), Canoa (0°27'42" South 80°27'8" West), and Pedernales (0°4'43" North 80°2'52" West) cities (Figure 1).

The camp in Canoa (Figure 1b) is administered by a local NGO, Deja Tu Huella por Manabi, while the Ecuadorian Army operates the other two camps described here. All the families in the camps had access to necessary services, including electricity, toilets, showers, water, medical support, playgrounds, social services, training facilities for adults, and educational facilities for the children. All the services were provided for free. A total of 120 families living in these shelters were selected for the survey using a stratified random sampling method.

A structured questionnaire was prepared after field-testing in the Manta earthquake shelter. The household-based questionnaire was administered between May 28, 2016 – June 5, 2016. The survey team consisted of the author and an additional researcher, Nicolás van Drunen. In addition, several focus group discussions were undertaken with the affected people and relevant organizations in charge (i.e. the Army Corps of Ecuador and the local NGOs that are providing support) to understand the overall situation in the shelters and the process of recovery from the disaster. Questions were asked about demographic information, economic status, change of occupation, damaged house (year of construction, material type, ownership pattern), damage and losses due to earthquakes, household preparedness, problems in the shelters, and future housing and livelihood plans to recover from the earthquakes. Some generalized findings from this household-based survey of 120 families are summarized in the following pages.

<sup>1</sup> Further discussion of these issues can be found in 2 EEFIT reports: Franco et al. (2016) "The April 16 2016 MW7.8 Muisne Earthquake in Ecuador—Observations & Conclusions from the EEFIT Reconnaissance Mission of May 24 - June 7." Earthquake Engineering Field Investigation Team, Institution of Structural Engineers, London, UK.

Franco et al. (2017) "The April 16 2016 MW7.8 Muisne Earthquake in Ecuador—Preliminary Observations from the EEFIT Reconnaissance Mission of May 24-June 7." In Proceedings of the 16th World Conference on Earthquake Engineering, 16WCEE 2017, Santiago Chile, January 9th to 13th 2017, Paper N° 4982

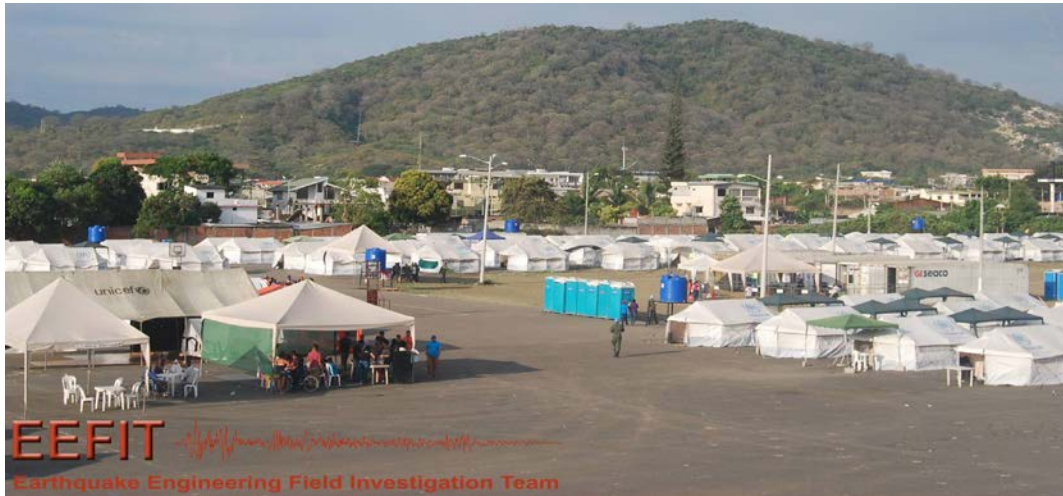


Figure 8-1. The earthquake refugee shelters in (a) Portoviejo, (b) Canoa, and in (c) Pedernales, Ecuador. Source: Bayes Ahmed, field visit, June 2016.

### 8.1.1 Demographic Characteristics

Fifty-three percent of the population was found to fall within 18 – 65 years of age, meaning they were employable. The second largest group was between 6-17 years (30%), and the remaining were either under the age of five or over the age of 65. The average family size was four. The male and female ratio was found balanced with 49% male and 51% female. Forty-seven percent of people had completed their primary education, while 39% finished secondary education. Six percent were found to be illiterate and 5% had finished an undergraduate level education.

## 8.1.2 Economic Status

No notable variation in monthly household income was found. On average, around 24% of the households in the shelters earn US\$ 151-300 monthly, and 20% reported US\$ 76-150 and US\$ 301-450, respectively. After the earthquake, a change in primary household occupation was found as a major issue. Approximately 55% of the respondents lost their jobs because of the earthquake. Most of the people in shelters lost jobs in retail business (17%), fishing/fish selling (7%), construction (4%), hotel business (4%), day labor (3%), and tourism (3%) sectors (Table 8-1).

Table 8-1. Changes in occupation pattern.

Before Earthquake			After Earthquake			Changes
Occupation	Freq.	%	Occupation	Freq.	%	(%)
Bartender	2	1.67				-1.67
Beauty Parlour	1	0.83	Beauty Parlour	1	0.83	0
Business	1	0.83				-0.83
Butcher	1	0.83				-0.83
Carpenter	1	0.83				-0.83
Coconut Sell	1	0.83	Coconut Sell	1	0.83	0
Construction	11	9.17	Construction	6	5.00	-4.17
Cook	2	1.67	Cook	1	0.83	-0.84
Day Labour	7	5.83	Day Labour	4	3.33	-2.5
Delivery	1	0.83	Delivery	1	0.83	0
Driver	6	5.00	Driver	4	3.33	-1.67
Engineer	1	0.83				-0.83
<b>Fishermen/ Fish Business</b>	<b>15</b>	<b>12.50</b>	<b>Fishermen/ Fish Business</b>	<b>7</b>	<b>5.83</b>	<b>-6.67</b>
Garments	1	0.83				-0.83
Hotel	5	4.17				-4.17
Housemaid	2	1.67	Housemaid	1	0.83	-0.84
Housewife	6	5.00	Housewife	3	2.50	-2.5
Job Others	2	1.67	Job Others	2	1.67	0
Laundry	1	0.83	Laundry	1	0.83	0
Magazine Sell	1	0.83				-0.83
Professor	1	0.83	Professor	1	0.83	0
Public Job	7	5.83	Public Job	6	5.00	-0.83
<b>Retail</b>	<b>25</b>	<b>20.83</b>	<b>Retail</b>	<b>5</b>	<b>4.17</b>	<b>-16.66</b>
Security Guard	3	2.50				-2.5
Singer	1	0.83	Singer	1	0.83	0
Teacher	2	1.67	Teacher	1	0.83	-0.84
Technician	4	3.33	Technician	2	1.67	-1.66
Tourism	3	2.50				-2.5
<b>Unemployed</b>	<b>5</b>	<b>4.17</b>	<b>Unemployed</b>	<b>71</b>	<b>59.17</b>	<b>+55</b>
Waste Collect	1	0.83	Waste Collect	1	0.83	0
Total	120	100	Total	120	100	0

### 8.1.3 Information on Survey Respondent Homes

The results of the survey suggest that most of the shelter occupants came from damaged houses (42%) that had been recently built (in the 2000s). Eighteen percent of houses were constructed recently (>2010), and 24% of the houses were built in the 1990s. The damaged houses were mostly one (46%) and two stories (45%). Houses of mixed construction materials (wood, brick, concrete) were the most damaged (39%) followed by concrete structures (31%). Figure 8-2 provides more detail. Approximately 58% of the respondents were homeowners, while the rest were renters. The shelter refugees basically came from city centers/urban areas (93%), and most of their houses were completely destroyed (65%).

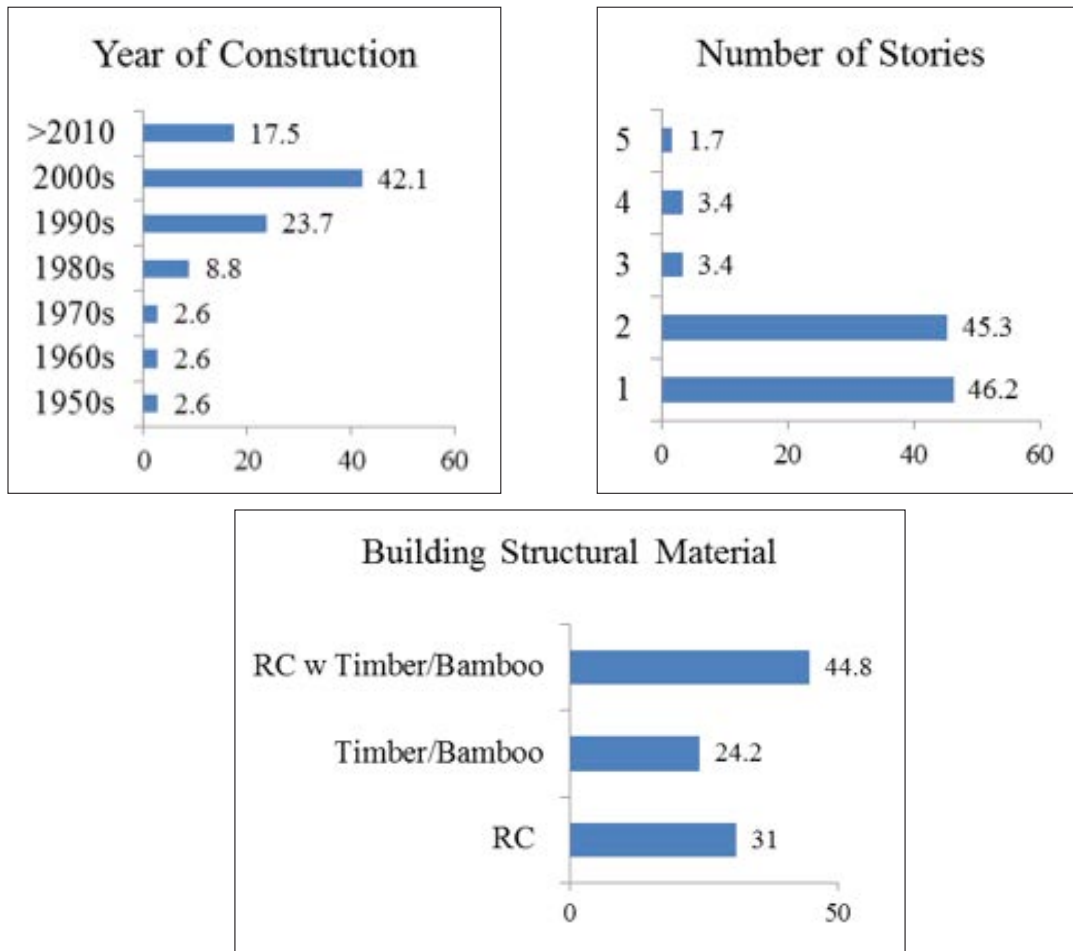


Figure 8-2. Distribution of building characteristics derived from 120 interviews at shelters (in %)

### 8.1.4 Problems in the Shelters

The survey participants were asked about their plans to recover from the earthquake. Most of them were not prepared (98%) for the earthquake. When asked to select the top two problems that they were facing while living in the shelters, they identified food shortages (26%) and water supply (18%) as problems, with 23% reporting no problem. When asked about a second level of problems, 45% said they were not facing further problems, but hot weather (26%) and lack of proper sanitation (15%) were identified as secondary problems by the remaining respondents.

### 8.1.5 Future Direction

As part of their recovery process, a majority of the respondents desired to get employment (59%) and housing (34%) to return to their pre-earthquake lifestyle. When the same group was asked a second level of concerns, some desired to get loans (25%) and relocate to other places (17%). Most of the affected families prefer to move back to a one-story building (88%), with a preference for wood (52%) or bamboo (17%). Thirty-eight percent of the respondents wanted to stay in a city center or an urban area.

### 8.1.6 Summary Findings

The following general findings emerged from the household survey:

- The typical family size of the survey respondents in the three shelter camps was an average of four people, with a fairly even gender balance.
- Most of the people are adult working-class (18–65 years), without a higher education (most having just completed primary level).
- They are low-earning households (US\$75-300/month), involved primarily in retail business, fishing, construction, and as day laborers. After the earthquake, they are unemployed and their first priority is to find a source of earning.
- The survey respondents were primarily homeowners from one-story buildings made of mixed materials (wood, brick, and concrete) or concrete, the homes that were totally destroyed were mostly recently built (in the 2000s), primarily located in urban areas.
- Survey respondents were not prepared for this earthquake disaster. They want to go back to their normal lives, with a preference now for one-story houses made of wood and/or bamboo, and they want to continue their livelihoods in urban areas.

The summary of survey results presented here describes families who were living in one of three shelter camps, representing only families who either lost their houses or were unable to live in their previous homes due to the earthquake. Their views do not necessarily represent the broader affected communities, but rather offer a window into how the earthquake affected a segment of the population. In the camps, some of the families were too affected to participate in the survey. There was limited time for surveying at each shelter and as such the questionnaire was kept as short as possible. To be most effective, community vulnerability research needs more time and interactions with vulnerable populations. Moving forward, it is hoped that additional researchers can further explore these issues of vulnerability and resilience.



Figure 8-3. Rebuilding a fishing village using bamboo and wood structures. Source: Bayes Ahmed, fieldwork, June 2016

## 8.1.7 Acknowledgments

Bayes Ahmed<sup>1,2</sup>, a PhD student at the Institute for Risk and Disaster Reduction, University College London (UCL), UK is the author of this report. He is grateful to: the EEFIT for funding this fieldwork; Guillermo Franco for being a superb team leader and guiding always in the right direction; Nicolás van Drunen and Everth Mera for assisting during the questionnaire surveying; the highly enthusiastic EEFIT reconnaissance team for their motivation; to Maj. Manuel Querembas and the Ecuadorian Army for their help getting access to the shelters; and the respective officials and local people for their cooperation during the fieldwork.

---

1 Institute for Risk and Disaster Reduction, Department of Earth Sciences, University College London (UCL), Gower Street, London WC1E 6BT, UK. Email: bayes.ahmed.13@ucl.ac.uk

2 Department of Disaster Science and Management, Faculty of Earth and Environmental Sciences, University of Dhaka, Dhaka 1000, Bangladesh. Email: bayesahmed@gmail.com

## REFERENCES

- Adger, W.N. Vulnerability. *Glob. Environ. Chang.* 2006, 16, 268–281.
- Alexander D, Magni M. Mortality in the L'Aquila (Central Italy) Earthquake of 6 April 2009: A Study in Victimisation. *PLOS Currents Disasters*. 2013 Jan 7 . Edition 1. doi: 10.1371/50585b8e6efd1.
- Alexander, D. 2000. *Confronting catastrophe: New perspectives on natural disasters*. Terra Publishing, Harpenden, England, 282 pp.
- Alexander, D.E. Communicating earthquake risk to the public: the trial of the "L'Aquila Seven". *Nat Hazards* (2014) 72: 1159. doi:10.1007/s11069-014-1062-2
- Alexander, D.E. Resilience and disaster risk reduction: An etymological journey. *Nat. Hazards Earth Syst. Sci.* 2013, 13, 2707–2716.
- David Alexander. "A Tale of Three Cities and Three Earthquake Disasters" (2012). URL: [http://works.bepress.com/david\\_alexander/2/](http://works.bepress.com/david_alexander/2/)
- Hewitt, K. (Ed.) *Interpretations of Calamity from the Viewpoint of Human Ecology*, 1st ed.; Allen & Unwin: London, UK, 1983.
- Lewis J. The Good, The Bad and The Ugly: Disaster Risk Reduction (DRR) Versus Disaster Risk Creation (DRC). *PLOS Currents Disasters*. 2012 Jun 21 . Edition 1. doi: 10.1371/4f8d4eaec6af8.
- Lewis, J. *Development in Disaster-Prone Places: Studies of Vulnerability*; Intermediate Technology: London, UK, 1999.
- Wisner, B.; Blaikie, P.; Cannon, T.; Davis, I. *At Risk: Natural Hazards, People's Vulnerability and Disasters*, 2nd ed.; Routledge: London, UK, 2004.